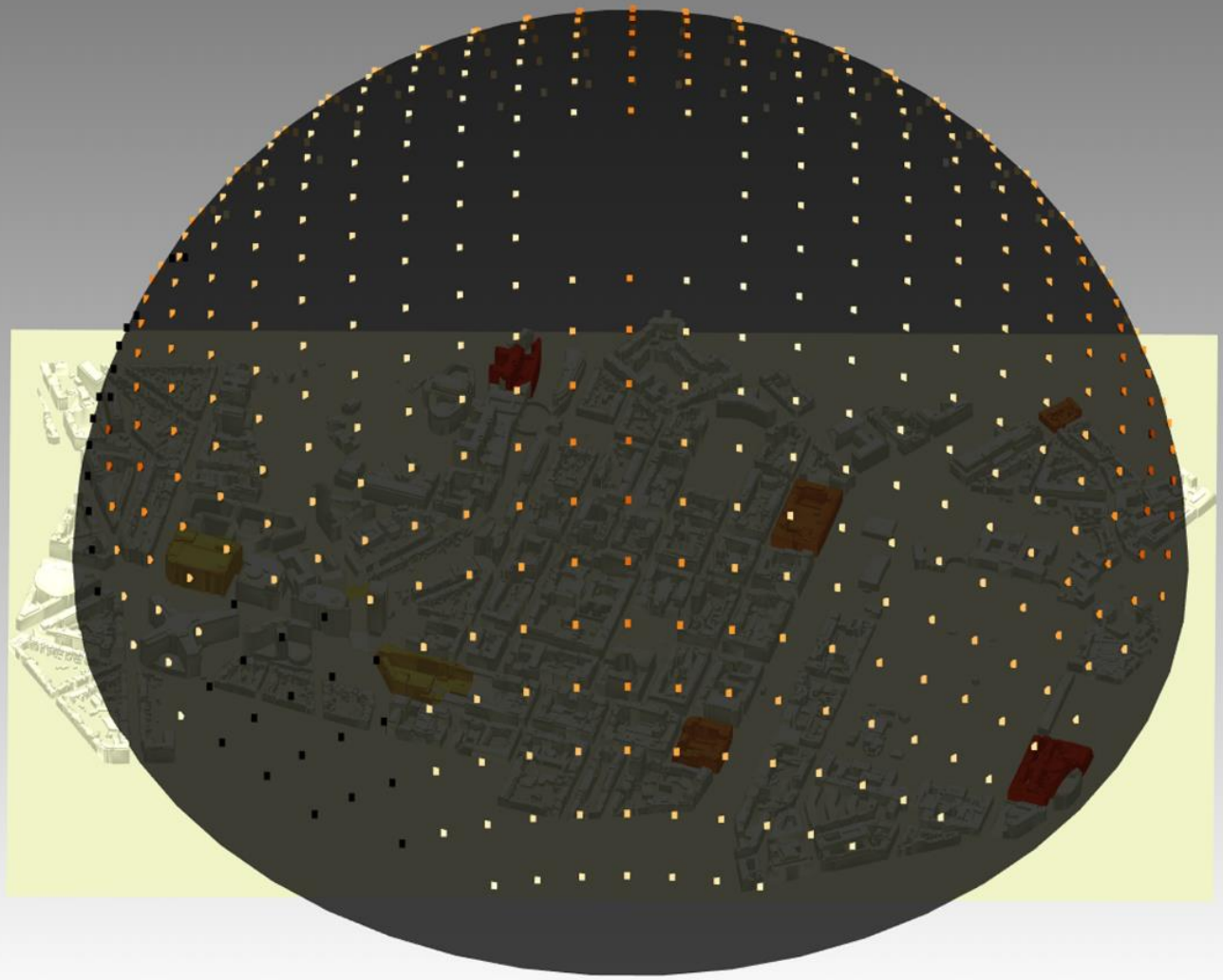

# Identification of the best 3D viewpoint within building models

Romain Neuville
Dissertation
ULiège

# 3D Geovisualization

## Identification of the best 3D viewpoint within building models

**By**

Romain Neuville

Thesis submitted for the fulfillment of the degree of Doctor of Philosophy in Sciences

**December 2019**

Université de Liège

Faculté des Sciences

Département de Géographie

© Romain Neuville

This dissertation has been approved by

| | |
|---|---|
| Prof. Dr. Roland Billen | Co-director of research |
| Prof. Dr. Jacynthe Pouliot | Co-director of research |

The doctoral committee is composed of

| | |
|---|---|
| Prof. Dr. Roland Billen | Université de Liège, Belgium |
| Prof. Dr. Maria Giulia Dondero | Université de Liège, Belgium |
| Prof. Dr. Pierre Hallot | Université de Liège, Belgium |
| Prof. Dr. Jacynthe Pouliot | Université Laval, Canada |

The jury is composed of

| | |
|---|---|
| Prof. Dr. Roland Billen | Université de Liège, Belgium |
| Prof. Dr. Sidonie Christophe | IGN-France, France |
| Prof. Dr. Arzu Çöltekin | FHNW, Switzerland |
| Prof. Dr. Maria Giulia Dondero | Université de Liège, Belgium |
| Prof. Dr. Pierre Hallot | Université de Liège, Belgium |
| Prof. Dr. Jacynthe Pouliot | Université Laval, Canada |


This dissertation was carried out at the geomatics unit of the University of Liège, from October 2015 to December 2019.

© 2019 R. Neuville (ORCID 0000-0003-1949-1332)

# Abstract

Geospatial data visualization, known as geovisualization, often provides great support in the comprehension of the geographic information. For instance, geovisualization is fully integrated in urban planning, from the exploratory phase (e.g., for facilitating the diagnosis of areas where something needs to be done) to the monitoring stage (e.g., for evaluating dynamics phenomena). Initially carried out in 2D, this process increasingly extents to the third dimension as a way to enhance the visual perception of the surrounding world, which is fundamentally 3D. However, this shift is not without pitfalls, both in the graphical design of 3D model and the viewpoint selection. To promote the use of the third dimension, it is therefore essential to propose new strategies that facilitate this transition. As a result, this thesis intends to contribute to 3D geovisualization field development via the first proposal that aims to formalize its process into a knowledge network including both an expression (i.e., visual stimuli) and content plan (i.e., semantic world). Following this formalization effort, we realized that moving to the 3rd dimension strengthens the role of the viewpoint, especially in order to enhance the visualization techniques relevance in achieving visual targeted purposes. Indeed, as the camera is no longer simply oriented in a classic top-down direction (which is usually the case in 2D), the point of view needs now to be configured; and, due to the 3D graphical representation, this configuration is complex, in particular because occlusion issues are inevitable. This is why this research mainly tackles the best 3D viewpoint selection issue via a geocomputational method that

automates and optimizes its identification within 3D scene. Note that specific attention has been carried out to incorporate the solution into a global semantic driven visualization process. Eventually, the proposal is validated through the development of an experimental framework that aims to evaluate our solution for a given visual selectivity task: visual counting. For that purpose, an empirical test has been conducted with experts in the form of interviews using an online questionnaire.

# Résumé

La visualisation de données géospatiales, connues sous le terme de géovisualisation, est généralement d'un grand soutien dans la compréhension de l'information géographique. A titre d'exemple, la géovisualisation est pleinement intégrée au sein de la planification urbaine, depuis l'étape exploratoire (e.g. pour faciliter le diagnostic du territoire) jusqu'à l'étape de surveillance (e.g. dans l'évaluation des phénomènes dynamiques). Initialement opéré en 2D, ce processus s'étend de plus en plus à la troisième dimension afin d'améliorer, entre autre, la perception du monde environnant, fondamentalement 3D. Cependant, ce passage n'est pas exempt d'écueils, à la fois dans la conception graphique du modèle 3D et le choix du point de vue à adopter. Afin de promouvoir l'utilisation de la troisième dimension, il est dès lors essentiel de proposer de nouvelles stratégies qui facilitent cette transition. En conséquence, cette thèse souhaite contribuer au développement de la géovisualisation 3D au travers d'une première proposition visant à formaliser son processus et ce, sous la forme d'un réseau de connaissances incluant à la fois un plan de l'expression (i.e. les stimuli visuels) et un plan du contenu (i.e. le monde sémantique). Suivant cet effort de formalisation, nous nous sommes rendus compte que le passage à la troisième dimension renforce le rôle du point de vue, en particulier afin d'améliorer la pertinence des techniques de visualisation à accomplir des objectifs visuels donnés. En effet, puisque la caméra n'est plus simplement orientée selon une direction « top down » (ce qui est généralement le cas en 2D), le point de vue devient un paramètre configurable; et en raison de la représentation graphique 3D,

cette configuration est relativement complexe, essentiellement parce que les problèmes d'occlusion sont inévitables. C'est la raison pour laquelle cette recherche se focalise essentiellement sur le problème de la sélection du meilleur point de vue 3D au travers d'une méthode géoinformatique qui automatise et optimise son identification au sein de la scène 3D. Notez qu'une attention spécifique a été portée afin d'incorporer cette solution au sein d'un processus global de visualisation à base sémantique. Finalement, notre proposition est validée au travers du développement d'un cadre expérimental visant à évaluer notre solution pour une tâche visuelle donnée de sélectivité : le comptage visuel. A cet effet, un test empirique a été conduit auprès d'experts sous la forme d'interviews utilisant un questionnaire en ligne.

# Acknowledgements

This thesis is the achievement of four years, during which I had the privilege to be supported by several people.

Four years ago, my supervisor, Professor Roland Billen, gave me this great opportunity to carry out this doctorate. Since the beginning, he truly assisted me with enthusiasm and guided me with patience. I sincerely thank him for his time and his knowledge that allowed me to progress in my work life.

After a year, Professor Jacynthe Pouliot is become my co-supervisor. Expert in the 3D visualization of geospatial data, she shared her expertise and gave me lots of constructive comments. Moreover, my internship at the Université Laval was extremely instructive and will remain a wonderful adventure of my life, both professional and personal.

From the beginning, I also received great support from Professor Pierre Hallot and his opening to additional application domains helped me to broaden my vision about my work. With her expertise in the semiotics field, Professor Maria Giulia Dondero allowed me to put this thesis into a broader context of the visual language.

I would also like to express my sincere thanks to Professor Jean-Paul Donnay for his valuable advice in this thesis formulation, his attentiveness and all the support offered to achieve this thesis under the best possible conditions.

I would like to thank Professor Yves Cornet as well for the extensive discussions about the practical issues that I met throughout this thesis. He devoted invaluable time and was always available to answer any of my questions.

Thanks to the whole geomatics unit of the University of Liège, especially to Marc Binard for his continued support in the IT aspects, and Anna Poletto for her help in the administrative follow-up.

I would also to sincerely thank my colleagues and friends Cécile Deprez, Gilles-Antoine Nys and Florent Poux for their good mood, their listening and their help during these four years.

Thanks to my entire family for their presence and their unconditional support.

Thanks to all people that I met during this thesis and thanks to all those who contributed to my personal development and my happiness.

*Our point of view determines our perception.*

# Table of Contents

# List of Tables

# List of Figures

# CHAPTER 1

# Introduction

## 1.1 Context

With a data feed of up to $10^7$ bits per seconds, sight is the most powerful sensory medium among all human senses (Franke, 1977). For this purpose, vision is extensively used in apprehending geospatial phenomena and is become a research area, called geovisualization. Defined as the field that provides both theories and methods for visually exploring, analyzing, summarizing and presenting geospatial data (MacEachren & Kraak, 2001), geovisualization aims to process and interpret the data into information, and ultimately into knowledge.

Conventionally, geospatial data have been visualized in two dimensions (i.e., via a set of planimetric coordinates) until recent and significant developments in data acquisition techniques (LiDAR, photogrammetry, and remote sensing) and computer sciences (storage and processing) make the third geometric dimension (mainly the height or the Z coordinate of objects) more accessible for both experts and non-professional users (Kwan, 2000). Technically, 3D geovisualization, i.e. the three-dimensional visualization process of 3D geospatially referenced data, intends to display a 3D geospatial model, i.e., a volumetric representation of real objects, to users (Wang, 2015). This is usually performed on digital screens (e.g., desktop computer, laptop, and tablet), but the development of technologies, such as head-mounted displays and CAVE (Cave Automatic Virtual Environment) systems, now makes the stereoscopic 3D experience possible (Milgram & Kishino, 1994).

From a cognitive perspective, there is clear evidence that shifting to the third dimension enhances the geospatial data apprehension as it is more consistent with the human visual system (Jobst & Döllner, 2008; Ware et al., 1993). Indeed, due to a more natural interaction with the spatial content (Carpendale, 2003; Egenhofer & Mark, 1995; Jobst & Germanchis, 2007), 3D enables a more direct cognitive reasoning about geographical and temporal phenomena. For instance, the perception of depth may be enhanced, in particular via psychological (e.g., linear perspective and occlusion) and even physiological cues (e.g., binocular disparity and eye convergence) (Kraak, 1988; Okoshi, 1976). On the other hand, overlapping situations (e.g., property units within a multi-story building, utilities networks located above and under the ground) are better supported in 3D as the third dimension improves the visual understanding of their multi-level properties (Kwan & Lee, 2005; Zlatanova et al., 2004); this is especially the case for cadastre (Figure 1) and systems used for evacuating people from large public and business buildings (Meijers, Zlatanova, & Pfeifer, 2005; Pouliot et al., 2018).

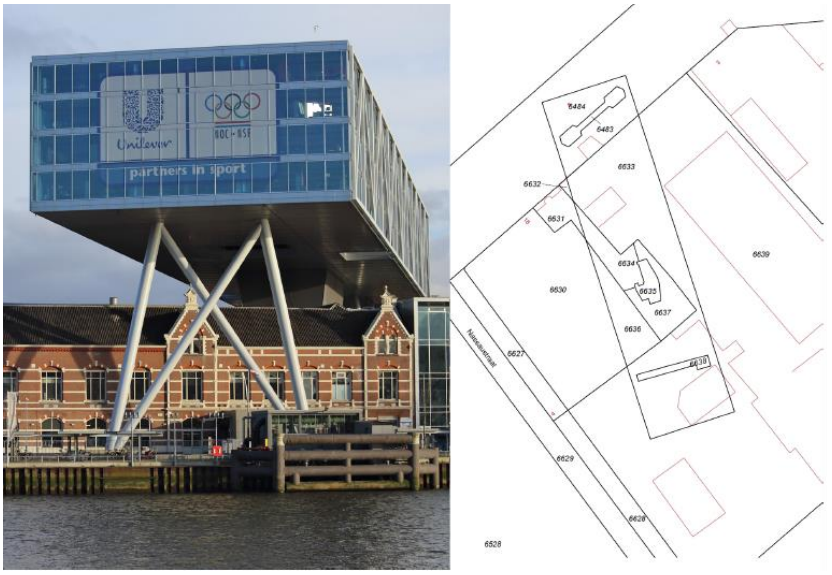


**Figure 1**: Example of overlapping situations in the Netherlands. The 2D cadastral map shows its limits in the graphical representation of the complex estate property, from (Biljecki et al., 2015)

Hence, an ever-increasing number of processes, from education to business applications (e.g., civil engineering, geology, and archeology), and decision-making procedures nowadays incorporate virtual 3D models to support their achievement (Abdul-Rahman & Pilouk, 2008; Bandrova, 2005; Calcagno et al., 2008; Huk, 2006; Jazayeri et al., 2014; Kaden & Kolbe, 2013; Lee, 2012). For instance, virtual 3D city models (i.e., virtual urban environments with a three-dimensional representation of common geometric urban objects (Billen et al., 2014)) have become extremely valuable for cities as they facilitate and support the planning and managing of urban areas, both for contractors (e.g., real estate developers, renovation and construction companies), political decision

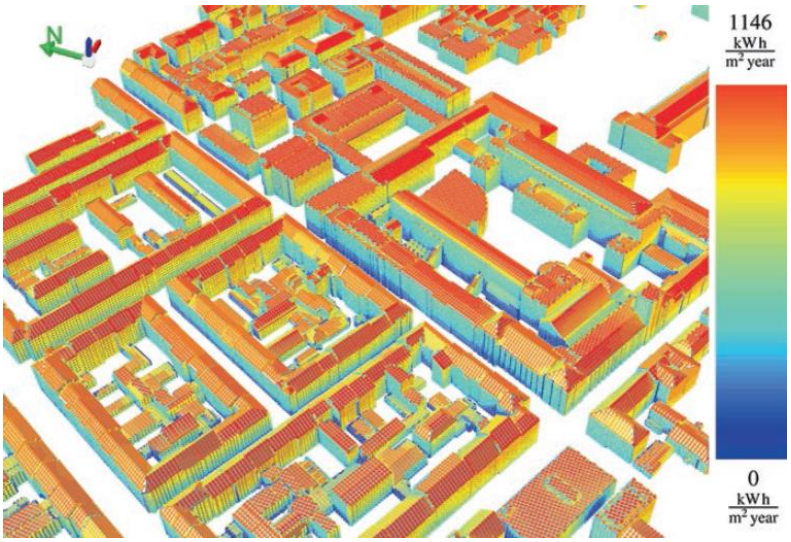


**Figure 2**: Yearly irradiation sum (expressed in kWh/m²/year) for building points at the Technical University of Munich campus and surrounding buildings, from (Willenborg et al., 2018)

makers, and citizens. This is why, to date, an ever-greater number of cities (e.g., Berlin, Montreal, Paris, Zürich, Rotterdam, Helsinki, and Abu Dhabi) manipulate virtual 3D city models for the management, integration, presentation, and distribution of complex urban geoinformation (Figure 2) (Döllner et al., 2006).

## 1.2 Problematics

### 1.2.1 Graphical inconsistency issue

From a theoretical and methodological point of view, 3D geovisualization is partly based on the rules of the graphics, i.e. the graphical section of semiotics. Defined as the field that studies the relationship between the expression plan (i.e., visual stimuli within the graphics) and the content plan (i.e., the semantic world)[1] (Edeline et al., 1992), graphics has already provided a wide range of semiotic connections (also called codes). For that matter, Bertin's visual variables, combined with his interpretation tasks, are a clear example of the contribution of graphics to 2D geovisualization, and whilst a transposition of these semiotic relationships is feasible in 3D, some caution is needed.

Indeed, although numerous scientific studies have shown that the third dimension improves the understanding of geospatial phenomena in many application contexts (Dubel et al, 2014; Herbert & Chen, 2015; Kwan & Lee, 2004; Shojaei et al., 2013; Zhou et al., 2015), they also highlight the higher complexity within the visualization process of such data in three dimensions. Indeed, moving to the third dimension implies additional

[1] The existence of these two plans (expression and content) assume that the conflicts occurring on them are inherently associated in order to produce semiotic relationships, i.e. codes.

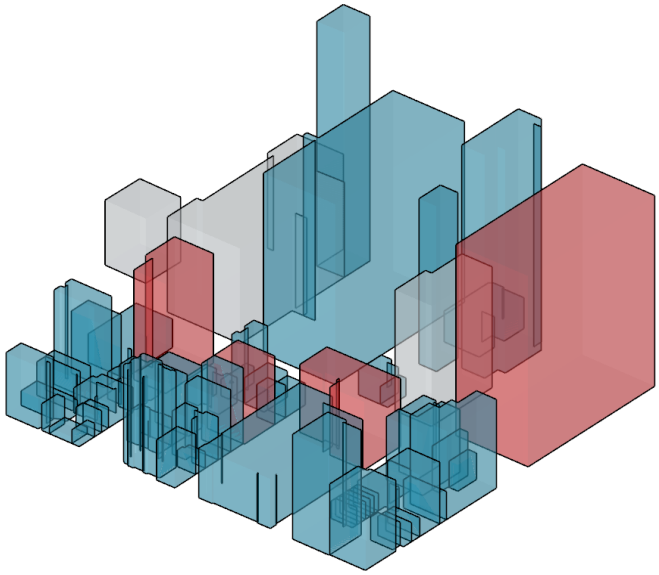

**Figure 3**: The application of transparency (as an occlusion management technique) induces a visual superposition of hue among the geometric objects (building features of a virtual 3D LOD1 city model of New York provided by the Technical University of Munich).

configurations, especially linked to the rendering of the 3D scene (e.g., lighting, shading, and depth of field). For instance, shading is usually applied to volumetric objects as it assists in revealing their shapes (Ware, 2012). Although useful, this rendering setting leads to locally influence the visual objects' perception in lightness and saturation (Jobst et al., 2008), which in the end may distort the underlying semantic information. The same is also true among mapping visualization techniques. For example, transparency (as an occlusion management technique) may induce a superposition of retinal variables (Figure 3).

As a result, in this research project, we hypothesize that the formalization of graphic design principles is possible and corresponds to a valuable approach to prevent the appearance of graphical (and subsequently semantic) inconsistency when mapping and rendering 3D models.

### 1.2.2 3D viewpoint selection issue

Aside the aforesaid issue, shifting to the 3rd dimension also strengthens the role of the viewpoint in the visualization process of geospatial data. Indeed, as the camera is no longer simply oriented in a classic top-down direction (which is usually the case in 2D), the point of view now needs to be configured; and, due to the 3D graphical representation of geometric objects[2], this configuration is complex, in particular because occlusion issues are inevitable. This is especially true for 3D city models where the high density of 3D geometric objects to be displayed and their location (both above and under the ground) necessarily lead to visual clutter and occlusion, which eventually may make the representativeness of objects and their spatial relationships more complex (Andrienko et al., 2008; Elmqvist & Tudoreanu, 2007; Li & Zhu, 2009).

[2] In a 3D visualization context, geometric objects are defined as any objects located in a 3D universe (x,y,z) and built from one of the geometric primitives (point, curve, surface, and volume) defined within the spatial schema ISO 19107:2003 (Pouliot, Badard, Desgagné, Bédard, & Thomas, 2008).

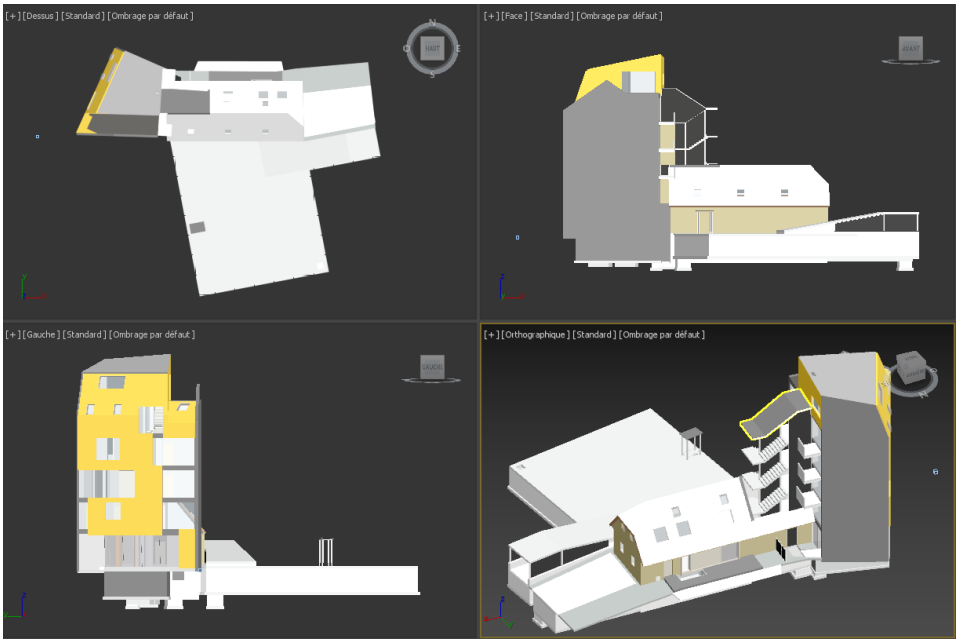


**Figure 4**: Multiple viewports of a 3D building (up, front, left and at 45°) provided by Autodesk® and visualized through Autodesk® 3ds Max

For that purpose, a taxonomy of 3D occlusion management techniques has been carried out in (Elmqvist & Tsigas, 2007). More than twenty methods have been analyzed and classified into five archetypical design patterns: multiple viewports (Figure 4), projection distorter (Figure 5), interactive exploder, tour planner, virtual X-Ray (Figure 6). Technically, this categorization has been established on the basis of six properties: the visual task to be primarily performed, the maximum handled objects' interaction, the strength of disambiguation cues, the layout of the visual substrate, the user's interaction, and the degree of objects' invariance (in terms of location, geometry, and appearance).

**Figure 5**: Projection distorter: multi-perspective view of a virtual 3D city model, from (Lorenz et al., 2008)

From a practical point of view, this taxonomy is helpful in selecting the most appropriate occlusion technique(s) as a function of the 3D environment setting and the visual task(s) to be executed. For instance, using transparency (classified into the virtual X-Ray category) can significantly improve the visibility of objects enclosed or contained within other objects (e.g., rooms inside a 3D building, pipes and electricity networks under the ground). However, it also reduces the perception of depth and makes the spatial relations evaluation more complex. As a result, the choice of the most suitable occlusion technique(s) is a function of the user's requirements, and is thus defined on a case-by-case basis.

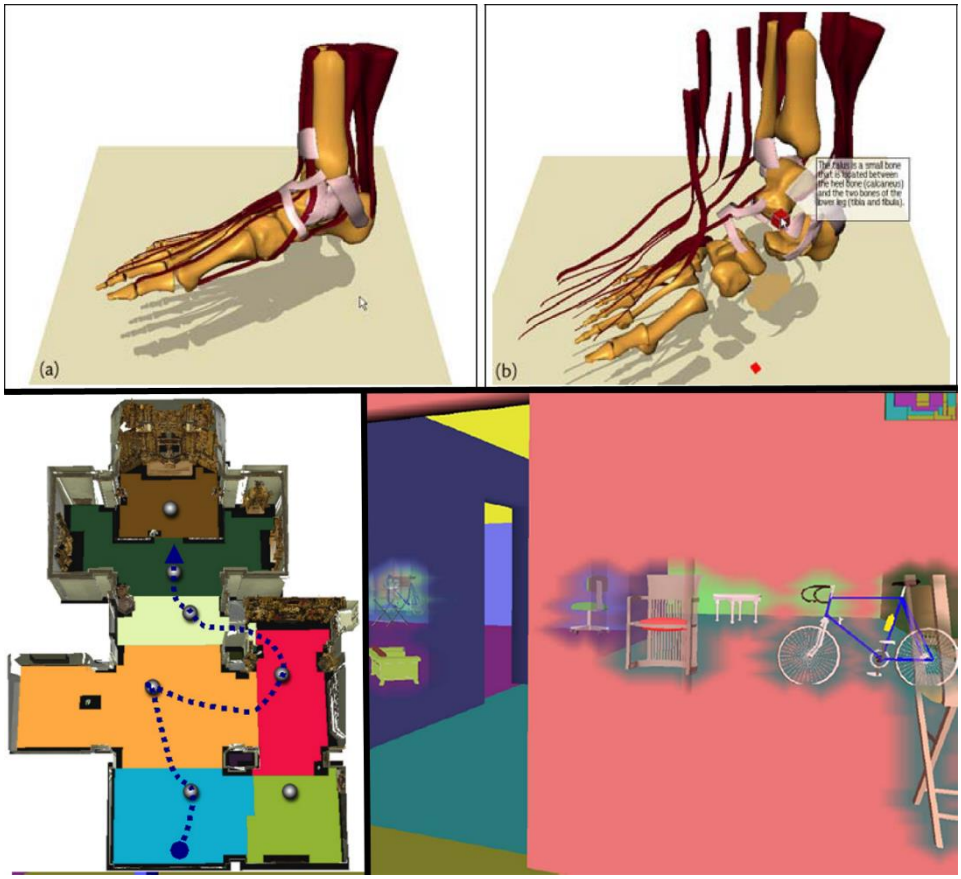


**Figure 6**: Interactive exploder of a 3D foot model on the upper image, from (Sonnet et al., 2004); tour planner within a 3D church model on the lower left image, from (Andujar et al., 2004); and virtual X-Ray (dynamic transparency) on the lower right image, from (Elmqvist et al., 2007)

Nevertheless, there is one aspect that is common to all occlusion situations and that no existing technique currently solves: the point of view selection inside the 3D scene. Independently of the occlusion technique(s) applied

to the 3D model, an unsuitable 3D viewpoint[3] can drastically reduce or even totally annihilate the visibility of given geometric objects within the 3D scene. For instance, the application of transparency, the use of multiple visualization windows, and/or a multi-perspective view of the 3D scene can significantly decrease the quantity of hidden objects (Lorenz et al., 2008; Röhlig & Schumann, 2016; Wang et al., 2017), although this affirmation is conditioned by the ultimate 3D point(s) of view from which users visualize the objects. This is why managing the virtual camera inside the 3D environment is prominent (Rautenbach et al., 2015); and finding the most appropriate point of view out for a set of 3D geometric objects is usually a high time-consuming task, which especially depends on the 3D model complexity and is independently of the user's expertise.

## 1.3 Research questions

On the basis of above, this thesis supports the idea that the viewpoint is a fundamental parameter in 3D geovisualization, making the use of visualization techniques relevant for the development of a semiotics linked to 3D geospatial data. To emphasize this proposal, 3D

[3] A 3D viewpoint is defined as the cross-product of four components: the camera position, orientation, the focal length, and the vision time. The two first parameters are 3D vectors which respectively represent a 3D camera location and a 3D viewing direction into the world coordinate system. The focal length is the distance between the projection center and projection plane, which sets the field of view. Eventually, in case of a computer animation combining multiple points of view, a vision time can be given to each 3D viewpoint.

geovisualization must first and foremost be formalized so as to encompass the 3D point of view into a global semantic driven visualization process. Furthermore, as the field remains unstructured, especially from a semiotic point of view (i.e., incorporating both an expression and content plan), this initial stage will also tackle the graphical inconsistency issue and we do believe that it might improve the 3D visualization process of geospatial data.

In this research, the attention is focused on the visualization of virtual 3D buildings as these volumetric features are both part of 3D city models (employed in more than 100 application domains (Biljecki et al., 2015)) and constitute the backbone of the building information modeling (BIM), of which the objective is to assist the construction, management, and maintenance of facilities (Abbasnejad & Moud, 2013; Azhar, 2011; Czmoch & Pękala, 2014). This is why we raise the following global research question:

**Does it exist an optimal 3D viewpoint for visualizing a set of geometric objects within 3D building models?**

In this thesis, we claim that there exists at least one optimal 3D viewpoint, and this point of view is a function of the objects' view area inside the viewport, i.e. the visualization window inside a digital display.

Additionally, three specific questions are raised in order to incorporate the semantic world into the global context of this research. Attention is focused on a given interpretation task: the selectivity purpose, i.e. the

visual capacity to extract a set of 3D objects belonging to the same semantic category. Furthermore, the default software points of view are used in the evaluation of our proposal. Hence, the specific research questions are:

1. Is a 3D viewpoint based on the maximization of 3D geometric objects' view area **more accurate** for the selectivity task of a set of objects within a virtual 3D building model compared to the default combined software points of view?

2. Does a 3D viewpoint based on the maximization of 3D geometric objects' view area **enhance the user's certainty** when visually selecting a set of objects within a virtual 3D building model compared to the default combined software points of view?

3. Does a 3D viewpoint based on the maximization of 3D geometric objects' view area make the selectivity task of a set of objects **faster** within a virtual 3D building model compared to a given default software point of view?

## 1.4 Research objectives

The global aim of this thesis is to **enhance the 3D visualization process of virtual building models in achieving given user-centered visual purposes**. The achievement of this goal is carried out through the definition of three specific objectives:

1. Formalizing the 3D visualization process of geospatial data in order to produce more consistent (i.e., unambiguous) graphic (and ultimately semantic) representations;

2. Proposing a theoretical and operational solution to the 3D viewpoint selection issue in order to enhance the visualization of the underlying semantic information;

3. Evaluating the proposal for a given visual task related to the selectivity purpose.

## 1.5 Research methodology

In order to address the research objectives, a three levels approach is elaborated and is in accordance with the scientific hypothetico-deductive method.

First, an extensive **literature review** of academic papers and books is carried out in order to provide a clear understanding of the 3D geovisualization field along with previous research outcomes. It lays the foundation of **key concepts** related to the 3D visualization process of geospatial data and defines the **connections** among them. As a result, this former stage aims to establish the theoretical background of this research and to give structure to 3D geovisualization (the first research objective).

Then, we address the ubiquitous 3D viewpoint selection issue via **a theoretical and operational solution that automates and optimizes its**

**identification** within a broad semantic driven visualization process. This second phase is carried out to achieve the second goal of this research.

Eventually, a **validation stage** is performed in order to evaluate the previous solution in achieving a given visual selective task: visual counting. For this purpose, a specific case study is designed and aims to support the proposal through an empirical study carried out with specialists. As such, this stage addresses the third objective of this thesis.

## 1.6 Contributions of this work

The main contributions of this research can be summarized as follows:

1. The first attempt to formalize the 3D geovisualization process through the development of a knowledge network from which researchers can take advantage for the definition of suitable graphic design guidelines;
2. The development of a geocomputational method that automates and optimizes the 3D viewpoint selection as a way of maximizing the visualization of the underlying semantic information;
3. The development of an experimental framework that evaluates graphic design guidelines, which is the prerequisite to support the development of user-centered solutions;
4. The first client-server application that assists users in the 3D visualization process of geospatial data, both in the graphical representation and the 3D viewpoint selection.

## 1.7 Thesis organization

Chapter 2, **3D Geovisualization**, gives an overview of the literature in the 3D geovisualization field, extracts its key components from the graphics and computer graphics fields, and formalizes its process both in the expression and content plans (research objective 1). This chapter is based on *A Formalized 3D Geovisualization Illustrated to Selectivity Purpose of Virtual 3D City Model*, an article published within the "ISPRS International Journal of Geo-Information" in May 2018.

Chapter 3, **3D Viewpoint Management**, addresses the 3D viewpoint selection issue through an automatic camera management within the 3D scene (research objective 2). A geocomputational method is designed and aims to maximize the view area of selected 3D geometric objects in the user's visualization window. This chapter is based on *3D Viewpoint Management and Navigation in Urban Planning: Application to the Exploratory Phase*, an article published within the "Remote Sensing" journal in January 2019.

Chapter 4, **Experimental Study**, deals with the evaluation of our proposal within building information modeling. As a result, this chapter presents the design, implementation and statistical analysis of an empirical test related to visual counting of assets within a building model (research objective 3). This chapter is based on *Identification of the Best 3D Viewpoint within the BIM Model: Application to Visual Tasks Related to Facility Management*, an article published within the "Buildings" journal in July 2019.

Chapter 5, **Back to this research**, provides a reflexive feedback on the previous chapters and addresses a set of future research opportunities into a broader context of 3D geospatial data acquisition and visualization.

Chapter 6, **Conclusions and Recommendations**, goes back to research questions and objectives. It also highlights the outcomes of this research and how it contributes to knowledge. Ultimately, this chapter ends with research perspectives.

The thesis organization (as described above) is schematically presented in Figure 7.

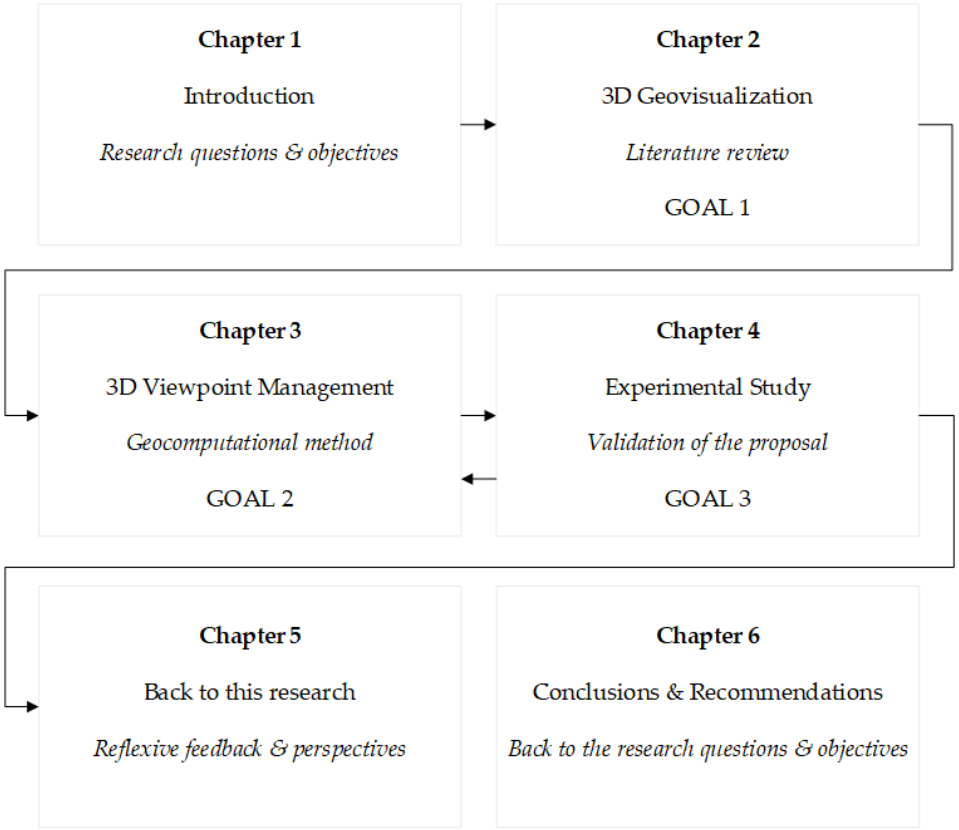


**Figure 7**: Thesis organization

CHAPTER 2

# 3D geovisualization formalization

## 2.1 Preface

This chapter is based on *A Formalized 3D Geovisualization Illustrated to Selectivity Purpose of Virtual 3D City Model*, an article published within the "ISPRS International Journal of Geo-Information" in May 2018. It reviews the literature related to the 3D geovisualization field and establishes the theoretical framework of this research. In this way, it proposes the first attempt to formalize the 3D visualization process of geospatial data from a semiotics point of view. Developed as a knowledge network that encompasses the key 3D geovisualization components, it aims to tackle the graphical inconsistency issue when designing 3D geospatial models. Furthermore, this chapter formalizes the key role of 3D viewpoint as a fundamental parameter that determines the visibility of geometric objects to which visualization techniques have been applied. However, to date, its management is manually fixed by the designer, who tries to reduce at best the occlusion issue on a set of selected features. Hence, the automation of the 3D viewpoint selection within the 3D scene is still a challenge to be solved and is tackled in Chapter 3.

## 2.2 Abstract

Virtual 3D city models act as valuable central information hubs supporting many aspects of cities, from management to planning and simulation. However, we noted that 3D city models are still underexploited and believe that this is partly due to inefficient visual communication channels across 3D model producers and the end-user.

With the development of a formalized 3D geovisualization approach, this chapter aims to support and make the visual identification and recognition of specific objects in the 3D models more efficient and useful. The foundation of the proposed solution is a knowledge network of the visualization of 3D geospatial data that gathers and links mapping and rendering techniques. To formalize this knowledge base and make it usable as a decision-making system for the selection of styles, second-order logic is used. It provides a first set of efficient graphic design guidelines, avoiding the creation of graphical conflicts and thus improving visual communication. An interactive tool is implemented and lays the foundation for a suitable solution for assisting the visualization process of 3D geospatial models within CAD and GIS-oriented software. Ultimately, we propose an extension to OGC Symbology Encoding in order to provide suitable graphic design guidelines to web mapping services.

**Keywords:** 3D geospatial data; 3D geovisualization; Styled Layer Descriptor; Symbology; Encoding; virtual 3D city model; 3D semiotics; graphics; computer graphics; mapping; rendering; graphical conflict

## 2.3 Introduction

In the administration of cities, virtual 3D city models are extremely valuable, as they constitute 3D geovirtual environments serving many application fields: e.g., urban planning, facility management, mobile telecommunication, environmental simulation, navigation, and disaster management (Altmaier & Kolbe, 2003; Döllner et al., 2006; Sinning-Meister

et al., 1996). For that matter, the development of standards, such as CityGML (Open Geospatial Consortium, 2006), played a key role in extending virtual 3D city models into relevant central information hubs to which many applications can attach their domain information (Kolbe, 2009). However, it does not necessarily mean that people can directly and efficiently communicate with each other because they have a common information model at their disposal.

To achieve this, a communication channel must be designed and set up across stakeholders. As sight is one of the key senses for information communication (Ward et al., 2010), the link could be carried out by an appropriate 3D geospatial data visualization as a means of effectively exchanging contextual knowledge (Batty et al., 2000; Glander & Döllner, 2009). Nevertheless, there is still a crucial issue to solve: how to efficiently show 3D geospatial data in order to produce relevant visual communication? There are plenty of 3D visualization techniques (e.g., transparency, hue and shading), but they are not all compatible with each other, leading to potential graphical conflicts that may cause misunderstanding across stakeholders. Furthermore, their application is often specific to the type of data to be visualized, the task to be performed, and the context in which the task is to be executed (Métral et al., 2014). As a result, selecting appropriate 3D visualization techniques is quite complex, especially for non-experts who often deal with new combinations of criteria (data, task, and/or context).

In this research project, we thus hypothesize that the formalization of graphic design principles is possible and corresponds to a valuable approach to support users in the visualization process of 3D geospatial data. This is why we propose to formalize (from a semiotics point of view) 3D geovisualization as a knowledge network by extracting its key components (from graphics and computer graphics fields) and establishing connections between camera settings, visualization techniques (expression plan), and targeted purposes (content plan). The goal is to build a knowledge network by gathering and connecting an ever-increasing number of visualization techniques from different application fields. This knowledge network could even automatically and intelligently be structured through machine learning (Brasebin et al., 2015): the more a visualization technique is used, the more it fits specific requirements, and subsequently the more it is helpful.

Following this, interactive design support tools could then be implemented to provide designers with feedback about the suitability of their representation choices. This seems necessary, since current CAD and GIS-oriented software does not warn against graphical conflicts that may appear during the visualization pipeline. The same applies to 3D geoinformation diffusion through the OGC web 3D services. While Neubauer and Zipf (Neubauer & Zipf, 2007) have already provided an extension to Symbology Encoding for the visualization of 3D scenes, this process remains unstructured. Additional elements should be incorporated to provide suitable graphic design guidelines.

This chapter is structured as follows. Sections 2.4 and 2.5 are dedicated to the 3D geovisualization field and aims to provide theoretical insights. They also deal with the visualization process of virtual 3D city models and the graphical conflicts issue. Section 2.6 presents a second-order logic formalism applied to the 3D geovisualization process and illustrates its role within the visual selectivity purpose for virtual 3D city models. In Section 2.7, the formalism is implemented in three different kinds of applications. Ultimately, we discuss the results, conclude, and address some research perspectives.

## 2.4 3D Geovisualization

### 2.4.1 Definition

Based on (MacEachren & Kraak, 2001) definition, 3D geovisualization is defined as the field that provides theory, methods, and tools for the visual exploration, analysis, confirmation, synthesis, and communication of spatial data. It incorporates approaches from a wide range of fields, such as scientific computing, cartography, image analysis, information visualization, exploratory data analysis, and geographic information systems.

The development of 3D geovisualization relies heavily on computer graphics, the technologies to design and manipulate digital images of 3D environment (Bleisch, 2012). Through this field, it is also possible to incorporate interaction (the ability for the user to move or to apply a

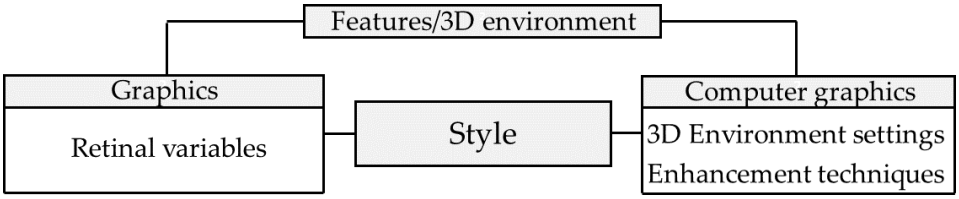


**Figure 8**: Key components of 3D geovisualization

motion to objects) and to improve the immersion experience) with the use of head-mounted display or CAVE (Cave Automatic Virtual Environment) (Heim, 2000; Kraak, 2003; MacEachren et al., 1999). Besides, many application fields, such as education, geoscience, and human activity-travel patterns research showed their great usefulness in the visualization of 3D geospatial data (Billen et al., 2008; Kwan, 2000; Philips et al., 2015). Figure 8 is a simplified configuration of key components involved in 3D geovisualization and defines style as the application of graphic elements from graphics and computer graphics fields to features and the 3D environment. The next section explains these concepts in detail.

### 2.4.2 Graphics

To fulfil geospatial visualization challenges, theoretical and methodological approaches from graphics are used in 3D geovisualization (Andrienko et al., 2008; MacEachren & Kraak, 2001). Within the framework of graphics representation, components are visual (or retinal) variables sensed in accordance with group levels,

**Table 1**: State-of-the-art of static retinal variables defined over the last fifty years

| Visual Variable | Author (Date) | Example |
|---|---|---|
| Arrangement | Morisson (1974) | 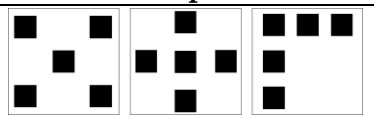 |
| Crispness | MacEachren (1995) |  |
| Grain | Bertin (1967) | 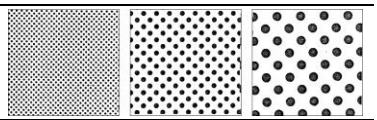 |
| Hue | Bertin (1967) |  |
| Lightness/Value | Bertin (1967) |  |
| Material | Carpendale (2003) | 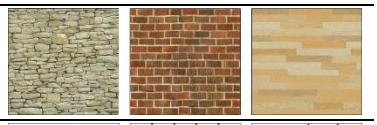 |
| Orientation | Bertin (1967) | 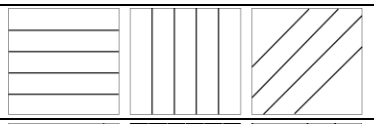 |
| Pattern | Carpendale (2003) | 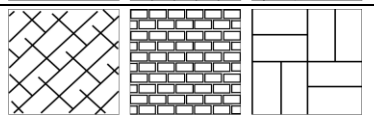 |
| Perspective height | Slocum et al. (2010) | 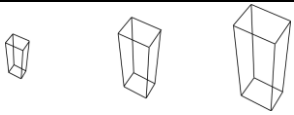 |
| Position | Bertin (1967) | 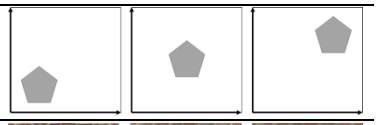 |
| Resolution | MacEachren (1995) | 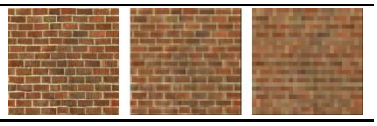 |

| | | |
|---|---|---|
| Saturation | Morisson (1974) |  |
| Shape | Bertin (1967) | 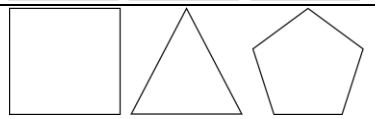 |
| Size | Bertin (1967) | 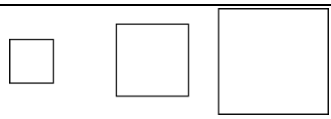 |
| Sketchiness | Boukhelifa et al. (2012) | 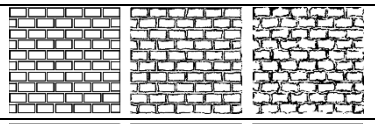 |
| Spacing | Slocum et al. (2010) |  |
| Transparency | MacEachren (1995) | 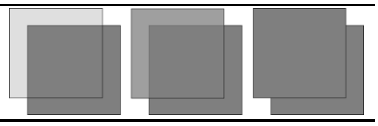 |

equivalent to the four scales of measurement: nominal, ordinal, interval, and ratio (Stevens, 1946). Over the last fifty years, many authors, including (Bertin, 1967), (Morrison, 1974), (MacEachren, 1995), (Carpendale, 2003), (Slocum t al., 2010), and (Boukhelifa, et al., 2012), have supplied a wide range of static retinal variables (summarized in Table 1). Initially developed on 2D geometries (points, curves, surfaces), these static retinal variables can be easily extended to volumes and subsequently to the third dimension.

When using visual variables, users must keep in mind the suitability of these variables to perform specific visual tasks (one variable may perform

**Table 2**: Interpretation tasks of static retinal variables (Bertin, 1967)

| **Interpretation Task** | **Signification** | **Question** |
|---|---|---|
| ***Selectivity*** | The capacity to extract categories | Does the retinal variable variation identify categories? |
| ***Associativity*** | The capacity to regroup similarities | Does the retinal variable variation group similarities? |
| ***Order perception*** | The capacity to compare several orders | Does the retinal variable variation identify a change in order? |
| ***Quantitative perception*** | The capacity to quantify a difference | Does the retinal variable variation quantify a difference? |

well while another is less suitable). The suitability for graphics is in the interpretation tasks they are able to carry out. In Table 2, we present the perceptual properties classes as defined by (Bertin, 1967). Note that additional definitions exist in the literature, as do alternative criteria to measure the suitability of retinal variables (MacEachren, 1995).

Retinal variables have different degrees of consistency to achieve these visual tasks. This is why research has been conducted in 3D graphics. For instance, the following studies (Pouliot et al., 2014; Pouliot et al., 2014; Pouliot et al., 2013; Wang et al., 2012) show that colour is one of the most relevant variables for selectivity tasks in 3D cadastre visualization. This is

also the conclusion of (Rautenbach et al., 2015), who identify (in the specific context of urban planning) hue (and texture) as the most adapted visual variables for selectivity. Ultimately, retinal variables are also suitable for managing specific 3D geovisualization challenges: e.g., transparency for occlusion issues (Avery et al., 2009; Coors, 2003; Elmqvist et al., 2007; Elmqvist & Tsigas, 2007).

### 2.4.3 3D Environment Settings

While 3D geovisualization is partly based on graphics, it also incorporates additional settings from computer graphics that greatly influence the final display. (Haeberling, 2002) distinguishes the following rendering parameters:

- Projection: parallel or perspective;
- Camera: position, orientation, and focal length;
- Lighting: direct, ambient, or artificial light;
- Shading;
- Shadow;
- Atmospheric effect.

The previous list can be extended with viewport variations that change the projection (parallel or perspective) progressively or digressively in order to efficiently reduce occlusion issues in 3D geospatial environments. (Lorenz et al., 2008) show that it does not modify the dynamic aspect of virtual 3D city applications and (Jobst & Döllner, 2008) even conclude that it allows a better perception of 3D spatial relations.

### 2.4.4 Enhancement techniques

Besides static visual variables and 3D environment settings, additional techniques have been developed in order to improve the visualization of 3D geospatial environments. (Bazargan & Falquet, 2009) show the suitability of seven enhancement techniques (illustrative shadows, virtual PDA, croquet 3D windows, croquet 3D interactor, 2D medial layer, sidebar, and 3D labels) for the depiction of non-geometric information, while (Trapp et al., 2011) classify object-highlighting techniques useful for the visualization of user's selection, query results, and navigation. The classification is carried out based on the type of rendering: style-variance techniques (focus-based style or context-based style), outlining techniques, and glyph-based techniques. They conclude that context-based style variance and outline techniques seem to be the most relevant techniques, since they highlight (to some extent) hidden objects in the scene.

## 2.5 Virtual 3D City Models

### 2.5.1 Definition and Benefits

Virtual 3D city models are defined as three-dimensional digital representations of urban environments (Hajji & Billen, 2016; Stadler & Kolbe, 2007). Their development and usage are linked to the drawbacks of photorealistic displays. Unlike 3D models, photorealistic depictions present (Döllner & Buchholz, 2005b):

- A higher cost for data acquisition due to the required higher quality of geometries and facade textures;
- A more difficult integration of thematic information owing to the visual predominance of textured facades, roofs, and road systems in the image space;
- A more complex visualization of multiple information layers on account of photorealistic details;
- A more complex display on lower-specification devices (e.g., mobile phones, tablets) that generally require a simplification and aggregation process to be efficiently visualized (Ellul & Altenbuchner, 2014).

Virtual 3D city models mainly focus on common aboveground and underground urban objects and structures such as buildings (Figure 9), transportation, vegetation, and public utilities, of which they are able to store geometric, topologic, and semantic information with the development of common information models such as IFC, indoorGML and CityGML (Kim et al., 2014; Liu et al., 2017; Open Geospatial Consortium, 2006, 2018). For example, CityGML is organized in thematic classes and incorporates the "level of details" concept, both related to geometry, appearance, and semantics (Biljecki et al., 2016; Biljecki et al., 2014; Löwner et al., 2013).

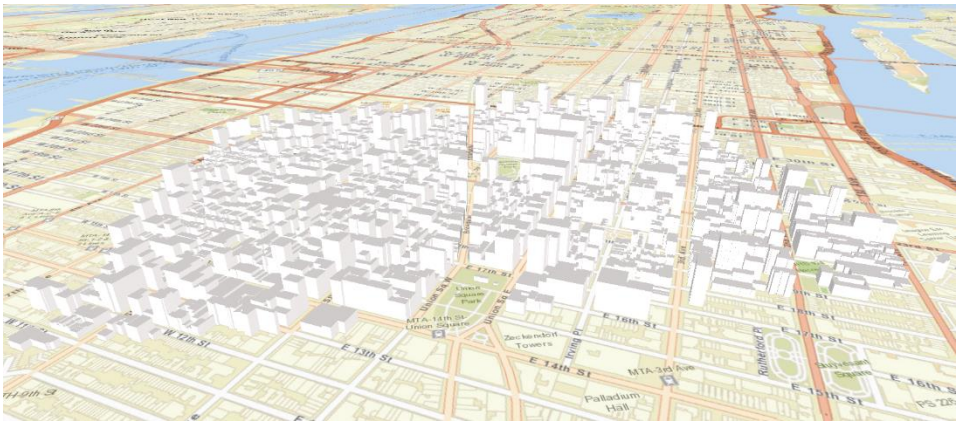


**Figure 9**: Part of a virtual 3D LOD1 city model of New York (building features) provided by the Technical University of Munich and visualized with ArcGlobe

This concept is used to describe a series of different representations of real-world objects, to meet the requirements of a wide range of application fields and to enhance the performance and quality of the visualization process (Biljecki, 2017; Gröger & Plümer, 2012; Luebke et al., 2012). However, within a typical 3D visualization process, objects' appearance and geometry are one aspect; another is the graphical representation of their semantic information, and this is developed in the next section.

### 2.5.2 Semantic Driven Visualization

The development of CityGML as a standard for the representation and exchange of semantic 3D city models extended their initial purpose of visualization to thematic queries, analytical tasks, and spatial data mining (Zhu et al., 2009). As a result, a semantic driven visualization emerged, aiming to relay semantic information, and ultimately to improve the

global usability of virtual 3D city models (Benner et al., 2005). However, the magnitude and complexity of virtual 3D city models raise the question of how to expressively and efficiently produce such a visualization (Jobst et al., 2010). In a paper published in 2015, (Semmo et al., 2015) present a 3D semiotic model incorporating the studies of several researchers. They distinguish five processing stages in the visualization process:

1. The modelling of real-world phenomena, which can be carried out by different kinds of sensors: passive (photogrammetry), active (ground laser scanner, airborne LIDAR), or hybrid (imagery and laser range sensors, hybrid DSM, aerial image and 2D GIS) (Hu, You, & Neumann, 2003).
2. The filtering stage to produce a primary landscape model where only the required information for further processing is selected.
3. The mapping of the primary model to a cartographic model via symbolisation (i.e., the application of static retinal variables (e.g., hue, size, transparency) to selected objects).
4. The rendering of the cartographic model; that is, the definition of 3D environment settings (e.g., projection, camera attributes, lighting, and atmospheric effects) and potentially the application of enhancement techniques.
5. The perceptional aspects of the 3D graphic representation, such as psychological and physiological cues. When used carefully, they facilitate the communication process (Buchroithner et al., 2000).

Note that the mapping and rendering stages include the design aspects of (Jobst et al., 2008) and (Häberling et al., 2008). In addition to the filtering stage, they constitute the visualization process defined by (Ware, 2012), that can also incorporate the generalisation processes (Foerster et al., 2007).

The main weakness of this 3D semiotic model concerns the user's involvement across the visualization process (stages 2 to 4) (Semmo et al., 2015). Indeed, it is common that the visualization of 3D geospatial data collection requires the application of more than one visualization technique (Ogao & Kraak, 2002). In this case, the selected visualization techniques must at least be able to convey the desired information, and mainly not negatively interfere with each other (Khan & Khan, 2011; Métral et al., 2012). Indeed, graphical conflicts may occur in the visualization process, especially between the mapping and rendering stages. For instance, shadow may hide 3D objects in the 3D environment, making the application of any visual variables useless. In a paper published in 2008, (Jobst et al., 2008) present a first set of graphical conflicts. While this study introduces graphical conflicts, it has some limitations. First, it only considers incompatibilities among visualization techniques, while they also exist among their targeted purposes (e.g., their perceptual properties). It also does not present a methodological framework that takes additional visualization techniques into account and does not define further connections among visualization techniques and their targeted purposes. Ultimately, the study does not provide a graphic design support tool for assisting the visualization process.

## 2.6 Knowledge Network Configuration

### 2.6.1 Introduction

To address previous limits, we propose a formalization of the 3D geovisualization. We do not pretend to solve all graphical conflicts, but we do believe that with a deep understanding of how 3D geovisualization works, we can at best avoid them and subsequently produce a more efficient visualization of 3D geospatial data. This section aims to present and extend the initial formalism developed by Neuville et al. (Neuville et al., 2017). The insertion of camera settings in the mathematical framework as well as their connections to visualization techniques are new, and enhance the formalization process.

3D geovisualization is formalized with second-order logic, from which we use the mathematical language for defining and connecting its components. Working at this level of abstraction allows a deep understanding of the process and an integration at numerous scales, both for domain experts who define their own graphic design guidelines and users who apply them. First, this section presents the mathematical framework. As such, key components of 3D geovisualization are stored in collections of entities. Then, a set of functions define their role(s) in the 3D geovisualization process and express their connections.

**Table 3**: Sets and operators definition

| Notation | Signification |
|---|---|
| $a \in A$ | a *is an element of* A |
| $\lvert A \rvert$ | Number of elements in A |
| $A \times B$ | A *cross-product* $B = \{(a, b)\ a \in A, b \in B\}$ |
| $\mathbb{R}$ | Set of reals |
| $\mathbb{N}$ | Set of integers |
| $\mathbb{R}^+$ | Set of positive reals $([0; +\infty[)$ |
| $\mathbb{R}^3$ | $\mathbb{R} \times \mathbb{R} \times \mathbb{R}$ |
| $\cup$ | Union of two sets |
| $\cap$ | Intersection of two sets |
| $\vee$ | OR boolean operator |
| $\wedge$ | AND boolean operator |
| $\rightarrow$ | IMPLICATION operator |
| $\neg$ | NOT operator |

Functions are classified into three categories in order to distinguish functions related to camera settings (geometry-related), camera settings and visualization techniques (geometry and attribute-related), and visualization techniques (attribute-related). In order to clarify the process, sets and operators are presented in Table 3. Ultimately, this section illustrates the formalism on a subset of static retinal variables and their targeted purposes.

## 2.6.2 Mathematical Framework

### *2.6.2.1 Collections of Entities*

Collection A (Equation (1)) gathers camera settings and corresponds to the cross-product of camera position ($A_1$), camera orientation ($A_2$), focal length ($A_3$), and vision time ($A_4$). It incorporates a subset of variables of vision defined by Jobst et al. (Jobst et al., 2008), to which we add vision time (i.e., time spent visualising a given viewpoint). The value is infinity for a static viewpoint, while it is a positive real in a motion with multiple viewpoints. Mathematically:

$$A = A_1 \times A_2 \times A_3 \times A_4, \quad (1)$$

with

$$A_1 = \mathbb{R}^3, \quad (2)$$

$$A_2 = \mathbb{R}^3, \quad (3)$$

$$A_3 = \mathbb{R}^+ \cup \{\infty\}, \quad (4)$$

$$A_4 = \mathbb{R}^+ \cup \{\infty\}. \quad (5)$$

Then, collection B (Equation (6)) gathers visualization techniques. It includes static retinal variables from Table 1 as well as 3D environment settings and enhancement techniques from Sections 2.4.3 and 2.4.4:

$$B = \{[\text{Static retinal variables}], [\text{3D environment settings}], [\text{Enhancement techniques}]\}. \quad (6)$$

Thirdly, collection C (Equation (7)) defines the targeted purposes arising from the application of collections A and B. It incorporates the fulfilment of interpretation tasks (Table 2), solutions to 3D geovisualization challenges (Sections 2.4.3 and 2.4.4), and globally all perceptions conveyed by A and B (e.g., scale, security, and pollution).

$$C = \{[\text{Interpretation tasks}], [\text{3D geovisualization challenges}], [\text{Perceptions}]\}. \quad (7)$$

Ultimately, collection O (Equation (8)) corresponds to 3D geometric objects (e.g., buildings, transportation, and vegetation) inside the 3D geospatial environment.

$$O = \{[\text{3D geometric objects}]\}. \quad (8)$$

*2.6.2.2 Geometry-Related Functions*

Function F (Equation (9)) means that A determines the visibility of 3D geometric objects. Mathematically, it goes from the set of A to (→) the set of O parts (P(O)) and from an "a" element of A is associated (↦) the part of O that includes the "o", such as "a" implies "o".

$$F{:}A \longrightarrow P(O){:}a \mapsto \{o \in O{:}a \rightarrow o\} \quad (9)$$

Then, the completeness of a specific entity "a" (camera position, orientation, focal length, and vision time) is defined as the number of visible 3D geometric objects (Equation (10)):

$$|F(a)|. \quad (10)$$

Due to the magnitude and complexity of virtual 3D city models, the completeness of "a" can be less than the total number of 3D geometric objects returned by the query. To solve this issue, several solutions are feasible, such as the application of static visual variables (e.g., transparency), enhancement techniques (e.g., outlining technique), and viewport variations. However, if these options are not feasible, the

completeness can be improved with a motion which seeks to display the missing information. Mathematically, the motion is defined as the addition of two (or more) entities of A and its completeness (Equation (11)) as the sum of each entity completeness, from which we subtract the completeness of the intersections (two by two).

$$|F(a_1)| + |F(a_2)| - |F(a_1) \cap F(a_2)| > |F(a_1)|, |F(a_2)|. \quad (11)$$

Function G (Equation (12)) aims to connect collection A to collection C, meaning that an entity "a" is associated to a part of C (targeted purposes). For instance, a low-angle shot may imply a *scale* perception.

$$G{:}A \longrightarrow P(C){:}a \mapsto \{c \in C{:}a \rightarrow c\}. \quad (12)$$

### 2.6.2.3 Geometry- and Attribute-Related Function

Function H (Equation (13)) aims to link collection B to collection C. However, this connection requires the involvement of collection A, since the targeted purpose(s) of any entity "b" implies at least the visibility of this entity. Function H means that a combination of an entity "a" and an entity "$b_1$" or a set of entities "$b_n$" is associated to a part of C. For instance, hue is selective and associative; transparency solves occlusion issues; a *dilapidated city* perception may require the combination of several visualization techniques, such as the simultaneous application of haze (3D environment setting) and damaged facade materials (static retinal variable).

$$H_n{:}\ A \times B^n \longrightarrow P(C){:}(a, b_1, \ldots, b_n) \mapsto \{c \in C{:}(a, b_1, \ldots, b_n) \rightarrow c\}, \quad (13)$$

with

$$n \in \mathbb{N}.$$

#### *2.6.2.4 Attribute-Related Functions*

The following functions aim to determine the interactions occurring between entities of collections B and C.

Function I (Equation (14)) means that the application of an entity "$b_1$" induces the use or the indirect application of an additional entity "$b_2$". For example, the production of a shadow implies the use of a directional light; the application of perspective height as a static retinal variable indirectly implies the application of size. This function defines a **consequence** connection among visualization techniques.

$$I{:}B \longrightarrow P(B){:}b_1 \mapsto \{\, b_2 \in B{:}b_1 \rightarrow b_2\}. \tag{14}$$

Function J (Equation (15)) means that an entity "$b_1$" is **compatible** with another entity "$b_2$".

$$J{:}B \longrightarrow P(B){:}b_1 \mapsto \{\, b_2 \in B{:}b_1 \wedge b_2\}. \tag{15}$$

Function K (Equation (16)) means that an entity "$b_1$" is **incompatible** with another entity "$b_2$".For example, size is incompatible with perspective projection since the latter modifies the perception of size as a function of object position in the 3D geospatial environment.

$$K{:}B \longrightarrow P(B){:}b_1 \mapsto \{\, b_2 \in B{:}\neg\, (b_1 \wedge b_2)\}. \tag{16}$$

Function L (Equation (17)) means that "$c_1$" (the targeted purpose of an entity "$b_1$") is **compatible** with "$c_2$" (the targeted purpose of an entity

"$b_2$"). For example, the simultaneous application of size and hue on a single 3D object combines the specific targeted purpose of these static visual variables (the *order* interpretation task with size and the *associative* interpretation task with hue).

$$L_{b1,b2}{:}H_1(b_1) \longrightarrow P(H_1(b_2)){:}c_1 \mapsto \{\, c_2 \in H_1(b_2){:}c_1 \vee c_2\}. \quad (17)$$

Function M (Equation (18)) means that "$c_1$" (the targeted purpose of an entity "$b_1$") is **incompatible** with "$c_2$" (the targeted purpose of an entity "$b_2$"). For example, the simultaneous application of pattern and grain on a single 3D object does not maintain their specific *selectivity* interpretation task, since grain interferes in the pattern perception.

$$M_{b1,b2}{:}H_1(b_1) \longrightarrow P(H_1(b_2)){:}c_1 \mapsto \{\, c_2 \in H_1(b_2){:}\neg\, (c_1 \vee c_2)\}. \quad (18)$$

### 2.6.3 Illustration with Static Retinal Variables and 3D Environment Parameters for Selectivity Purposes

#### *2.6.3.1 Collection of Entities*

In this chapter, we consider a subset of visualization techniques and their targeted purposes. Hence, collection B (Equation (19)) first gathers a subset of static retinal variables (Table 1). We do not consider the position visual variable of Bertin, since changing the 3D object position alters its spatial relation to other elements. Note however that this variable remains very useful for semantic information representation, such as labelling (Stein & Décoret, 2008). Collection B also includes 3D environment settings (Section 2.4.3), while the only selectivity interpretation task (Table 2) is considered in collection C (Equation (20)).

| | |
|---|---|
| B = {arrangement, atmosphere effect (haze), crispness, depth of field, environment projection, grain, hue, lightness/value, directional lighting, material, orientation, pattern, perspective height, resolution, saturation, shading, shadow, shape, size, sketchiness, spacing, transparency} | (19) |
| C = {selectivity} | (20)) |

Then, connections between collections B and C are defined, which is carried out by a review of the existing literature but also through empirical tests performed on a part of the virtual 3D LOD1 city model of New York (Figure 9). In the following section, we provide a set of figures to illustrate the statements.

#### *2.6.3.2 Truth Values of Functions*

Equation (14) addresses the consequence connection among the entities of B. It links the following entities:

- the production of a shadow induces the use of a directional light (Figure 10a);
- the application of transparency indirectly implies the application of lightness/value and saturation (Figure 10b);
- the application of grain indirectly implies the application of spacing. In Figure 10c, two levels of grain are applied to the same building, which also implies a spacing variation between points.
- the application of perspective height indirectly induces the application of size. In Figure 10d, two different perspective heights

are applied to the same red building, which also implies a size variation of this building.

Equations (15) and (16) refer to compatibility and incompatibility connections among the entities of B. On the basis of previous studies, the following incompatibilities can be extracted:

- Atmosphere effect (haze) influences the perception of lightness/value and saturation (Figure 11a) (Jobst et al., 2008);
- Shading influences the perception of lightness/value and saturation (Figure 11b) (Jobst et al., 2008);
- Directional lighting influences the perception of lightness/value and saturation (Figure 11c) (Jobst et al., 2008);
- Shadow influences the perception of lightness/value and saturation (Figure 11d) (Jobst et al., 2008);
- Depth of field changes the perception of size (Jobst et al., 2008), orientation (Wang et al., 2012), grain and spacing (Ware, 2012), but also perspective height and resolution.

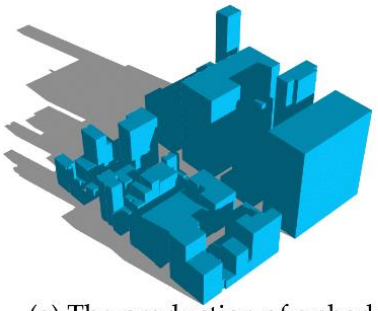

(a) The production of a shadow induces the use of a directional light.

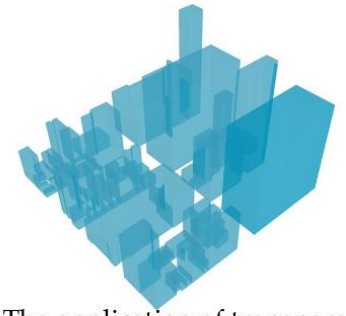

(b) The application of transparency implies indirectly the application of lightnessvalue and saturation

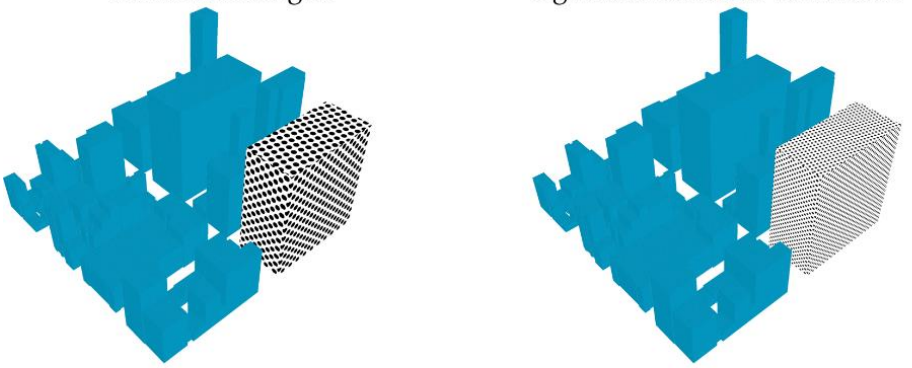

(c) A change of grain implies a change of spacing.

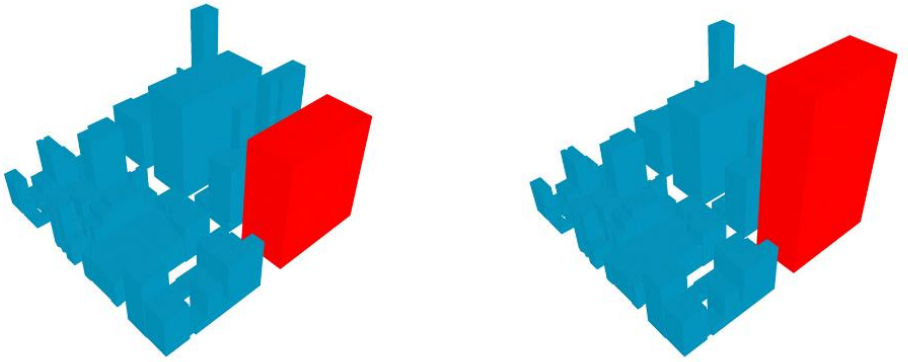

(d) A change of perspective height induces a change of size.

**Figure 10**: Consequences between a set of static visual variables and 3D environment settings

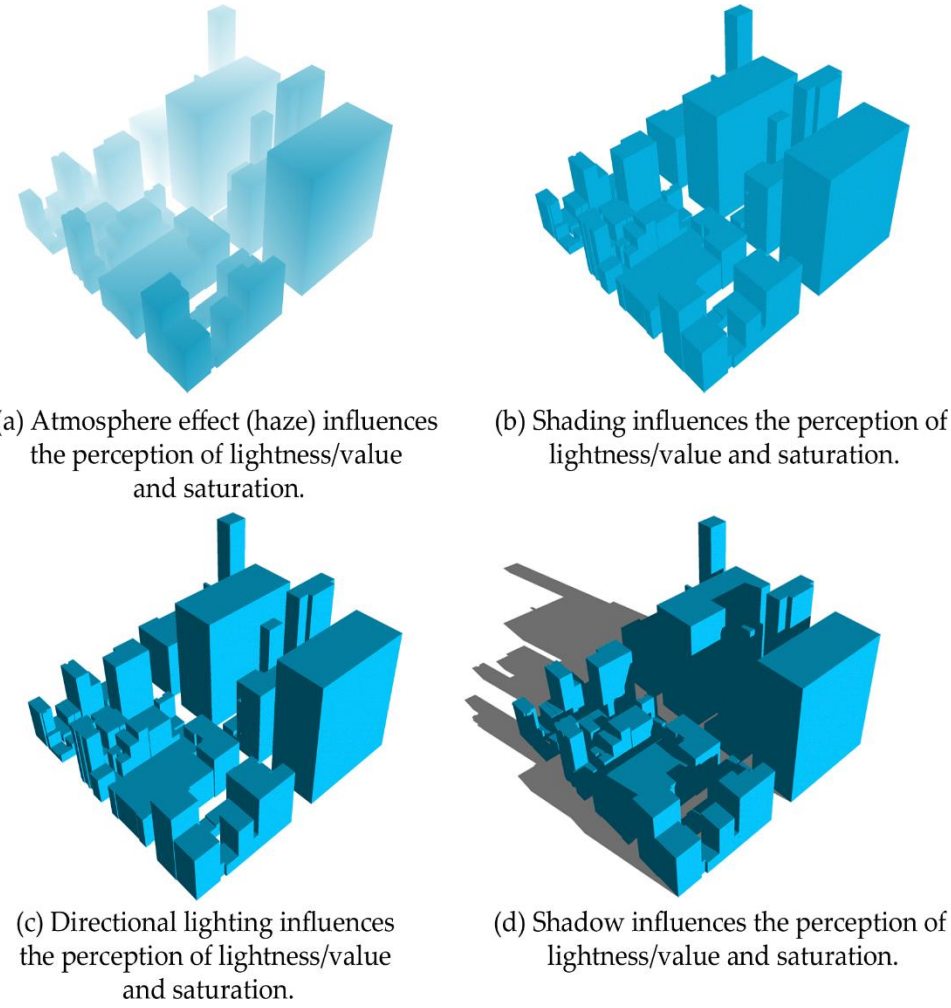

(a) Atmosphere effect (haze) influences the perception of lightness/value and saturation.

(b) Shading influences the perception of lightness/value and saturation.

(c) Directional lighting influences the perception of lightness/value and saturation.

(d) Shadow influences the perception of lightness/value and saturation.

**Figure 11**: Incompatibilities among a set of static visual variables and 3D environment settings

Equations (17) and (18) address compatibility and incompatibility connections among the targeted purposes of B (i.e., the entities of C). Among the selective entities of B, some are incompatible because their

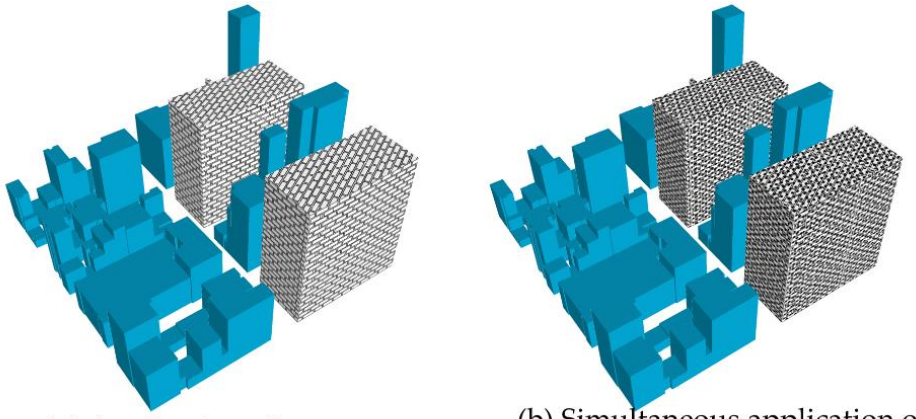


**Figure 12**: Incompatibilities between pattern and grain for selectivity purpose

selectivity perceptual property cancels when they are applied on a same 3D object. This is especially the case of grain, pattern, and sketchiness since their combination makes the specific extraction of each individual element more difficult (Figure 12).

Note that previous consequences and incompatibilities are quite direct (i.e., undeniable) and generic (i.e., independent of data to be visualised, the task to be performed, and the context in which task is executed). However, in practice, most graphical conflicts are difficult to predict, since they may depend on the spatial distribution of 3D objects. This is especially the case of transparency and shadow. The first may induce a superposition of static visual variables, while the second may hide a part of the 3D scene and subsequently make the application of any retinal variables useless (Figure 13a,b).

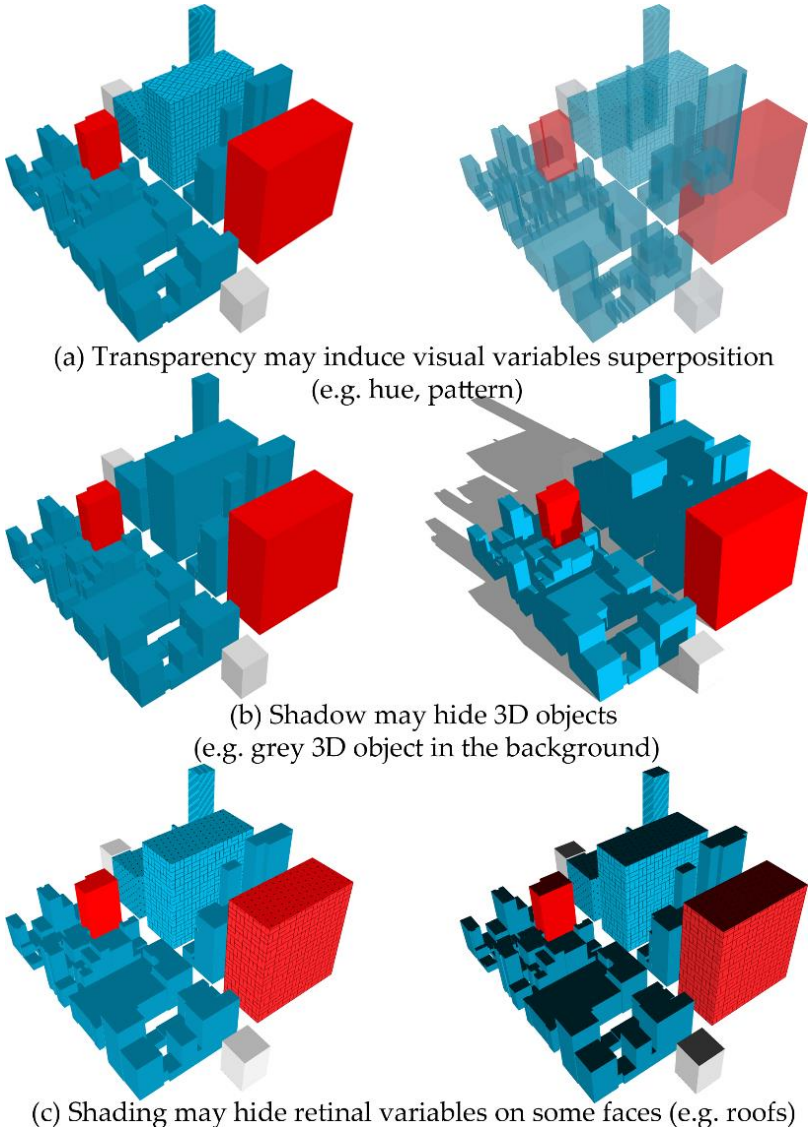


**Figure 13**: Potential incompatibilities between a set of visual variables and 3D environment settings.

Some incompatibilities may also be a function of the application level of visualization techniques. While shading is useful to emphasize the three-dimensional appearance, too much shading may hide retinal variables on

some faces (Figure 13c). However, too little shading may not highlight the geometric appearance of 3D objects.

## 2.7 Examples of Knowledge Network Application

In Section 2.6, we created the framework of a future knowledge network on 3D geovisualization through a formalization process. At this stage of development, experts (e.g., from urban planning) are able to define their own graphic design guidelines based on the previous mathematical framework. However, one challenge has yet to be solved: how to incorporate this knowledge into an operational solution that assists end-users in the visualization process of 3D models? To answer this question, we designed three applications. The first one is an application chart of the previous 3D geovisualization knowledge network. The second is a dynamic client WebGL application that implements the previous chart. Ultimately, we suggest an extension to the OGC Symbology Encoding so as to introduce knowledge in the visualization process of web mapping services.

### 2.7.1 Application Chart

In Section 2.6.3, we extracted connections (consequence, incompatibility, and potential incompatibility) between a set of static retinal variables and 3D environment settings for the purpose of selectivity. The following application (Figure 14) aims to bring the knowledge into a chart that assists the visualization process of virtual 3D city models. Static retinal variables (classified into three categories) and 3D environment settings are

displayed horizontally and vertically, respectively. Then, the use of four colors expresses the four categories of connections:

1. Compatibility connection in green;
2. Potential incompatibility connection in yellow; this refers to incompatibilities that may be linked to the spatial distribution of 3D objects and/or the application level of static visual variables used simultaneously.
3. Incompatibility connection in red;
4. Consequence connection in blue.

The chart reading is performed either through a selection of static retinal variables that constrains the use of 3D environment settings, or the reverse. As such, users can then find appropriate graphical expressions and avoid graphical conflicts. Note that the chart also shows connections among static retinal variables and 3D environment settings through the use of colored exponents (e.g., consequence connection between shadow and lighting, incompatibility connection between pattern and grain). Figure 14 illustrates the application chart and extends the version of Neuville et al. (Neuville et al., 2017) by reviewing some graphical conflicts.

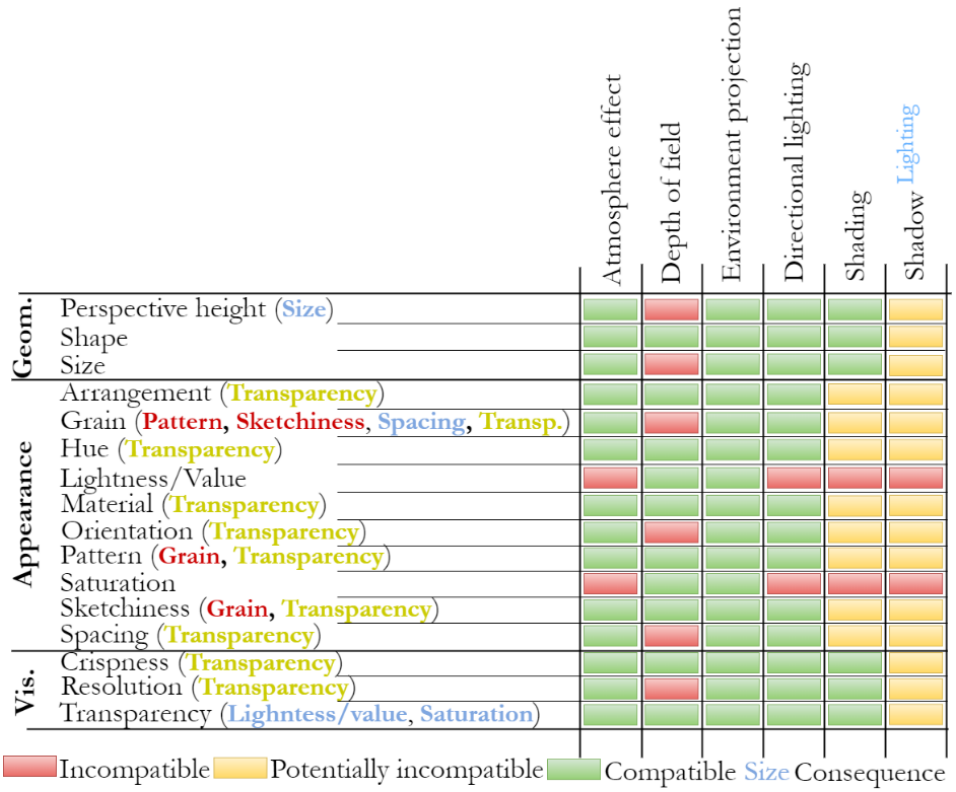


**Figure 14**: An application chart (extension version of (Neuville et al., 2017)) for assisting the visualization of selectivity purpose of virtual 3D city models. Static visual variables are categorized into three classes: visibility (vis.), appearance, and geometry (geom.).

### 2.7.2 Dynamic WebGL Application

In order to provide an operational solution that could be implemented into existing CAD and GIS-oriented software, we propose an interactive design plugin, developed with three.js, a cross-browser JavaScript library using WebGL. The application interface includes a 3D viewer and a sidebar that incorporates a set of static retinal variables and 3D

environment parameters. Unlike standard 3D viewers, the plugin brings intelligence into the visualization process. Indeed, two events are produced when the user applies a specific visualization technique. The first concerns the display of consequence, potential incompatibility, and incompatibility connections (through the previous colour coding), while the second explains these connections via a warning window. This is especially useful for potential incompatibilities where the inconsistency degree depends on specific factors such as the spatial distribution of 3D objects and/or the application level of other visualization techniques.

Figure 15 illustrates the WebGL application. To show the visual evolution of the 3D model, we present multiple views (times t1 to t3). In the first step, the user downloads the 3D model without applying any visualization techniques (upper image). In the example, shading is then used to highlight the 3D geometric appearance of 3D objects (second image). After that, hue is used for some buildings for the purpose of selectivity (lower image).

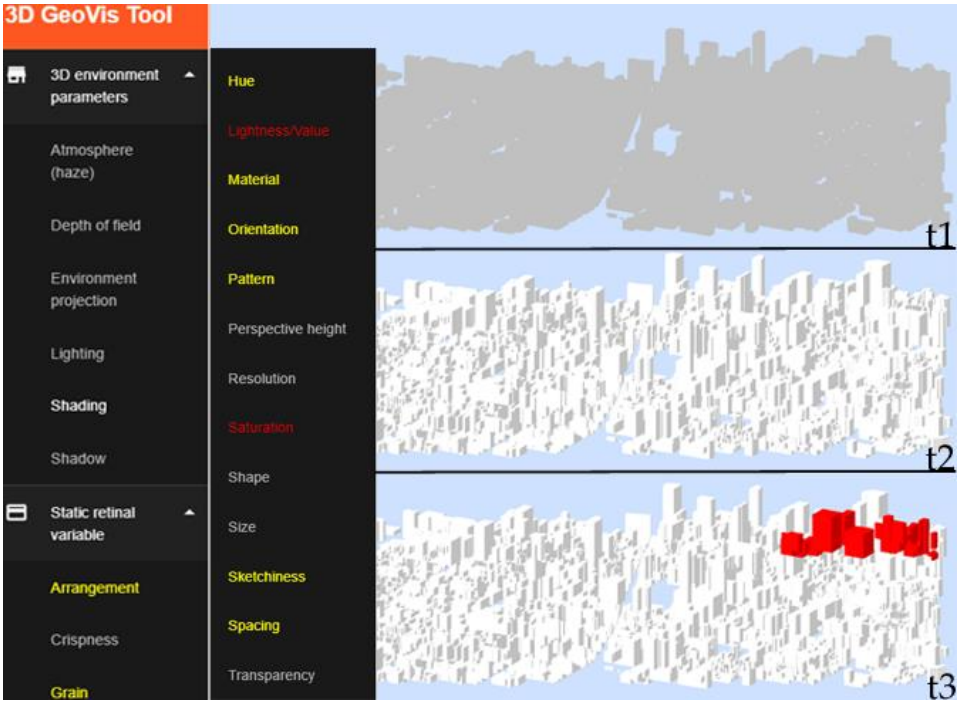


**Figure 15**: A dynamic WebGL application for assisting the visualization process of 3D geospatial data. Multiple views of the 3D model (times t1 to t3) are shown to highlight the visualization process.

During the whole visualization process, the sidebar is continuously updated to inform user of compatible, incompatible, and potentially incompatible visualization techniques. As shown in Figure 15, the application of shading constrains the use of additional visualization techniques, which is carried out with the use of the same colour coding as in Figure 14.

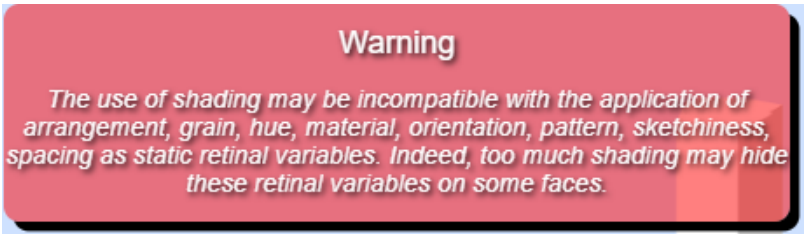


**Figure 16**: A warning window to inform users against potential incompatibilities.

Note that we applied hue despite the constraint established by the use of shading (Figure 14). As a reminder, there is a potential incompatibility among these two variables. Indeed, too much shading may hide hue on some 3D object faces. Since a low level of shading was applied on the 3D model, this visual variable can be used without causing any graphical conflicts. Note that the plugin also displays a window for these kinds of incompatibilities in order to inform designers against potential graphical conflicts (Figure 16). As a result, suitable styles can be applied to features and the 3D environment.

### 2.7.3 OGC Symbology Encoding Extension

Ultimately, we suggest an extension to Symbology Encoding (SE). SE is an XML language for styling information that can be applied to the features and coverage data of web mapping services. While an extension of SE has been proposed in (Neubauer & Zipf, 2007), the visualization process remains unstructured and graphical conflicts may still appear. That is why we propose a new extension to SE in order to assist users in the

visualization process of web mapping services. To achieve this, we propose an additional XML element that deals with the suitability between the visualization techniques and their targeted purposes. The new element is called Suitability, and its format is shown in the following XML-Schema fragment:

```
<xsd:element name="Suitability" type="se:SuitabilityType">
</xsd:element>
<xsd:complexType name=" SuitabilityType">
<xsd:sequence>
    <xsd:element ref="se:Name" minOccurs="1"/>
    <xsd:element ref="se:Description" minOccurs="1"/>
    <xsd:element ref="se:TargetedPurpose" minOccurs="1"
maxOccurs="unbounded"/>
    <xsd:element ref="se:Consequence" minOccurs="0"
maxOccurs="unbounded"/>
    <xsd:element ref="se:Incompatibility" minOccurs="0"
maxOccurs="unbounded"/>
    <xsd:element ref="se:PotentialIncompatibility" minOccurs="0"
maxOccurs="unbounded"/>
</xsd:sequence>
</xsd:complexType>
<xsd:element name=" TargetedPurpose" type="xsd:string"/>
<xsd:element name="Consequence" type="xsd:string"/>
<xsd:element name="Incompatibility" type="IncompatibilityType">
</xsd:element>
<xsd:complexType name="IncompatibilityType">
    <xsd:simpleContent>
        <xsd:extension base="xsd:string">
            <xsd:attribute name=" TargetedPurposeFrom"
type="string" use="optional"/>
            <xsd:attribute name=" TargetedPurposeTo"
type="string" use="optional"/>
        </xsd:extension>
    </xsd:simpleContent>
</xsd:complexType>
```

```
    <xsd:element name="PotentialIncompatibility"
type="se:PotentialIncompatibilityType">
    </xsd:element>
    <xsd:complexType name=" PotentialIncompatibilityType">
        <xsd:sequence>
            <xsd:element name="Technique" type="xsd:string"/>
            <xsd:element name="Explanation" type="xsd:string"/>
        </xsd:sequence>
    <xsd:attribute name=" TargetedPurposeFrom" type="string"
use="optional"/>
    <xsd:attribute name=" TargetedPurposeTo" type="string"
use="optional"/>
    </xsd:complexType>
```

The *Name* element refers to a given visualization technique (static retinal variable, 3D environment setting, or enhancement technique) and the *Description* element clarifies the context in which the connections are defined (e.g., urban visualization). The *TargetedPurpose* element corresponds to the targeted purpose(s) arising from the application of the visualization technique (Equation (13)). The *Consequence* element refers to Equation (14). Incompatibility and Potential Incompatibility elements refer respectively to Equations (16) and (18). *TargetedPurposeFrom* and *TargetedPurposeTo* attributes express the incompatibilities among entities of C (i.e., the targeted purposes of visualization techniques). The following provides two application examples for hue and pattern visualization techniques.

```
<Suitability>
    <Name>Hue</Name>
    <Description>
        <Title>Hue usage in urban visualization</Title>
    </Description>
```

```
        <TargetedPurposeFrom>Selectivity</TargetedPurposeFrom>
        <PotentialIncompatibility>
            <Technique>Shading</Technique>
            <Explanation>Too much shading may hide hue on some
faces</Explanation>
        </PotentialIncompatibility>
        <PotentialIncompatibility>
            <Technique>Shadow</Technique>
            <Explanation>Shadow may hide 3D objects and
subsequently hue</Explanation>
        </PotentialIncompatibility>
    </Suitability>
    <Suitability>
        <Name>Pattern</Name>
        <Description>
            <Title>Pattern usage in urban visualization</Title>
        </Description>
        <TargetedPurposeFrom>Selectivity</TargetedPurposeFrom>
        <Incompatibility TargetedPurposeFromFrom="Selectivity"
TargetedPurposeFromTo="Selectivity">Grain</Incompatibility>
        <PotentialIncompatibility >
            <Technique>Shading</Technique>
            <Explanation>Too much shading may hide pattern on some
faces</Explanation>
        </PotentialIncompatibility>
        <PotentialIncompatibility>
            <Technique>Shadow</Technique>
            <Explanation>Shadow may hide 3D objects and
subsequently pattern</Explanation>
        </PotentialIncompatibility>
    </Suitability>
```

## 2.8 Discussion and Conclusions

In this chapter, we proposed to formalize, as a knowledge network, the parameters and components that influence the quality of efficient 3D geovisualization schema. Those parameters and components are classified into four categories as (1) camera settings (position, orientation, focal length, and vision time), (2) visualization techniques (from graphics and computer graphics fields), (3) targeted purposes (interpretation tasks, 3D geovisualization challenges, and perceptions), and (4) 3D objects. Furthermore, connections between the camera settings, the visualization techniques, and the targeted purposes are identified and formalized into a formal mathematical framework (second-order logic). We showed that 3D geovisualization components may be joined according to four kinds of connections: compatibility, incompatibility, potential incompatibility, and consequence. To demonstrate the utility of the proposal, the formalism is applied on a first set of visualization techniques for the purpose of selectivity. The mathematical framework is then used to connect visualization techniques and to provide a first set of graphic design guidelines. Ultimately, three applications are proposed as proofs of concept.

The knowledge network of key components for efficient 3D geovisualization is a clear contribution to the field, since we could not find such a proposal in the scientific literature or practices. It assists both domain experts in the definition of their own graphic design guidelines and non-professional users that manipulate and visualize 3D geospatial data. Indeed, the knowledge network and its formalization are written generically, such that it may be applicable to any 3D geospatial data. Additionally, the applications themselves—especially the WebGL plugin and the Symbology Encoding extension—contribute to the domain, since they can now be used and tested in various contexts.

Our work has some limitations. For example, the formalism was only applied to a small set of visualization techniques and targeted purposes. In the future, further entities will be incorporated in order to extend the preliminary results. Indeed, the formalism aims to build a knowledge network by gathering and connecting an ever-increasing number of entities.

In this chapter, we provided a first set of graphic design guidelines. Some are actually valid for any application fields manipulating 3D geospatial data (e.g., cadastre, augmented and virtual realities, and navigation), while others may be reviewed in order to fit specific contexts, data, and tasks. However, it is clear that static retinal variables "lightness/value" and "saturation" are not actually relevant in 3D geovisualization due to their numerous graphical conflicts with most 3D environment settings. Results also indicate that the degree of inconsistency among considered

visualization techniques is heavily connected to the spatial distribution of requested objects in the 3D geospatial environment and the application level of visualization techniques used simultaneously. This is especially the case for transparency, shadow, and shading, which should be used with caution. Furthermore, many graphical conflicts are difficult to predict. However, this does not mean that they are inevitable, at least if they are defined. This is why it is necessary to build a knowledge network on the visualization of 3D geospatial data. It could even be developed and distributed through XML documents via the new element Suitability.

Ultimately, CAD and GIS-oriented software should incorporate viewpoint management support tools. Indeed, camera settings (camera position, orientation, focal length, and vision time) are crucial in the 3D geovisualization process, since they determine the visibility of 3D objects to which visualization techniques have been applied. However, to date, the viewpoint is manually fixed by the designer who tries to maximise at best the visibility of 3D objects. This operation may be quite arduous, especially with 3D models at high density (e.g., virtual 3D city models). As a result, the temporal and spatial management of camera settings is still a challenge to be solved and is addressed in the next chapter.

CHAPTER 3

# 3D viewpoint management

## 3.1 Preface

This chapter is based on *3D Viewpoint Management and Navigation in Urban Planning: Application to the Exploratory Phase*, an article published within the "Remote Sensing" journal in January 2019. Following up the recommendation of the previous chapter on the need of automation in the 3D viewpoint selection, this chapter proposes a geocomputational method that assists users in the identification of the best point of view, i.e. maximizing the visibility of the 3D model semantic information. Via the development and implementation of two algorithms (called viewpoint management algorithm and flythrough creation algorithm), we propose the first theoretical and operational solution that aims to improve the 3D geovisualization process (especially the occlusion issue) based solely on suitable 3D points of view. Yet, this proposal will have still to be validated, which is the purpose of Chapter 4.

## 3.2 Abstract

3D geovisualization is essential in urban planning as it assists the analysis of geospatial data and decision-making in the design and development of land use and built environment. However, we noted that 3D geospatial models are commonly visualized arbitrarily as current 3D viewers often lack of design instructions to assist end-users. Hence, in this chapter, we propose a theoretical and operational solution to manage camera settings by automatically computing best viewpoints. Based on user's parameters, a viewpoint management algorithm initially calculates optimal camera parameters for visualizing a set of 3D objects of interest through parallel

projections. Precomputed points of view are then integrated into a flythrough creation algorithm for producing an automatic navigation within the 3D geospatial model. To illustrate our proposal, the algorithms are illustrated within the scope of a fictive exploratory phase for the public transport services access in the European quarter of Brussels.

**Keywords:** 3D geovisualization; visualization pipeline; 3D geospatial data; virtual 3D city model; viewpoint; occlusion; camera; urban planning; planning activities; urban indicators

## 3.3 Introduction

### 3.3.1 3D Geovisualization and Urban Planning

In urban planning, 3D geovisualization is fundamental as all planning activities are required, to a certain extent, to be displayed (Biljecki et al., 2015). In the exploratory phase, 3D geovisualization facilitates the diagnosis of areas where something needs to be done (Ranzinger & Gleixner, 1997), such as air quality and noise pollution (Congote et al., 2012; Lu et al., 2017). In the analysis phase, the presentation of results can be improved with an appropriate 3D geospatial data display (e.g., for assessing land use consumption and patterns) (Kaňuk et al., 2015). Finally, 3D geovisualization is also an integral part of the design, implementation, evaluation, and monitoring phases. For instance, it is respectively employed to assist park design (Liu & Sung, 2014), to identify urban objects that might interfere within a building project (Moser et al., 2010), to evaluate urban projects both for political decision-makers and citizens

(Wu et al., 2010), and ultimately to monitor urban dynamics (Calabrese et al., 2011).

However, based on the review in (Neuville et al., 2018), 3D geovisualization is commonly performed arbitrarily. Whilst 3D viewers provide a lot of tools for visualizing 3D geospatial data (e.g., type of projection, view controls, and transparency) (Cemellini et al., 2018), they still do not incorporate design instructions to assist end-users. Therefore, the graphical expression may be irrelevant due, for example, to an inappropriate set of visualization techniques. In urban planning, this is detrimental as it may alter the communication process among stakeholders (political decision-makers, contractors, and citizens). For instance, the shadow cast from a new building onto the neighborhood is not always easy to assess and we do believe that this situation is essentially due to the failure to assist users in the visualization of 3D geospatial data. Consequently, we defined in (Neuville et al., 2018) a 3D geovisualization framework that connects visualization techniques and defines their consistency according to four kinds of connections: compatibility, incompatibility, potential incompatibility, and consequence. Effective visual combinations, i.e., without graphical conflicts, can thus be found, leading to addressing the visualization of 3D geospatial models in a comprehensive and integrated way.

In this chapter, we enhance the 3D geovisualization framework of (Neuville et al., 2018) with a theoretical and operational solution to manage camera parameters, and subsequently occlusion issues within 3D

models. Indeed, while occlusion is one of the most fundamental depth cues (Ware, 2012), it can also make the representativeness of features and their spatial relationships more complex (Li & Zhu, 2009). This is why the occlusion management is one of the greatest challenges (if not the most notable one) in the visualization process of 3D geospatial data. Besides, most 3D virtual environments display a high density and diversity of 3D objects, leading necessarily to clutter and occlusion (Elmqvist & Tudoreanu, 2007). This is especially the case for virtual 3D city models that usually provide both aboveground and underground information (e.g., buildings, transportations, aqueducts, and gas pipelines).

### 3.3.2 3D Occlusion Management Review

In (Elmqvist & Tsigas, 2007), the authors performed a taxonomy of 3D occlusion management techniques. More than twenty methods have been analyzed and classified into five design patterns (Table 4). Following this research, it turned out that combining design patterns into hybrid interaction models, involving both user's interaction (active interaction model) and 3D data pre-treatment (passive interaction model), could be an interesting and promising solution for effectively managing occlusion. Indeed, they are an efficient tradeoff between active and passive interaction models since they respectively combine both flexibility and precision. For example, tour planner (passive interaction model) could be associated with an interactive exploder (active interaction model) in order to reduce occlusion in high local congestion areas. To produce such hybrid

**Table 4**: Taxonomy of 3D occlusion management techniques based on (Elmqvist & Tsigas, 2007)

| Design pattern | Signification | Example |
|---|---|---|
| **Multiple viewports** | Managing occlusion with two or more views (overview and detailed view(s)) | Tumbler, worldlets |
| **Virtual X-ray** | Managing occlusion in the image-space through fragment shaders | Perspective cutouts, image-space dynamic transparency |
| **Tour planner** | Managing occlusion with an exploration phase | Way-finder |
| **Interactive exploder** | Managing occlusion in the object-space through user's interaction | 3D explosion probe, deformation-based volume explosion |
| **Projection distorter** | Managing occlusion in the view-space through two or more integrated views | Artistic multiprojection, view projection animation |

interaction models, it is thus primordial to manage the camera as it determines the visibility of 3D objects to which visualization techniques (e.g., virtual X-Ray) have been applied. However, we noted that this operation is still manually handled by designers, who try to maximize at best the visibility of 3D objects; which is highly time-consuming.

As a first step in achieving hybrid interaction models, we therefore propose a flythrough creation algorithm (FCA) that automatically computes efficient camera paths to optimally visualize 3D objects of

interest. This algorithm is based on an existing viewpoint management algorithm (VMA) that automatically computes optimal static viewpoints, i.e., maximizing at best the visibility of selected features (Neuville et al., 2016; Poux & Neuville et al., 2017). Note that, besides saving processing time for users, VMA also addresses ethical issues about 3D views by providing self-reliant points of view, i.e., independent from the user's standpoint. Finally, incorporated into a computer animation creation algorithm, it intends to support urban planning by assisting the evaluation and cognition of complex spatial circumstances (Ninger & Bartel, 1998). In summary, the main contributions of this chapter are:

- The development of a new algorithm (flythrough creation algorithm) for producing automatic computer animations within virtual 3D geospatial models and subsequently supporting the spatial knowledge acquisition;
- The improvement of an existing viewpoint management algorithm (Neuville et al., 2016) at several levels: the equal distribution of points of view on the analysis sphere, the definition of a utility function, and the framing computation of viewpoints for parallel projections. Moreover, the original algorithm has been enhanced both in calculation time and computer resources;
- The integration of the two previous algorithms within a broader semantic driven visualization process of 3D geospatial data;
- The implementation of an operational solution for automatically generating spatial bookmarks and computer animations within virtual 3D geospatial models.

This chapter is structured as follows. Sections 3.4, 3.5 and 3.6 outline VMA and FCA into a broader 3D geovisualization framework, and explain the mechanics of each algorithm in more detail. Section 3.7 illustrates VMA and FCA within the scope of a fictive exploratory stage related to the public transport services access in the European quarter (Brussels). Eventually, the chapter discusses the algorithms and addresses perspectives for urban planning.

## 3.4 Methodological Framework

### 3.4.1 Overview

This section aims to give an overview of the viewpoint management and flythrough creation algorithms within a broader semantic driven visualization process (Figure 17). The algorithms are then explained and illustrated in the following sections.

From a theoretical point of view, the 3D geospatial data visualization pipeline is usually divided into three main stages (Semmo et al., 2015): (1) the filtering stage to select 3D objects into a primary landscape; (2) the primary model mapping to a cartographic model via symbolization; (3) the rendering of the cartographic model (e.g., projection, lighting, and shading). The filtering stage consists in (semantically and/or spatially) querying the 3D geospatial data in order to reduce the density of 3D geoinformation to be displayed, but also to distinguish objects of interests (OOIs) and visualization context objects (VCOs). OOIs are the subjects of study, and VCOs are the additional surrounding features.

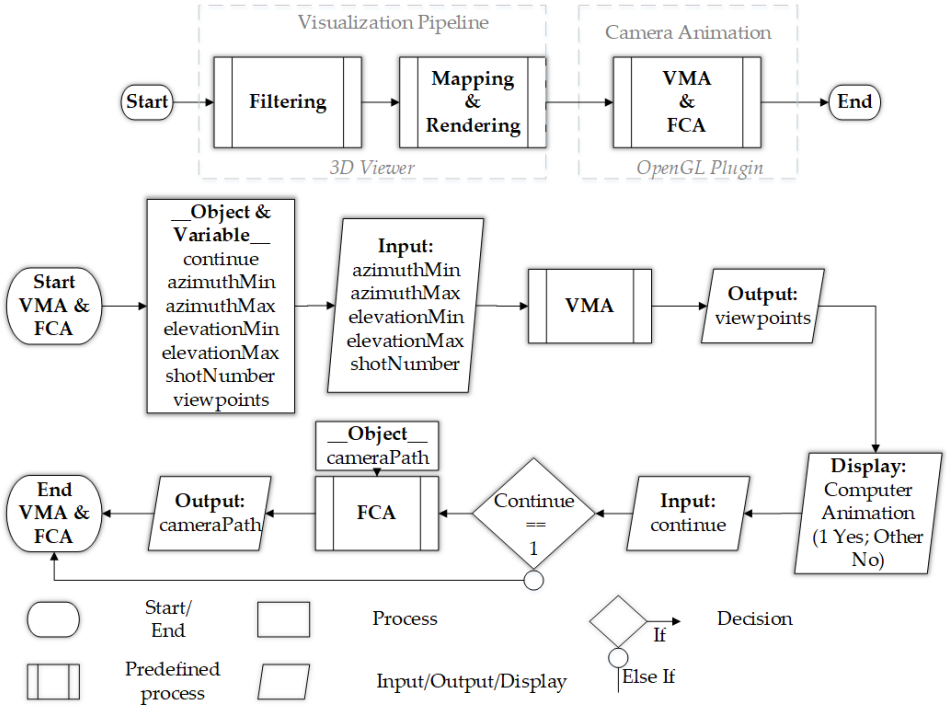


**Figure 17**: 3D geovisualization process including an automatic computer animation (ISO 5807). VMA: viewpoint management algorithm; FCA: flythrough creation algorithm.

Finally, the mapping and rendering stages aim to apply specific visualization techniques to OOIs, VCOs, and the 3D environment. Note that these two phases are co-dependent and some caution is needed to avoid graphical conflicts. Thereupon, we invite readers to refer to (Neuville et al., 2018) for a comprehensive study of the 3D geovisualization process.

The viewpoint management and flythrough creation algorithms have been designed as additional stages to the visualization pipeline, which

means that the user has initially divided the 3D geospatial data to be visualized into objects of interest and visualization context objects, and then applied particular visualization techniques to the objects and the environment. As the viewpoint management algorithm focuses on solving the occlusion issue with efficient camera parameters, only the visualization techniques including or managing occlusion are considered as they act on the objects' visibility and thereby on the viewpoints calculation. Such visualization techniques are, for instance, transparency (occlusion management technique), or shadow (inducing occlusion).

Before launching VMA, the user has to configure the algorithm by setting the viewpoints orientation (minimum and maximum azimuths, minimum and maximum elevations) and the number of points of view to be processed. These two parameters meet the user's requirements as he/she may restrict the viewpoints computation to his/her application needs. When the algorithm has been fully configured, it generates and processes a set of viewpoints, and returns (1) one best global viewpoint, i.e., the most efficient point of view visualizing all the objects of interest; and (2) a best local viewpoint for each object of interest, i.e., its best point of view regarding all the processed viewpoints. The viewpoint management algorithm is fully explained in Section 3.5.

Then, these two outputs become the inputs of the flythrough creation algorithm that aims to build a computer animation by spatially and temporally handling the precomputed static viewpoints into an efficient camera path. To produce an automatic navigation, FCA firstly produces

an overview of the 3D geospatial model which immerses users into the study area. Then, the camera automatically moves to the best global point of view before reaching the best local viewpoints for a deeper investigation of the objects of interest. Section 3.6 presents in more detail the flythrough creation algorithm.

### 3.4.2 Camera Settings

This section proposes a brief review of the camera settings within 3D viewers. First, a virtual camera behaves as a real camera since it "converts electromagnetic radiation from an object into an image of that object and projects that image onto a surface" (American Society of Civil Engineers, 1994). Within the framework of this research, the objects are in three dimensions and the projection surface is plane. Then, the virtual camera settings (A) can be formalized according to four components: a camera position (A1), a camera orientation (A2), a focal length (A3), and a vision time (A4).

Mathematically (Neuville et al., 2018):

$$A = A_1 \times A_2 \times A_3 \times A_4, \quad (1)$$

With

$$A_1 = \mathbb{R}^3, \quad (2)$$

$$A_2 = \mathbb{R}^3, \quad (3)$$

$$A_3 = \mathbb{R}^+ \cup \{\infty\}, \quad (4)$$

$$A_4 = \mathbb{R}^+ \cup \{\infty\}. \quad (5)$$

Figure 18 illustrates the previous virtual camera settings. The camera position and orientation are 3D vectors which respectively represent a 3D location and a 3D viewing direction into the world coordinate system. The focal length is the distance between the projection center and projection plane, and the vision time is defined as the time spent on visualizing a given viewpoint. Considering one or several objects of interest(s) to be displayed, the viewpoint management algorithm aims to compute the best viewpoints, i.e., the best camera positions and orientations, which are then integrated into a computer animation by the flythrough creation algorithm that assigns a vision time to each point of view.

To date, the algorithms only deal with parallel projections, which means that the camera focal length is set at infinite. This consideration is explained by the higher complexity to compute the most appropriate distance from which the camera should look at the 3D scene with perspective projections. As shown in Figure 19, moving to the camera position *2* enhances the framing as it crops the image on the objects of interest. As such, their projected area increases. However, this operation extends the hidden faces ratio with the perspective projection (left image).

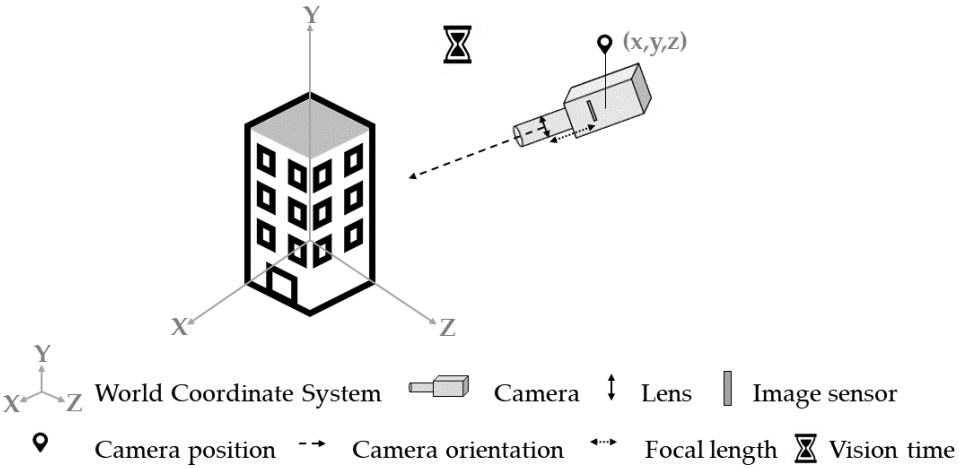


**Figure 18**: The virtual camera settings: camera position, camera orientation, focal length, and vision time

Indeed, the big building produces more hidden faces on the small building after moving to camera *2* (black section), which is not the case with the parallel projection (right image). As a consequence, a tradeoff between the OOIs' projected area gain and loss has to be found to get the optimal camera position. Nevertheless, it is different for each initial camera position as it depends on the camera elevation and the spatial distribution of OOIs. A discussion about this particular issue is provided in section 3.8.3.

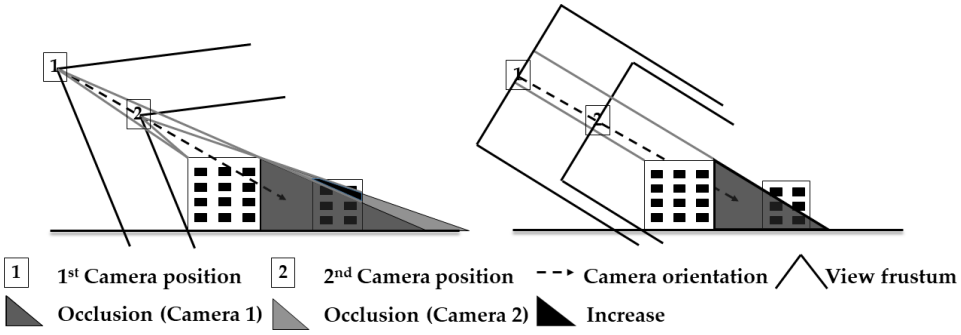


**Figure 19**: Hidden faces increase within perspective projections (left) versus parallel projections (right) when moving to camera position 2.

## 3.5 Viewpoint Management

### 3.5.1 Introduction

The best viewpoint selection is an old issue and several computation methods have already been proposed, such as the non-degenerated view method, the direct approximate viewpoint selection and the iterative viewpoint calculation (Dutagaci et al., 2010; Plemenos, 2003). These methods aim to calculate the most representative viewpoint for one or several object(s) of interest, i.e., maximizing object(s)' visible surface within the viewing window. In this chapter, we present a new iterative viewpoint calculation as it is the most suitable technique for visualizing complex "realistic" environments, like virtual 3D city models. To select the best viewpoints, numerous view descriptors have been developed and can be classified into the following list (Lee et al., 2005; Page et al., 2003; Polonsky et al., 2005; Vazquez et al., 2001): (1) the view area, (2) the ratio of visible area, (3) the surface area entropy, (4) the silhouette length, (5) the

silhouette entropy, (6) the curvature entropy, and (7) the mesh saliency. Note that these descriptors are complementary; none of these consistently provides the most suitable result. At this stage of development, only the view area descriptor is considered as it is most appropriate one for near real-time applications. In the next section, we present the viewpoint management algorithm, designed as an image processing algorithm using the graphics card hardware through the OpenGL application programming interface (API) for rendering 3D graphics, similarly to (Barral et al., 1999).

### 3.5.2 Method

First, the user has to distinguish the objects of interest (i.e., the subjects of study) from the visualization context objects (filtering stage). Next, he/she maps and renders the objects and the environment within the mapping and rendering phases. Once these three stages have been performed, the objects and their styles are loaded into a 3D scene, called the computation scene. As a reminder, only the visualization techniques including or managing occlusion are considered into the computation scene as they act on the objects' visibility.

Then, the user sets two parameters: the viewpoints orientation and the number of points of view to be processed. Based on these settings, the algorithm automatically generates a set of viewpoints on a sphere located on the center of the OOIs' bounding box (bbox). The sphere radius is computed based on the 3D bbox spatial extension, so that no object of interest is located outside the field of vision of any points of view. Note

that the camera orientation for each viewpoint is fixed and points to the bbox center. It guarantees that no OOIs are visually favored inside the 2D image. Moreover, it will optimize the framing computation for each point of view. Then, the viewpoints are distributed based on the formulae of the Lambert azimuthal equal-area projection (Snyder, 1987). This cartographic projection allows an equal points of view distribution on the sphere, avoiding an over-sampling at high latitudes and a sub-sampling at low latitudes. Technically, the algorithm firstly produces a set of 2D points, which are then positioned in 3D with the following formulae:

$$\lambda = arctan(\frac{-x}{y}) \tag{21}$$

$$\chi = \sqrt{2 * arcsin(\sqrt{\frac{x^2 + y^2}{4R^2}})} \tag{22}$$

With

$\lambda$ = the longitude,

$\chi$ = the colatitude,

$x$ = the 2D point abscissa coordinate,

$y$ = the 2D point ordinate coordinate,

$R$ = the radius of the sphere.

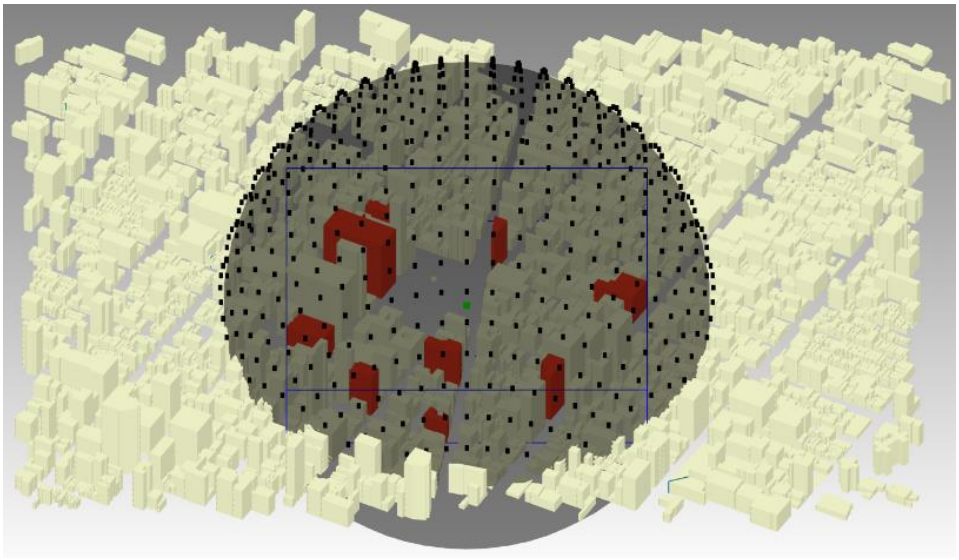

**Figure 20**: Sampling of viewpoints to be processed for visualizing randomly selected buildings around Madison Square Park (virtual 3D LOD1 city model of New York). Five hundred viewpoints (black) are equally distributed between 0 and 90 degrees of elevation. The selected buildings spatial bounding box is represented in blue and its center in green.

The sphere of view is illustrated on a part of the virtual 3D LOD1 city model of New York (building features) provided by the Technical University of Munich. Figure 20 shows a set of viewpoints automatically generated for visualizing randomly selected buildings (red) around Madison Square Park. First, the algorithm extracts the selected buildings spatial bounding box (blue) and centers the virtual sphere on the bbox center (green). In this example, the user has constrained the viewpoints computation between 0 and 90 degrees of elevation; there is no restriction

to the orientation of points of view. He/she has also set the number of viewpoints to be processed at five hundred.

Then, the algorithm processes each viewpoint in two following stages. First, as the viewing volume (defined by the camera frustum left, right, top, and bottom planes) is identical for each point of view, the framing can be optimized. Indeed, the camera frustum planes can be recalculated to better fit the 3D objects of interest in the 2D image. To solve this, the image coordinates of all the OOIs' bboxes vertices are computed; using the objects' bounding boxes reduces the computation time, especially if the objects' geometry is complex. At the end, the critical point, i.e., the closest 3D point from the 2D image edges, is identified. New camera frustum planes are then calculated based on the image distance ratio (in pixels) between the critical point and the image width or height.

A 2D image is next generated in which each object of interest is displayed with a distinct color. Figure 21 shows an example of numerical image to be processed in which the objects of interest are distinguished by their single grey level; the visualization context objects (i.e., the additional buildings) are in black. As such, the algorithm computes the OOIs' visibility by counting the number of distinct pixel colors. In order to accelerate the computation process, the image coordinates of all the OOIs' bboxes vertices are recalculated to focus the reading on the interest area, i.e., the image portion in which all the objects of interest are located. Note that the visibility of each OOI is defined by a minimum number of visible pixels within the 2D image. This parameter is not fixed and can be set as a

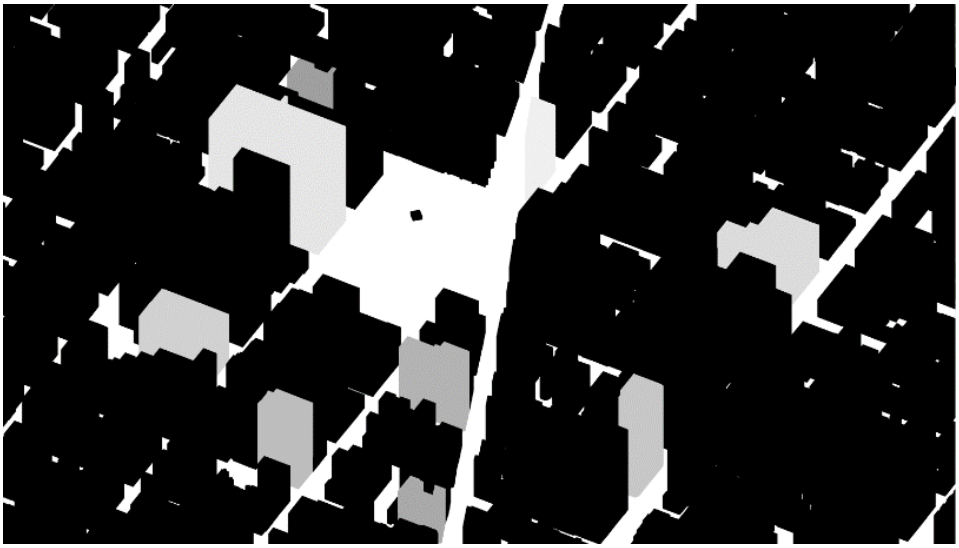

**Figure 21**: Example of numerical image to be processed. Selected buildings are displayed in different grey levels; additional buildings are in black

function of the screen resolution and the viewing distance from which the 3D geospatial data are visualized.

For each viewpoint, the number of visible objects of interest is stored, as well as the associated pixel values. After processing all points of view, the algorithm computes a standardized value for each viewpoint:

$$\sum_{i=1}^{n}(P_i/P_{iMax}) \tag{23}$$

With

$n$ = the number of 3D objects of interest,

$P_i$ = the number of visible pixels for the 3D object i,

$P_{iMax}$ = the maximum number of visible pixels for the 3D object i (considering all viewpoints).

The standardization aims to give the same visibility weight to each object of interest within the viewing window. The best global viewpoint is then defined as the point of view that visualizes all OOIs with the maximum standardized value. Additionally, the algorithm also provides a best local viewpoint for each object of interest, which is the point of view that maximizes its standardized value. Table 5 shows an example of outputs provided by VMA. For each viewpoint, the algorithm computes and stores the ratio of visible pixels per object, i.e., the number of pixels seen from this point of view divided by the maximum number of visible pixels (considering all viewpoints). The standardized value for each point of view is then the sum of ratios of visible pixels.

**Table 5**: Example of outputs provided by the viewpoint management algorithm. For each viewpoint, the algorithm stores the ratio of visible pixels per object and the total sum.

| | $P_1/P_{1Max}$ | $P_2/P_{2M}$ | $P_3/P_{3M}$ | $P_4/P_{4M}$ | $P_5/P_{5M}$ | $P_6/P_{6M}$ | $P_7/P_{7M}$ | $P_8/P_{8M}$ | $P_9/P_{9M}$ | Sum |
|---|---|---|---|---|---|---|---|---|---|---|
| View.1 | 0.278 | 0.350 | 0.300 | 0.440 | 0.387 | 0.103 | 0.264 | 0.376 | 0.390 | 2.89 |
| View.2 | 0.291 | 0.390 | 0.350 | 0.522 | 0.413 | 0.144 | 0.315 | 0.434 | 0.470 | 3.33 |
| View.3 | 0.278 | 0.388 | 0.349 | 0.529 | 0.386 | 0.134 | 0.329 | 0.437 | 0.486 | 3.32 |
| View.4 | 0.353 | 0.329 | 0.412 | 0.543 | 0.315 | 0.330 | 0.280 | 0.336 | 0.363 | 3.26 |
| View.5 | 0.341 | 0.330 | 0.422 | 0.415 | 0.288 | 0.353 | 0.295 | 0.303 | 0.364 | 3.11 |
| … | … | … | … | … | … | … | … | … | … | … |

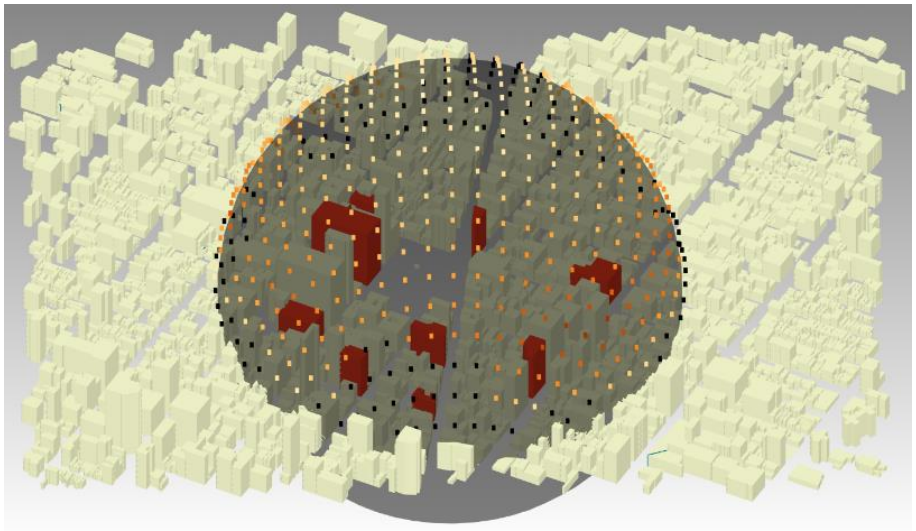

**Figure 22**: A visibility sphere. Viewpoints in black do not allow an overview of all objects of interest (red buildings). The other points of view are categorized with an equal interval ranking method.

Figure 22 shows the visibility sphere for the objects of interest, which displays the efficiency of each processed point of view. Viewpoints in black do not provide an overview of all OOIs; one or several object(s) of interest is/are either completely occluded or viewed under the visibility threshold. Then, an equal interval ranking method categorizes viewpoints standardized values for which all OOIs are simultaneously visible

At the end of the process, the algorithm provides a set of static viewpoints which efficiently visualize the objects of interest, both globally and individually. However, it does not temporally manage these points of view into a computer animation, which is essential to learn large-scale virtual environments such as virtual 3D city models (Chittaro & Burigat,

2004). The set of single viewpoints shall now be incorporated into a navigation process, which is performed by the flythrough creation algorithm and is explained in the next section.

## 3.6 Navigation

### 3.6.1 Introduction

According to Darken and Peterson (Darken & Peterson, 2001), navigation is the aggregate task of wayfinding (i.e., the cognitive element) and motion (i.e., the motoric element). A well-designed navigation aims to enhance the spatial knowledge acquisition, and makes the exploration and discovery feasible. Therefore, we present a flythrough creation algorithm for exploring virtual 3D models. It is designed for off-line explorations, as the camera path is firstly calculated off-line and the exploration is then undertaken (Sokolov et al., 2006).

First, FCA starts with the wayfinding phase, i.e., the camera path computation, with an overview of the 3D model. It aims to give users an overview of the geographic study area and is carried out at 45 degrees of elevation, which is recommended by (Häberling et al., 2008) for still keeping a 3D model overview and a perception of perspective. Note, however, that this viewing angle is not a constant and might be reviewed depending on the spatial extension of the 3D model, the 3D environment in which the 3D model is viewed, and/or the geographical distribution of 3D objects of interest within the 3D model. Then, the camera moves to the best global viewpoint before visualizing each OOI from its best point of

view. Note that the algorithm also considers the motion phase by defining how the camera moves from one viewpoint to another, i.e., its trajectory and velocity. The next section explains in more detail these two phases.

### 3.6.2 Method

First, the algorithm generates a parallel on a half sphere located upright to the center of the 3D geospatial model bounding box. As already mentioned, this parallel is at 45 degrees and its radius is computed based on the bbox spatial extension, so that no objects (of interest and from the visualization context) are located outside the field of vision of any points of view. Technically, the circle is approximated with Bezier curves, which is common in computer graphics for drawing curves in practice. Then, the 3D geospatial model overview is performed by sampling viewpoints on the parallel and by assigning a vision time for each point of view. The vision time per viewpoint is set by the frame rate (e.g., 0.03s at 30 fps, and 0.04s at 25 fps), and the speed of motion is a function of the number of viewpoints interpolated on the parallel. Higher the points of view to be interpolated, faster the camera motion. Note that the camera orientation is identical for each viewpoint and points to the bbox center. In Figure 23, the 3D geospatial model bounding box and its center are displayed in yellow. The camera moves successively clockwise to sampled viewpoints (black) on the 45th degree parallel to overview the 3D geospatial model.

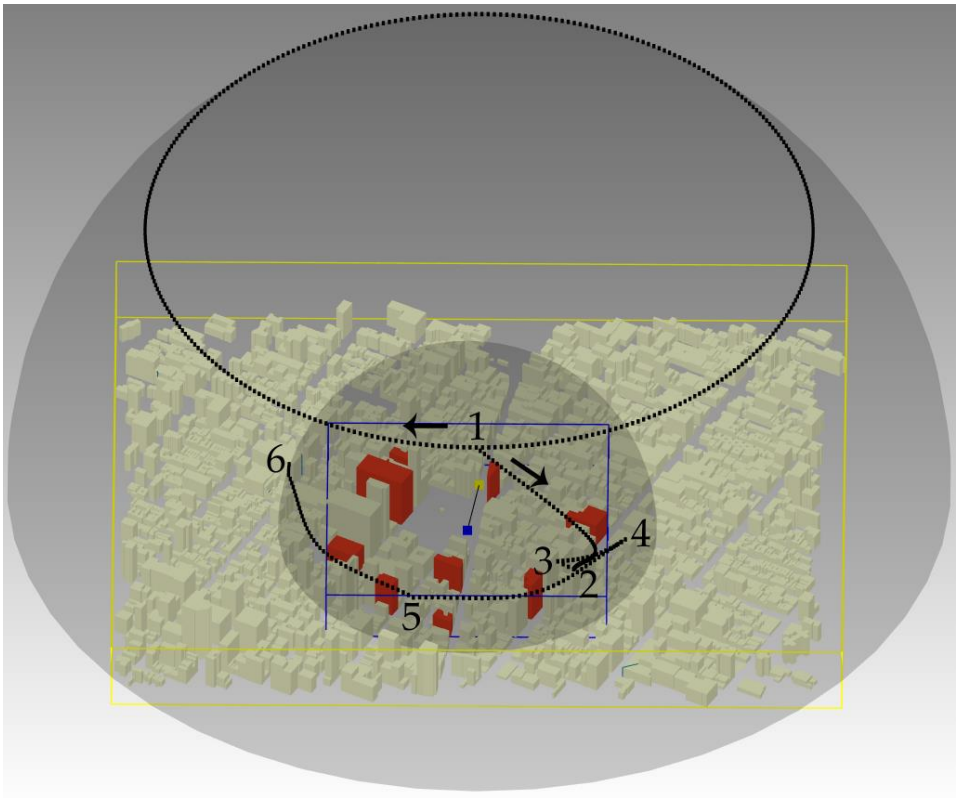


**Figure 23**: An automatic camera path for exploring a set of objects of interest (red buildings) within the virtual 3D city model of New York. Successive viewpoints are displayed in black. The 3D model overview starts at position 1 and turns clockwise. Then, the camera moves to the best global viewpoint (position 2) before visualizing local points of view (3, 4, 5, and 6). The 3D geospatial model and OOIs' bounding boxes and their center are respectively displayed in yellow and blue. Note that the camera orientation shifts to the OOIs' bbox center (blue) when moving to the global viewpoint.

After overviewing the geographic study area, the camera moves to the best global viewpoint (point of view 2). During the motion, the camera orientation shifts to the OOIs' bbox center (displayed in blue) and the view frustum is interpolated from the overview frustum to the best global viewpoint frustum. Once the camera reaches the destination, the flythrough stops, which allows users to visually focus on all the objects of interest. At this step, users may then undertake the urban planning phase (e.g., exploration, analysis, and evaluation stages). Next, users can continue the animation and move to best local viewpoints (points of view 3, 4, 5, and 6). The viewpoints sequence is set in order of importance. If two or more OOIs present the same best point of view, they are first visualized before seeing more "single" viewpoints (i.e., related to one single object of interest). This order aims to improve the scene understanding by firstly favoring viewpoints with a high quality of view. Then, a minimization criterion of distance between viewpoints is used to order same quality points of views, similarly to (Jaubert, Tamine, & Plemenos, 2006). Eventually, the camera motion between the points of view is based on the computation of orthodromy, which is the shortest path between viewpoints on the sphere.

## 3.7 Illustration to the Virtual 3D LOD2 City Model of Brussels

### 3.7.1 Web Application

As the World Wide Web is a democratized way to share and exchange information, the viewpoint management and flythrough creation algorithms have been implemented into a client-side web application. Technically, the web page has been designed with Bootstrap, an open-source front-end framework whereas the algorithms have been developed in WebGL, a cross-platform open source web standard for a low-level 3D graphics API based on OpenGL. As WebGL is a low-level API, the cross-browser Javascript library three.js has been used to simplify the programming writing.

Figure 24 illustrates the web application with the virtual 3D LOD2 city model of Brussels (provided by the Brussels Regional Informatics Centre). The *File* tab allows users to load the objects of interest and the visualization context objects, either separately (i.e., into two distinct files) or within the same file. In the latter case, the *Filtering* tab is used to divide the objects into the two previous categories. To date, the web application only loads the COLLAborative Design Activity (COLLADA) mesh file format as the latter supports the 3D objects' texturing and the 3D environment parameters, thus integrating the previous visualization pipeline phases (Figure 17). However, additional mesh file formats could be accepted, such as OBJ, FBX, and 3DS as they also store the 3D objects' appearance.


**Figure 24**: A web application developed as a 3D viewer and including the viewpoint and flythrough creation algorithms (Viewpoint and Animation tabs). The *Mapping* and *Rendering* tabs assist the 3D geovisualization process.

As the web application constitutes a proof-of-concept for future 3D "intelligent" viewers, i.e., incorporating design guidelines within the 3D geovisualization process, the *Mapping* and *Rendering* tabs warn users against graphical conflicts that might appear when applying a style to the features and/or the 3D environment. Eventually, the *Viewpoint* and *Animation* tabs respectively implement the viewpoint management and flythrough creation algorithms. Via these two tabs, users can parametrize (e.g., defining the viewpoints orientation to be processed) and launch the algorithms, as well as visualize the results.

### 3.7.2 Urban Indicator

In order to illustrate the theoretical and methodological framework, we designed a fictive exploratory phase related to the public transport services access in the European quarter of Brussels. The goal is to meet the upcoming Brussels Regional Express Network (RER) expectations in the European quarter as a significant increase in passenger traffic is foreseen. As such, the authorities might wonder if the existing public transport services accesses could meet this rise in new passengers, both from a human and material resources perspective. They thus would need to visualize them, and to some extent, their area of influence, which constitutes the urban indicator used to evaluate the passenger traffic increase related to each public transport service access.

To address this issue, we take into account the railway and subway stations spatial distribution. Only the railway and subway transports are considered as the future Brussels RER will use the existing railway network, and subway lines constitute an efficient way to travel within the quarter. In this exploratory phase, we do not deal with streetcar and bus stations as the quarter heart is not accessible by the tramway and buses are often stuck in congestion. Then, the area of influence of each station is computed based on the distances among stations. In Figure 25, the subway and railway stations are colored from yellow to red, respectively for small to large areas of influence. Note that the stations are represented either by their physical boundaries, or the total (or partial) city block in which they are located.

**Figure 25**: A virtual 3D LOD2 city model of the European Quarter (Brussels). The subway and railway stations are colored from yellow to red, respectively for small to large areas of influence.

Whilst the new Brussels RER is a real under construction project, we remind the reader that this exploratory phase is completely fictive. Thereby, this section aims to illustrate the algorithms feasibility. Additional indicators shall be included in the future to completely meet the Brussels RER outcomes.

### 3.7.3 Viewpoint Management Algorithm

For this exploratory phase, we set the viewpoints computation between 10 and 80 degrees of elevation; there is no restriction to the orientation of points of view. Constraining the elevation to such values insures perspective in viewpoints and avoids too much occlusion at low

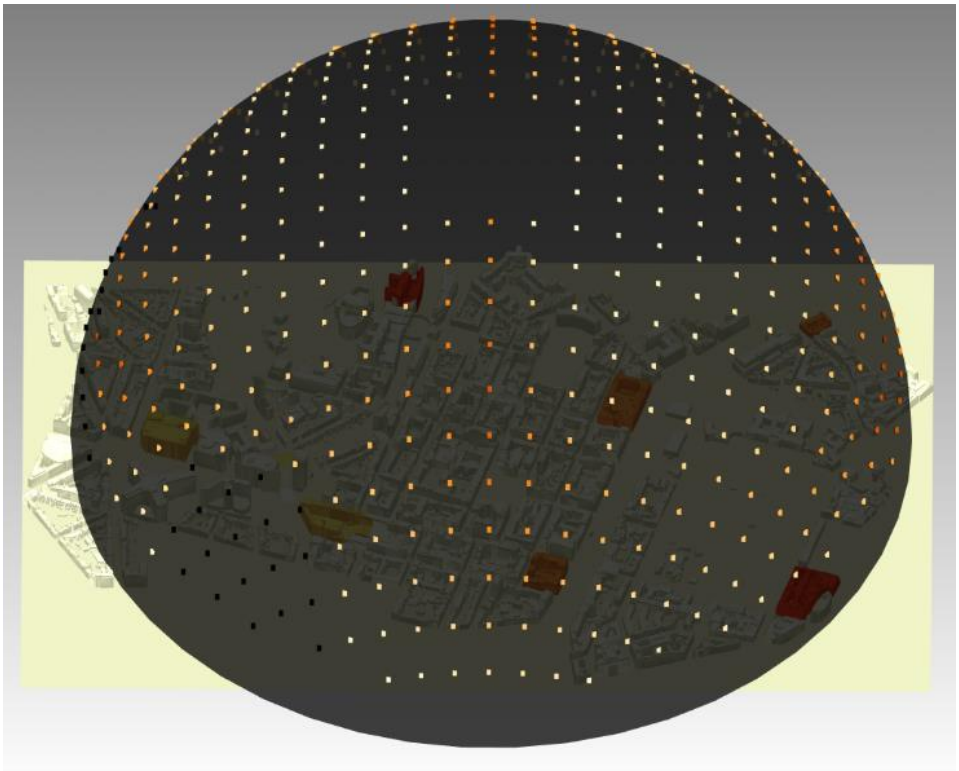

**Figure 26**: Viewpoints in black do not allow an overview of all stations. The other points of view are categorized with an equal interval ranking method.

elevations. Then, around five hundred points of view are generated. Figure 26 shows the visibility sphere. As a reminder, the viewpoints in black do not provide an overview of all stations. Note that the experimentation has been conducted on a laptop with an Intel Core i7 at 2.40 GHz (16 GB RAM) and an NVIDIA GeForce 845M. On average, the computation time is around 30 seconds.

**Figure 27**: The best global viewpoint for the whole set of railway and subway stations.

Figure 27 displays the best global point of view for the whole set of railway and subway stations within the European quarter.

Figure 28 shows the set of best local points of view in which optimally viewed stations are highlighted in green. Note that only four viewpoints are provided as several stations share the same local point of view.

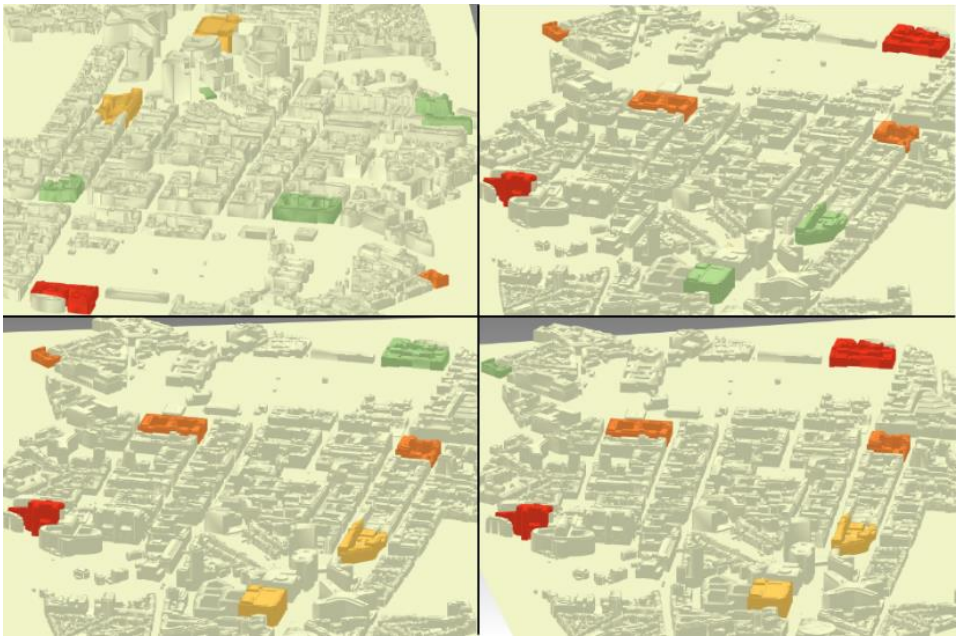

**Figure 28**: The best local viewpoints for the whole set of railway and subway stations. Optimally viewed stations are highlighted in green.

### 3.7.4 Flythrough Creation Algorithm

On the basis of above, the precomputed points of view are combined within an automatic computer animation, starting with a global 3D scene overview at 45 degrees of elevation. Afterwards, the camera moves and stops to the best global viewpoint. Users can then visualize all railway and subway stations through the point of view that maximizes their global visibility within the viewing window. Ultimately, the camera moves to each best local viewpoint. In Figure 29, the time is shown with a hues gradient, from white to red. The camera path starts at 45 degrees of elevation (1) and turns clockwise. Then, it continues to the best global viewpoint (2), before reaching the best local points of view (3, 4, and 5).

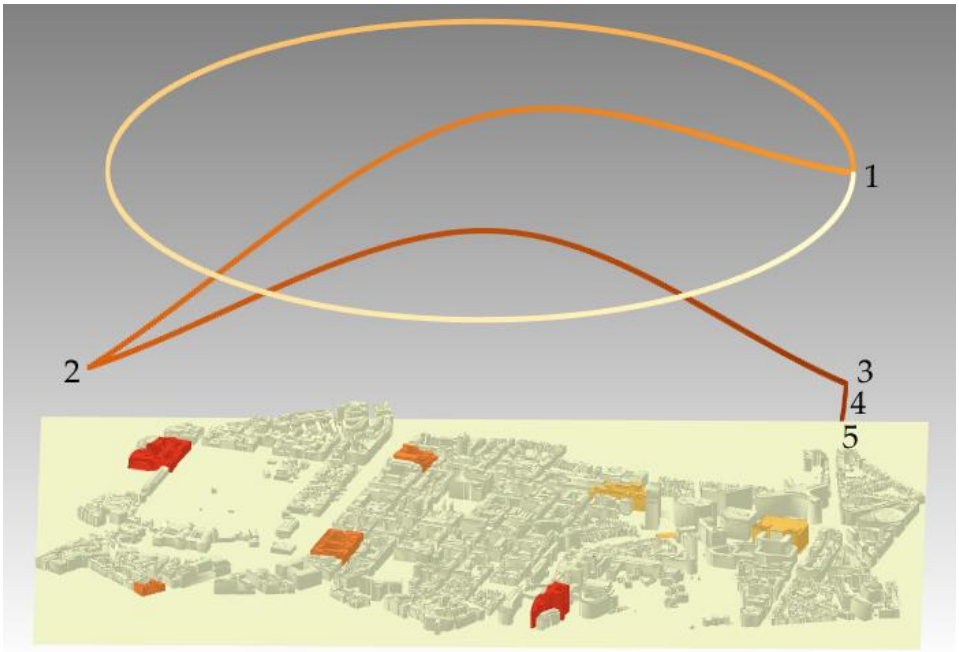


**Figure 29**: An automatic camera path for exploring the railway and subway stations within the virtual 3D LOD2 city model of Brussels (European quarter). The time flow is displayed with a hues gradient, from white to red.

### 3.7.5 Conclusion

In this section, we proposed a first implementation of both viewpoint and flythrough creation algorithms within a use case related to the public transport services access in the European quarter of Brussels. Whilst this exploratory phase is totally fictive, it highlights some benefits for urban planning. First, the algorithms facilitate the determination of right viewpoints, which is a time-consuming task for designers. By a simple interaction with the graphical interface, users can access and share

common points of view for visualizing the objects of interest within 3D geospatial models. These viewpoints constitute thus efficient spatial bookmarks that make the knowledge dissemination easier.

Then, the algorithms facilitate and make the production of computer animations more effective, which is convenient for both designers and end-users. First, the viewpoint management algorithm assists designers in the definition of the most appropriate viewpoints, i.e., visualizing at best the objects of interest. After that, the flythrough creation algorithm combines the selected points of view in order to improve the space understanding.

Eventually, the viewpoint management algorithm provides a visibility sphere, which is useful to explore alternative solutions proposed by the algorithm. Indeed, this sphere allows to get information about the poor and high visibility areas surrounding the objects of interest. As a consequence, designers and end-users could consider and visualize alternative viewpoints, and subsequently define new camera paths within the 3D geospatial model.

## 3.8 Discussion

### 3.8.1 Viewpoint Management Algorithm Complexity

The viewpoint management algorithm complexity is a function of two main parameters: the number of images to be processed (m) and the number of pixels to be analyzed (n). The higher the number of images and/or pixels, the longer the computation time. Thereby, the algorithm

complexity is O(m·n). The first factor (m) defines the calculation accuracy and depending on the application, a tradeoff between accuracy and processing time must be found. The second factor (n) depends on three parameters: the digital display size, the screen resolution, and the OOIs' spatial distribution. The two first settings are a function of the visual display (e.g., mobile phone, computer, and projector screen), while the spatial or attribute request sets the third parameter: the more scattered the objects of interest in space, the higher the number of pixels to be processed. Eventually, note that the algorithm complexity is O(m·n·o) with perspective projections as the distance from which the camera should look at the 3D scene (o) becomes a new parameter to be computed.

### 3.8.2 Advantages

The main advantage of the viewpoint management and flythrough creation algorithms is the independence from the 3D geospatial data to be analyzed. As the algorithms operate on the screen pixels, they can be applied to vector data, raster data, and even point clouds (Neuville et al., 2016). As such, the algorithms are an efficient solution to manage occlusion from any kinds of data and for any application domains. For instance, VMA has already facilitated the knowledge dissemination in archeology for an ancient mosaic in the oratory of Germigny-des-Prés (France) (Poux & Neuville et al., 2017). Then, the algorithms can run with any file formats and due to their implementation into a web application accessible from any HTML5-compatible browsers, they can be easily distributed and employed.

### 3.8.3 Limitations and Perspectives

The algorithms present also some limitations. First, the viewpoint management algorithm does not currently run with perspective projections. As already mentioned, the distance from which the camera should look at the 3D scene is a new unknown and shall be calculated for each point of view to be processed. Considering a given viewpoint, the algorithm shall firstly find all the potential objects that might hide the objects of interest. This operation could be performed by computing the circular sector in which each object of interest is located within the 2D image. Then, the algorithm shall calculate the 3D camera positions on the line of sight from which each object of interest is totally occluded. As such, only a small section of the line of sight would be analyzed in order to determine the optimal viewing distance. A heuristic search might also be used to speed up the process.

Then, the viewpoint management algorithm does not consider the recognition process for photorealistic displays yet. Defined as the capability to attach labels to objects for the identification to categorization processes (DiCarlo et al., 2012), it supposes that users can extract (i.e., visualize) specific items of the objects (Baddeley et al., 2002). For instance, recognizing a church within a 3D photorealistic environment may require to simultaneously visualize several key sections, such as a wall, a stained-glass window and the bell tower. In this case, the algorithm shall break the object down into its key components by uniquely coloring each element. Then, the 3D object recognition shall involve visualizing all sections at a

certain visibility threshold (defined in screen pixels). Note that, depending on the task to be performed (e.g., identification versus classification) and/or the object' visual characteristics (regarding itself or related to its context), more than one viewpoint per object might be required to fully accomplish the recognition process (Tjan & Legge, 1998). In that case, the algorithm shall compile several viewpoints and display them into a multiple viewports design pattern. Therefore, in the future, VMA could incorporate the recognition process, which might also be a gateway to take advantage of VMA in machine learning by improving the segmentation procedure.

To date, the viewpoint management algorithm only considers the view area descriptor to evaluate the representativeness of viewpoints. In the future, the algorithm could incorporate additional image and geometric descriptors in the assessment of viewpoint goodness. Indeed, it has been shown in (He et al., 2017) that 2D image features (e.g., hue and contrast) and 3D geometric features (e.g., surface visibility and outer points) are complimentary in the evaluation process of viewpoint representativeness. Furthermore, as some features are more effective, different weights could be assigned to each descriptor. The utility function (Equation 23) could therefore consider a global goodness score for each object of interest and then aggregate these scores into a viewpoint representativeness score. Eventually, note that these descriptors can be either applied to 3D objects or their key items to meet the specific objects' recognition process (as mentioned earlier).

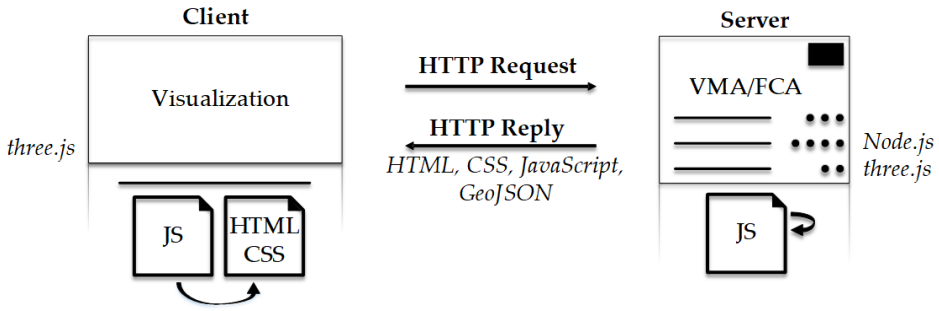


**Figure 30**: A full RESTful web application managing 3D viewpoint

Currently, the algorithms have been developed into a client-side application, which requires good computer memories and processing capacities. In order to develop a real RESTful web application, the visualization and processing stages shall be respectively divided into the client and the server (similarly than (Cemellini et al., 2018)). As the algorithm has been implemented in JavaScript, it could be carried out with an environment server such as Node.js. For instance, in Figure 30, the application is divided into a client (any HTML5-compatible browser) who visualizes the 3D geospatial data through the WebGL API, and a server that processes the data based on two libraries: Node.js and three.js. In a first step, the client would load, filter, map and render the 3D geospatial data. Then, the viewpoint management and flythrough creation algorithms would be remotely launched on the server thanks to the WebSocket API. Ultimately, the results (i.e., optimal camera parameters) would be sent to the client, who could thereby visualize the objects of interest in an efficient way, either statically and/or dynamically into an automatic computer animation.

For urban planning, this RESTful web application could even become an efficient tool for contractors, political decision-makers and citizens. In the analysis phase, it could help the presentation of results and therefore facilitate the understanding of urban aspects such as urban patterns and urban environmental issues. In the design and evaluation stages, it could support the comparison of urban projects as the application would allow a better view of pros and cons. In the implementation phase, it could assist the visualization of urban infrastructures that might interact with the land use development. Eventually, it could support the monitoring of cities by assisting the data acquisition on the field. Indeed, the algorithms could assist current flight planning (e.g., drone or airplane) in providing automatic camera viewpoints that efficiently visualize a set of objects of interest within a 3D environment. Furthermore, based on existing 3D CAD files, the algorithms could also support terrestrial laser scanning by effectively locating sensors, and therefore reducing occluded areas in the data acquisition process (Poux et al., 2018; Poux et al., 2017).

## 3.9 Conclusions

In this chapter, we proposed two algorithms for managing occlusion into future hybrid interaction models. They aim to enhance the spatial knowledge acquisition through efficient camera settings, which is a key element to assist contractors, political decision-makers and citizens in the urban planning process. First, an image processing algorithm, called the viewpoint management algorithm, computes a set of best points of view for a series of objects of interest. Then, these viewpoints are integrated into

a flythrough creation algorithm to produce an automatic navigation inside the 3D geospatial model. Ultimately, our algorithms have been illustrated within the scope of fictive exploratory phase for the public transport services access in the European quarter of Brussels.

The static and dynamic management of camera is a real contribution to the 3D geovisualization field, as the viewpoint(s) selection is an integral part of any 3D geospatial data visualization process. It could even be incorporated into 3D viewers as a plugin to efficiently solve the occlusion issue within all urban planning phases. However, there remains visualization issues to be solved, such as the objects' recognition process and the usage of the perspective projection. Eventually, our global proposal, i.e., **the existence of at least one optimal 3D viewpoint for visualizing a set of geometric objects within 3D building models**, is still to be validated, and is performed in the next chapter.

CHAPTER 4

# Experimental study

## 4.1 Preface

This chapter is based on *Identification of the Best 3D Viewpoint within the BIM Model: Application to Visual Tasks Related to Facility Management* (Neuville et al., 2019), an article published within the "Buildings" journal in July 2019. In Chapter 3, we developed a geocomputational method aiming to enhance the 3D visualization of geospatial data based solely on suitable 3D points of view. Through an experimental study conducted with experts, this chapter brings empirical evidence that supports our global hypothesis, i.e., **the existence of at least one optimal 3D viewpoint for visualizing a set of geometric objects within 3D building models**, in particular for a given selectivity task (visual counting) using a BIM model. Hence, this chapter addresses the specific research questions of this thesis and expand the knowledge basis of the 3D geovisualization field.

## 4.2 Abstract

Visualizing building assets within building information modeling (BIM) offers significant opportunities in facility management as it can assist the maintenance and the safety of buildings. Nevertheless, taking decisions based on 3D visualization remains a challenge since the high density of spatial information inside the 3D model requires suitable visualization techniques to achieve the visual task. The occlusion is ubiquitous and, whilst solutions already exist such as transparency, none currently solve this issue with an automatic and suitable management of camera settings. In this chapter, we therefore propose the first RESTful web application implementing a 3D viewpoint management algorithm and we

demonstrate its usability in the visualization of assets based on a BIM model for visual counting in facility management. Via an online questionnaire, an empirical test is conducted with architects, the construction industry, engineers, and surveyors. The results show that a 3D viewpoint that maximizes the 3D geometric objects' view inside the viewport significantly improves the accuracy and the certainty of a visual counting task compared to default software points of view, (i.e., combined front, back, left, and right viewpoints). Finally, this first validation lays the foundation of future investigations in the 3D viewpoint usability evaluation, both in terms of visual tasks and application domains.

**Keywords:** building information modeling; computer maintenance management system; facility management; assets; 3D geovisualization; 3D viewpoint; occlusion; usability; selectivity purpose; visual counting

## 4.3 Introduction

### 4.3.1 Context

Whilst initially employed within the Architecture, Engineering and Construction industry (AEC) as a new way for simplifying the design of a facility and simulating the construction sequencing (Azhar, 2011; Czmoch & Pękala, 2014), building information modeling (BIM) has recently been extended to facility management (FM) as a powerful tool for improving the building performance and managing its maintenance and safety throughout its lifetime (Abbasnejad & Moud, 2013). Defined as the organizational function that encompasses people, place, and process

within the built environment (ISO 41011, 2017), FM is crucial to maximize the lifespan of the building and its equipment (Wetzel & Thabet, 2016), and, if properly managed, it can save significant annual costs (Becerik-Gerber et al., 2012). Moreover, its early incorporation in the design phase can also facilitate maintenance during the operational stage of facilities (Wang et al. 2013).

Within the FM industry, 3D spatial data visualization is fundamental as it enhances the presentation of information, improves communication among stakeholders, enables spatial and spatiotemporal analyses not feasible in 2D, and assists decision-making in assets management (Akcamete et al., 2011; Kyle et al., 2002; Zhang et al., 2009). For instance, 3D geovisualization can facilitate the analysis of spatial relationships in work orders (for planning maintenance activities) or failure root cause detection (e.g., temperature control issues) (Akcamete et al., 2010; Motamedi et al., 2014). With this in mind, an innovative BIM interactive collaboration system for facility management has been newly proposed in (Lee et al., 2016). While this system integrates both a data arrangement and presentation module, the authors point out that it still lacks automation and assistance in data visualization. This is especially true in the 3D viewpoint identification from which the 3D building model should be displayed, since the high density and complexity of assets necessarily lead to occlusion (Elmqvist & Tudoreanu, 2007; Li & Zhu, 2009).

To date, 3D BIM software (such as Autodesk® Revit, Graphisoft® Constructor, and Bentley® Architecture (Azhar et al., 2008)) already

provides tools to manage occlusion by the display of a subset of assets, the application of transparency, the wireframe modeling, and/or through multiple viewports. For instance, the reduction of assets lightens the 3D model, while the application of transparency and the wireframe modeling enhance the visibility of assets that spatially interact with each other. Then, the 3D model can be visualized through a set of default software viewpoints: top-down, side, and at 45 degrees. While this occlusion-solving procedure significantly reduces the occlusion, it does not guarantee that all of the assets of interest are simultaneously visible, which is the prerequisite for any visual analysis or decision-making.

### 4.3.2 Viewpoint management algorithm

Hence, we have designed and implemented a Viewpoint Management Algorithm (VMA) in (Neuville et al., 2019; Neuville et al., 2016) which automates and supplies complete visibility of a set of 3D objects (extracted from spatial and/or semantical queries) within a 3D model. As a reminder, visualizing a 3D geometric object, i.e., any object located in a 3D universe (x,y,z) and built from one of the geometric primitives (point, curve, surface, and solid) defined within the spatial schema ISO 19107:2003 (Pouliot et al., 2008), requires a virtual camera, which acts as a real camera since it "converts electromagnetic radiation from an object into an image of that object and projects the image onto a surface" (American Society of Civil Engineers, 1994). In this research, the 3D geometric object is in three dimensions and the projection surface is plane. Then, a 3D viewpoint of the object can be produced based on the configuration of three parameters

(Neuville et al., 2018): the camera position, orientation, and the focal length. The camera position and orientation are 3D vectors that, respectively, represent a 3D location and a 3D viewing direction into the world coordinate system. The focal length is the distance between the projection center and projection plane, which sets the field of view associated to a camera position and location. In this research, this parameter is set to infinite as we only deal with parallel projections. Finally, note that, in the case of computer animation combining multiple points of view, a vision time can be given to a 3D viewpoint. Figure 18 illustrates the previous parameters.

The specific purpose of the viewpoint management algorithm is to provide an automatic 3D viewpoint that completely visualizes a set of 3D geometric objects. Technically, the algorithm computes the most appropriate camera position and orientation that maximize the 3D geometric objects' view area within the user's viewport, i.e., the visualization window inside a digital display (e.g., desktop computer, laptop, and tablet). To date, the viewport is a visualization window inside a desktop display.

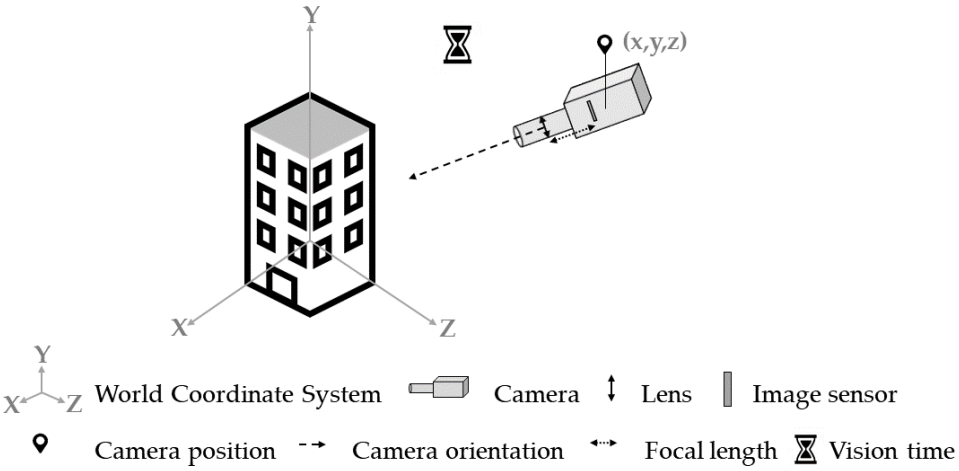


**Figure 18**: A 3D viewpoint and its components: camera position, orientation, focal length, and vision time from (Neuville et al. , 2019).

### 4.3.3 Case study and research questions

While our algorithm has already been used in archeology for facilitating the knowledge dissemination of an ancient mosaic in France (Poux & Neuville, et al., 2017), it has not been assessed for achieving visual tasks yet, which is the purpose of this chapter. It aims to validate the algorithm usability within the given context of facility management based on the BIM model, as it might constitute a promising solution to assist assets management. A specific case study has thus been designed and refers to a selectivity visual task, which is defined according to (Bertin, 1967) as the capacity to visually extract all 3D geometric objects belonging to a given category, and to perceive the image produced by this category. We specifically use color (hue) as the visual variable as it has been shown that

it is one of the most promising solutions for supplying a selectivity task (Pouliot et al., 2013; Rautenbach et al., 2015).

In this research, the visual task consists in visually counting bad condition assets within a 3D building model. The proposed case study extends another one presented in (Motamedi et al., 2014) where 3D visualization is used to identify potential causes of too-high-temperature incidents in a building. In this case study, 3D visualization aims to assist the company in charge of building safety, in particular in the assessment of an ongoing too-hot incident and the most appropriate response to emergency services. We therefore hypothesize that there exists at least one optimal 3D viewpoint for visualizing a set of 3D geometric objects and that this point of view is a function of the objects' view area inside the viewport.

Then, we aim to confirm or reject the suitability of this 3D point of view for visual counting of a set of objects within a virtual 3D building model, which is carried out with the use of the usability criterion. Indeed, usability is the most common variable for user-centered evaluation studies (Van Velsen et al., 2008), and it has already been discussed and employed in the visualization of 3D building models, especially in the 3D cadastre field (Oosterom et al., 2010; Shojaei et al., 2013). Most recently, this criterion has even been considered in the evaluation of transparency for delimitating property units with their physical counterparts (Wang et al., 2017). According to the ISO 9241-11, usability refers to the "extent to which a system, product or service can be used by specific users to achieve specified goals with effectiveness, efficiency, and satisfaction in a specified

context of use". Within the literature, there exists multiple interpretations linked to these three criteria (effectiveness, efficiency, and satisfaction). In this chapter, we refer to the definitions proposed in (Abran et al., 2003):

1. Effectiveness, i.e., how well users accomplish their objectives with the system;
2. Efficiency, i.e., the resources used to accomplish the objectives;
3. Satisfaction, i.e., users' feelings about the use of the system.

Note that only two quality conditions have been considered: effectiveness and satisfaction. Effectiveness is measured by two distinct indicators: the accuracy in performing the visual counting and the amount of time required to visually detect one 3D geometric object on the condition that visual counting has been accomplished with success. Finally, satisfaction is measured by the participants' certainty in achieving the visual task. Note that the participant's certitude has been preferred to his/her satisfaction for a more visual task-centric appreciation, similar to (Wallach & Scholz, 2012). To sum up, three quality indicators are considered:

- The accuracy in performing the visual task;
- The speed in carrying out the visual task;
- The certainty degree with which the user undertakes the visual task.

Ultimately, the usability of our best 3D point of view is also assessed according to the user's attributes, i.e., his/her background training, his/her decision-making level and his/her experience in 3D visualization.

### 4.3.4 Software architecture

Whilst initially developed into a client-side application, we propose in this chapter the first VMA implementation within a complete RESTful web application, with the visualization and processing stages divided between the client and the server. This has been made possible by the use of Node.js, a Javascript runtime (built on Chrome's V8 Javascript engine) that offers a Javascript environment server-side. As seen in Figure 30, the 3D spatial data visualization is performed on any HTML5-compatible browser through the WebGL API, while the best 3D viewpoint computation is supplied remotely by the server. Contrary to a client-side application, this architecture better addresses the end-users' needs as it does not require powerful visualization tools in terms of computer memories and high-end graphics boards. Moreover, the application tends to be more seamless. Technically, the client connects to the website of the application, from which he/she can upload a 3D model. Then, he/she is able to filter, map, and render the spatial data as a function of the semantic information that he/she intends to display. Once the latter has been carried out, the client sends the 3D model with its mapping and rendering aspects to the server via the WebSocket API. After that, the server recreates a partial copy of the 3D model based on the client's visual configuration.

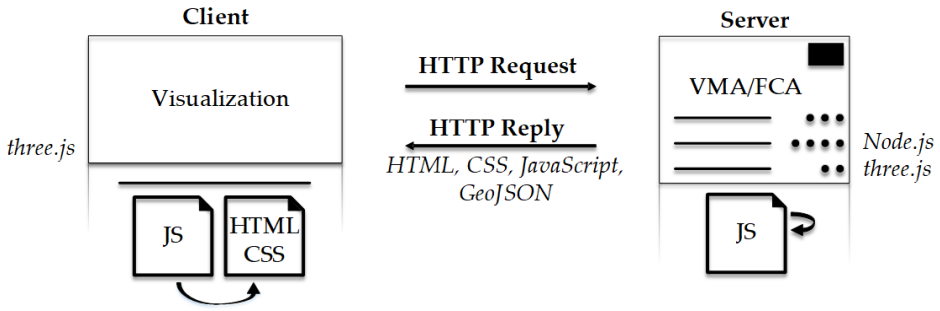


**Figure 30**: A complete RESTful web application managing the 3D viewpoint. The 3D visualization process is carried out client-side (via WebGL) while the computation process is supplied server-side thanks to Node.js and three.js, from (Neuville et al., 2019))

The geometric objects of the 3D scene are then divided into two categories: the objects of interest (i.e., the subjects of the study) and the visualization context objects (i.e., the additional surrounding features). The data are then processed and the server sends the results to the client, i.e., two sets of three-dimensional coordinates, which optimally locate and orientate the camera in the 3D scene in order to maximize the visibility of the objects of interest within the viewport.

The chapter is structured as follows. Section 4.4 is dedicated to the experimentation design and illustrates the study case. Section 4.5 statistically analyzes the results, while Section 4.6 discusses the outcomes, presents the research limitations, and addresses perspectives.

## 4.4 Experimentation design

### 4.4.1 Empirical approach

As it has been reported that the data visualization field requires empirical evidence to support its development (Green, 1998), an empirical approach is thus employed to answer the research questions. Moreover, this scientific method also constitutes the cornerstone of user-centered design in software development (Wallach & Scholz, 2012).

Technically, the empirical study was carried out in the form of interviews with the use of an online questionnaire, which has the advantages of simultaneously dealing with a larger number of participants and automating the data recording. Within this questionnaire, participants have to answer a set of twelve independent tests that always provide the same questions and potential answers. Note that the visualization techniques applied to the 3D model are kept constant over time, which means that the 3D viewpoint and the set of selected assets are the only parameters that change among the simulations.

Then, we specifically invited several groups of experts to participate in the survey and complementary information was provided to improve the visual task understanding. Whilst this strategy is more restrictive than a real online questionnaire released on the web in terms of participant numbers (Lazar et al., 2010), it guarantees a better comprehension of the task and therefore more reliable results (even with a smaller sample size).

Indeed, it has been shown that only five participants already detect 80% of usability issues (Virzi, 1992).

### 4.4.2 3D Building model

The case study was carried out on an existing architectural and mechanical, electrical and plumbing (MEP) project provided by Autodesk® Revit from which a non-textured black and white 3D model was extracted. Then, we hypothesized that a computer maintenance management system (CMMS) was integrated to the BIM model, which enabled a constant asset condition update through multiple sensors located inside the building, similar to (Motamedi et al., 2014). Figure 31 illustrates the 3D building model and shows some windows in red as an example of visual detection of rooms with an internal too-high temperature. Only a small set of assets from the initial BIM model was kept in order to enhance the overall visibility of the 3D model. Furthermore, the black and white appearance enables a better visual contrast between the highlighted windows and the surrounding environment. Transparency was then applied to all windows to improve the realism of the model and consequently its visual understanding. Ultimately, the lighting of the 3D model consists of a global ambient light and a directional light emitted from the camera location in the direction of the 3D model, which specifically enhances the lighting in the viewing direction of highlighted windows. Note that a shading effect is also produced as it assists in revealing the objects' shape.

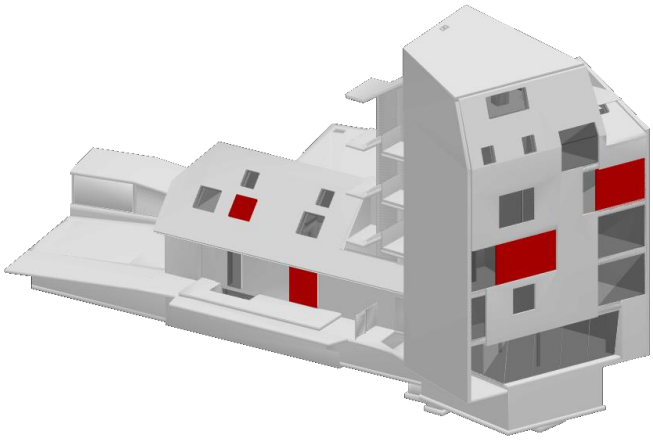

**Figure 31**: A 3D building model and example of visual detection of rooms with an internal too-high temperature

Then, the case study consisted in visually counting the number of highlighted windows within the 3D model from one or multiple 3D viewpoints. Twelve fictive internal too-high temperature incidents were created and were either visualized from:

- The four default combined software side points of view (4 simulations out of 12);
- A single side point of view, i.e., either from a front, back, left, or right viewpoint (4 simulations out of 12);
- Or a point of view that maximizes the 3D geometric objects' view area inside the viewport, and provided by the viewpoint management algorithm (4 simulations of out 12).

Note that the simulations are independent of each other, which means that there is no correlation between the tests; all configurations are possible and might partially reappear. As a result, the carryover effect is avoided. Furthermore, the overall complexity linked to the visual counting achievement is kept as constant as possible among the three sorts of point of view. Indeed, the four simulations linked to each kind of viewpoint include the visual counting of either four, five, six, and seven highlighted windows.

### 4.4.3 Online questionnaire

The online questionnaire has been built as a website designed with Bootstrap, an open-source front-end framework. It incorporates a MySQL server for storing the participants' profile and their responses. The questionnaire contains three main sections:

1. The first section is related to the participant's attributes. For this purpose, the participant must answer four questions linked to: his/her training background, the decision level to which he/she usually works, his/her frequency of visualizing 3D building models, his/her potential color perception deficiency.
2. The second section presents the 3D building model of the survey, sets the context of the case study, and proposes a demonstration test from which the participant gets acquainted with the questions and the procedure for answering.
3. The third section is the survey. The participant must answer twelve questions related to fictive too-high temperature incidents

occurring inside the building. As a reminder, three kinds of viewpoint are provided: the four default combined software side points of view, a single point of view, and the point of view provided by the viewpoint management algorithm.

Figure 32 illustrates the first section of the questionnaire with the four questions related to the participant's profile. Figure 33 shows the contextual setting of the survey and Figure 34 displays the first three simulations of the survey. As shown in Figure 34, the participant must answer two questions for each simulation:

- Question 1: How many distinct windows are highlighted in red in the 3D model?
- Question 2: What is the degree of certainty of your answer? Possible options: totally certain, quite certain, quite uncertain, and totally uncertain.

The first question aims to measure the effectiveness parameter, i.e., the participant's ability to visually count the number of bad condition assets within the 3D model correctly. The purpose of the second question is to measure the satisfaction linked to the visual counting task, i.e., the certainty with which the participant answers the first question. Then, the response time to complete the task is also stored as a measurement of the effectiveness criterion.

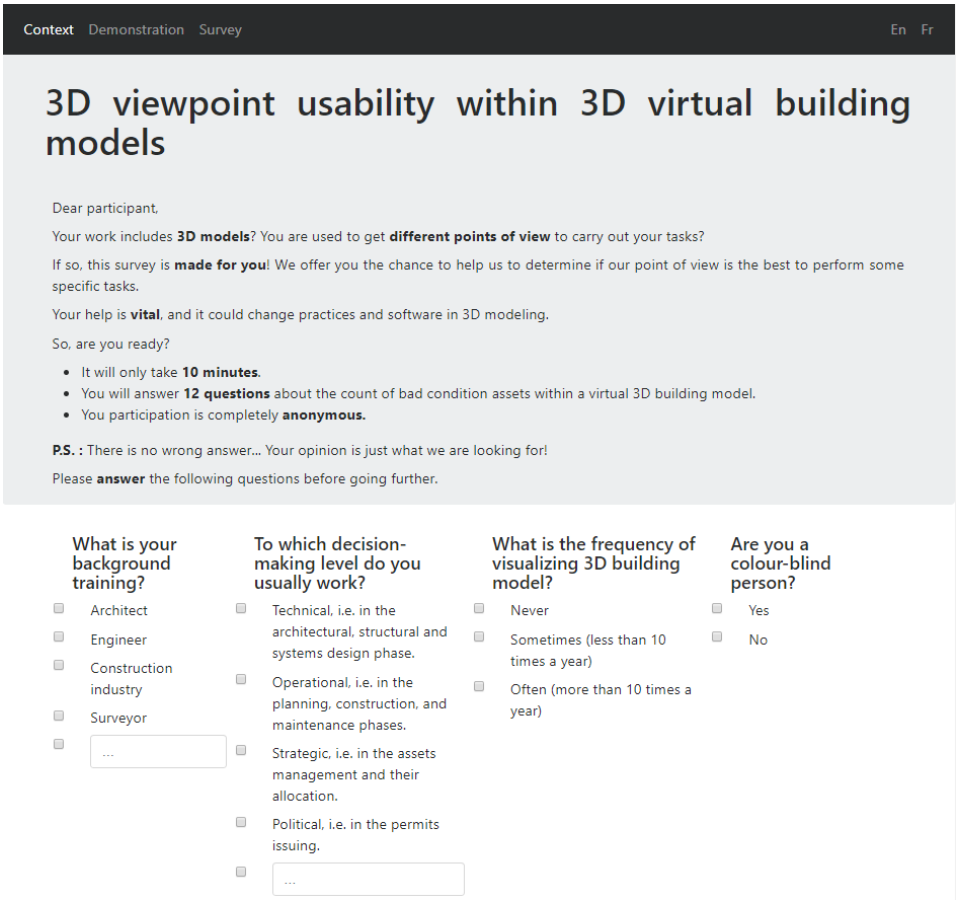


**Figure 32**: Website: Participants' attributes (section 1 of the questionnaire)

Note that the timer is not activated for the traditional four side points of view. Indeed, the analysis of four images inevitably entails a longer response time compared to a single point of view. Finally, since the number of objects to be visually detected impacts the overall response time, the latter is reduced to a visual counting time per object in the statistical analysis.

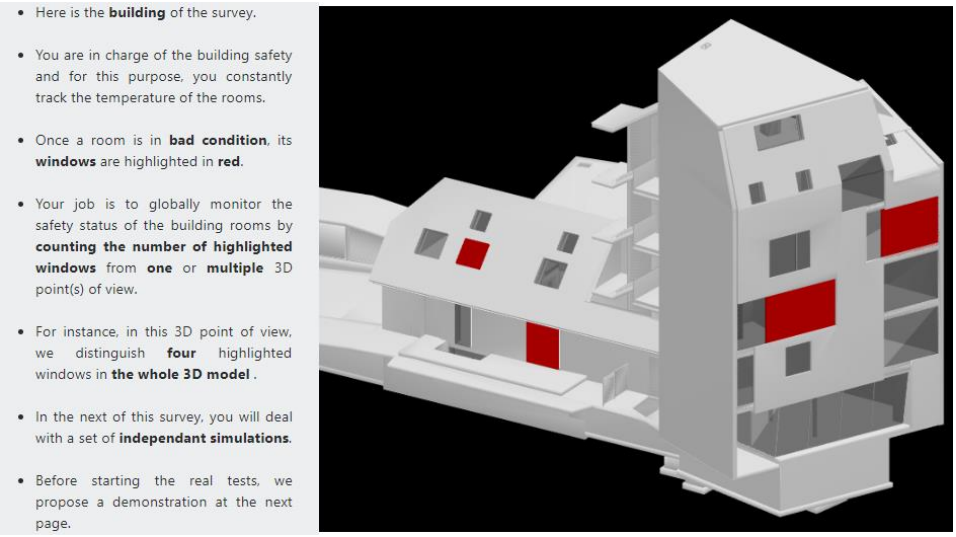


**Figure 33**: Website: contextual setting of the survey (section 2 of the questionnaire)

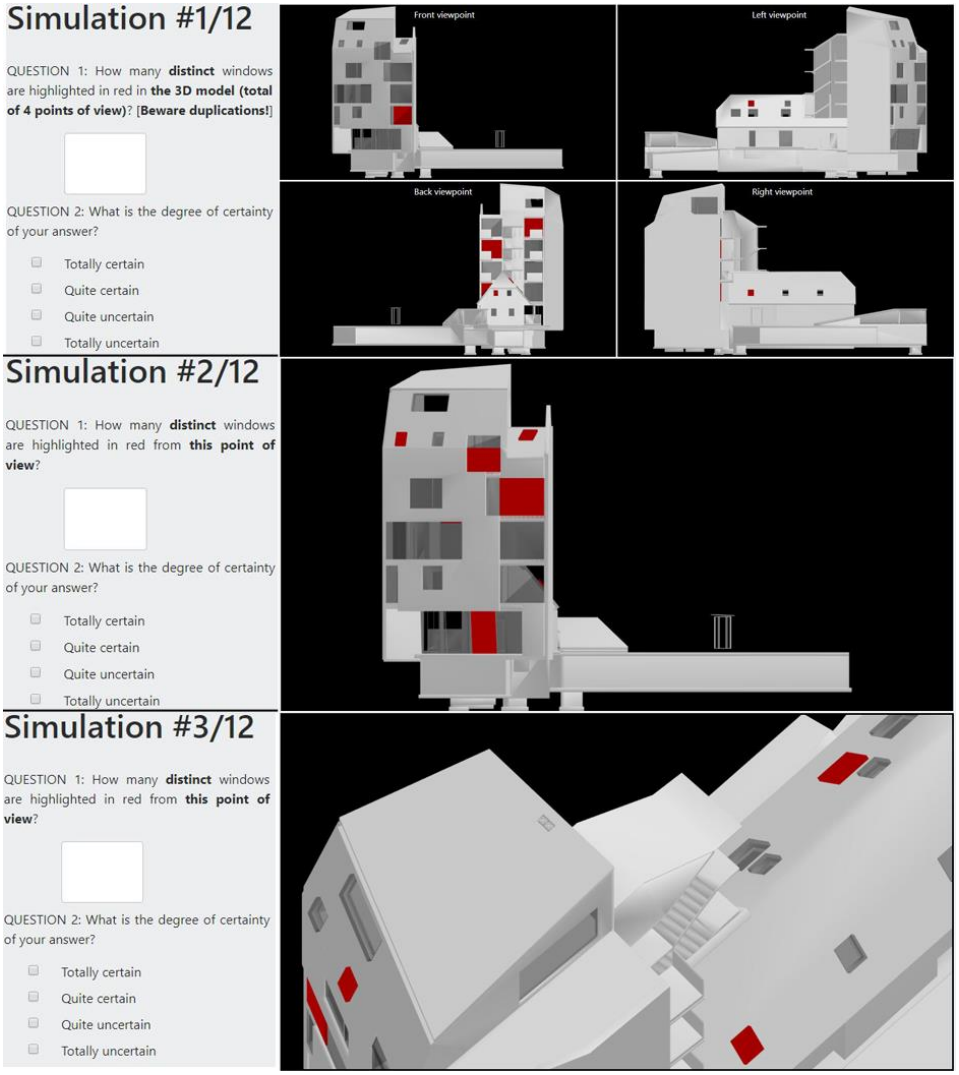


**Figure 34**: Website: the first three simulations of the survey (section 3 of the questionnaire)

## 4.5 Results

### 4.5.1 Participants' profile

Accessible through a consistent URL (3dviewpoint-survey.uliege.be), the website was visited by 48 participants from May to July 2019. Among these participants, six suffered from color perception deficiency and six did not fully complete the questionnaire. The statistical analysis was thus performed on a set of 36 participants[4] with the following characteristics:

- Background training: 13 surveyors, 13 engineers, 9 architects, and 1 expert from the industry construction.
- Decision-making level: Most of the participants (27 out of 36) usually worked at the technical level (i.e., in the architectural, structural, or systems design phases); 6 worked at the operational level (i.e., in the planning, construction, or maintenance phases); and 3 participants worked at the strategic level (i.e., in the assets management and their allocation).
- 3D visualization experience: More than half of the participants (29 out of 36) were used to visualizing 3D building models: 21 on a regular basis (i.e., more than ten times a year) and 8 more sporadically (i.e., less than ten time a year). Note that only 7 participants had never visualized 3D building models before the experiment.

[4] The survey results (anonymous) are provided in Appendix 1.

**Table 6**: Research questions and associated statistical methods.

| *Research question* | Criterion | Type of input data | Statistical method | Alpha |
|---|---|---|---|---|
| ***Accuracy*** | Effectiveness | Quantitative (ratio and discrete) | Exact binomial | 5% |
| ***Speed*** | Effectiveness | Quantitative (ratio and continuous) | ANOVA (one-way) | 5% |
| ***User's Certainty*** | Satisfaction | Qualitative (ordinal) | Chi-2 | 5% |

### 4.5.2 Statistical Analysis: Overview

The statistical analysis was carried out with the software environment R[5]. Three distinct statistical methods were applied to answer the research questions: the exact binomial test, the Anova (one-way) and the Chi-2 test. They are summarized in Table 6 and discussed in more detail in the next sections.

### 4.5.3 Is a 3D viewpoint based on the maximization of 3D geometric objects' view area more accurate for the selectivity task of a set of objects within a virtual 3D building model compared to the default combined software points of view?

The exact binomial test shows that maximizing the 3D geometric objects' view area inside the viewport significantly improves the achievement of a

[5] The statistical analyses codes are provided in Appendix 2.

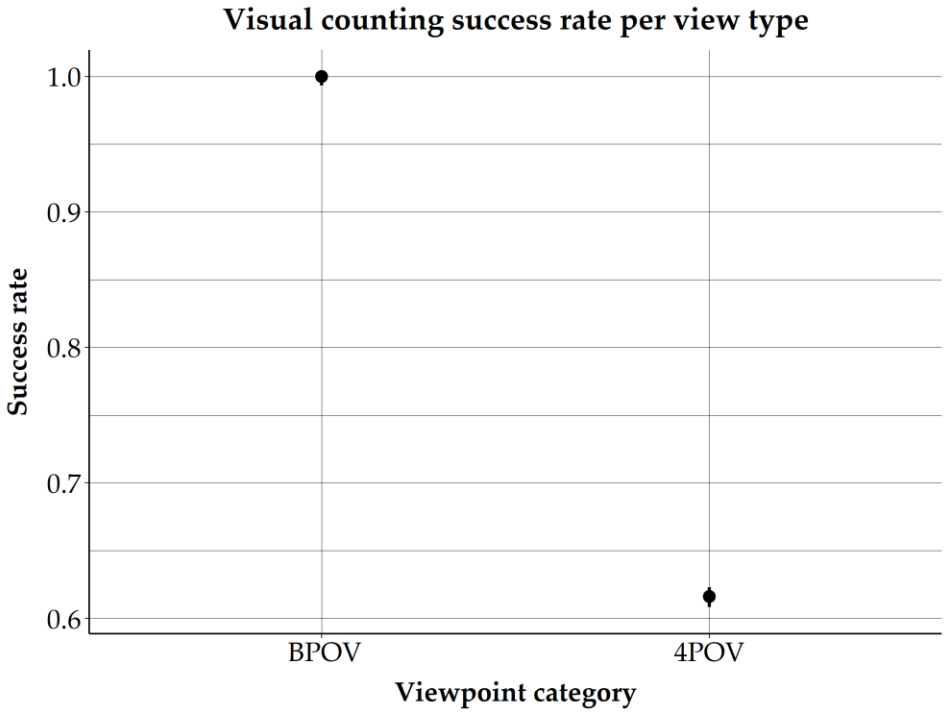


**Figure 35**: Exact binomial test. Visual counting success rate associated to the 3D viewpoint maximizing the 3D geometric objects' view area inside the viewpoint (BPOV) and the four default combined software side points of view (4POV).

visual selectivity task compared to the four default combined software side points of view. The overall mean success rate associated to the four side points of view is around 59.7%, while it reaches 100% for the point of view generated by the viewpoint management algorithm (Figure 35). Note that the exact binomial test has been preferred to the standard binomial test as the 3D viewpoint that maximizes the 3D geometric objects' view area did not meet the initial application condition of a standard binomial

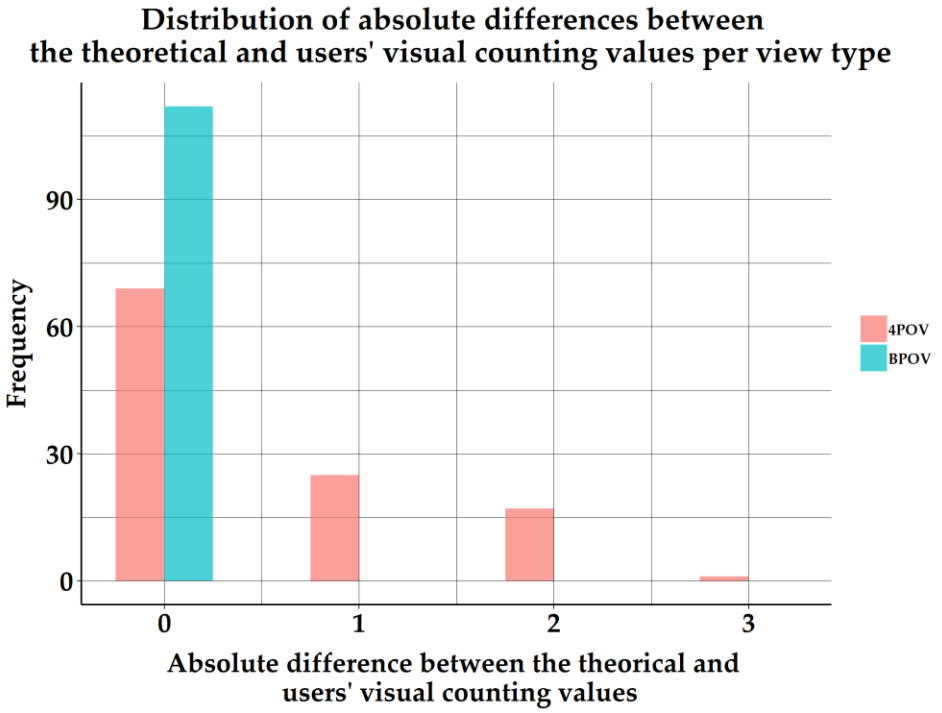


**Figure 36**: Distribution of absolute differences between the theoretical and user's visual counting values per view type. 4POV: the four default combined software side points of view; BPOV: the best point of view, i.e., the viewpoint maximizing the 3D geometric objects' view area within the viewport.

test; n*p*q was lower than nine (n being the number of observations, p the probability of success, and q the probability of failure). Finally, a further analysis of the answers (Figure 36) shows that users, when miscounting the exact number of windows, usually committed an error of one window in visual counting.

### 4.5.4 Does a 3D viewpoint based on the maximization of 3D geometric objects' view area enhance the user's certainty when visually selecting a set of objects within a virtual 3D building model compared to the default combined software points of view?

Prior to the statistical Chi-2 test, the initial measurement scale was reduced to two categories in order to meet the minimum number of observations per class (5). To achieve that, the frequencies associated to the totally uncertain, quite uncertain, and quite certain classes were merged; the totally certain class was not rearranged. Then, the application of the Chi-2 test showed that maximizing the 3D geometric objects' view area significantly improves the degree of certainty of participants when achieving the counting task (p-value: $2.2 \times 10{-}16 < 0.05$). As shown in Figure 37, participants are usually totally certain (category 3) when performing the visual counting from this point of view. In contrast, they are generally less confident when dealing with the four default combined software side points of view. Besides, note that the participants were never uncertain when performing the visual task with the best point of view. They were at least quite certain of their answer.

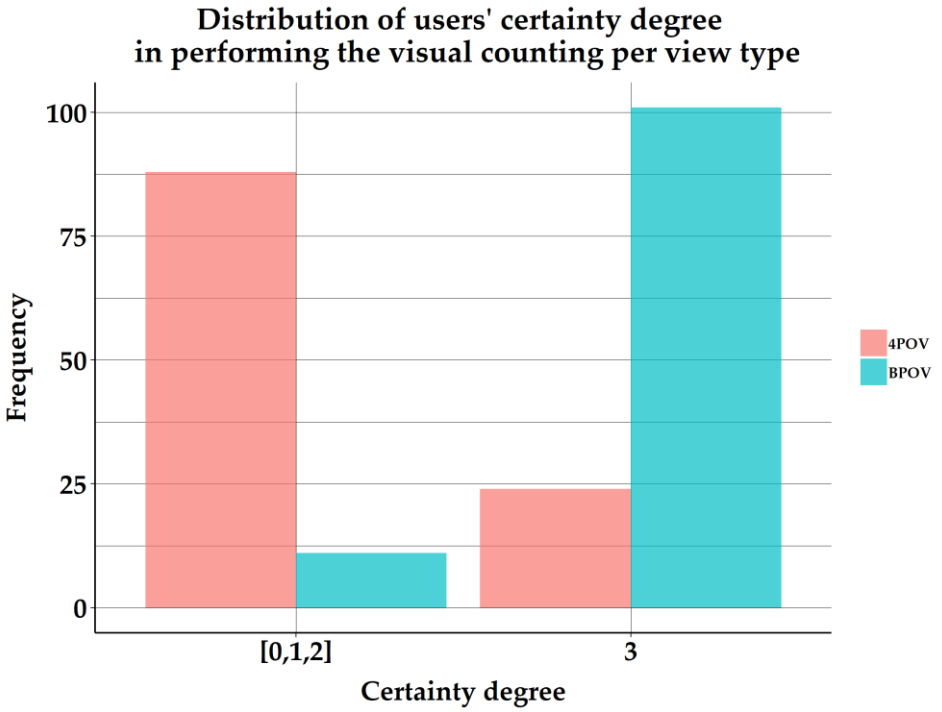


**Figure 37**: Distribution of users' certainty degree in performing the visual counting per view type; 4POV: the four default combined software side points of view; BPOV: the best point of view, i.e., the viewpoint maximizing the 3D geometric objects' view area within the viewport. The categories 0, 1, and 2 (respectively, totally uncertain, quite uncertain, and quite certain) have been merged to meet the minimum number of observations per class (5).

### 4.5.5 Does a 3D viewpoint based on the maximization of 3D geometric objects' view area make the selectivity task of a set of objects faster within a virtual 3D building model compared to a given default software point of view?

Before conducting the ANOVA, the response time was firstly reduced to a visual counting time per object. Furthermore, only response times related to questions correctly answered were considered in the statistical analysis. Performed on these time values, the statistical analysis shows no significant difference in speed between a single side point of view and the viewpoint maximizing the 3D geometric objects' view area inside the viewport (p-value: 0.07 > 0.05). The average visual detection speed per object is around 1.57 s, while it reaches 2.0 s with the side point of view. Figure 38 displays the distribution of registered visual counting times per object, which are grouped by view type.

Note that two outliers (from the single side point of view) were visually removed to improve the reading; their values exceeded 24 s. Whilst no significant difference could not be demonstrated (at the confidence level of 95%), it is worth noticing that the single side point of view shows a higher variability in the response times compared to the best 3D viewpoint.

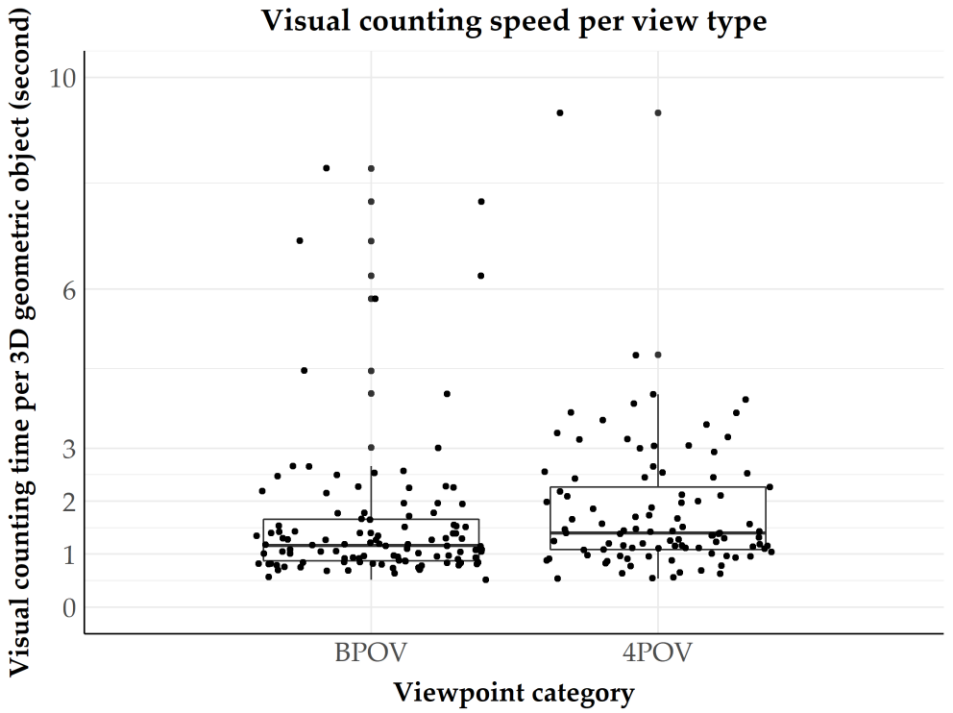


**Figure 38**: One-way ANOVA. Visual counting speed per view type associated to the 3D viewpoint maximizing the 3D geometric object's view area inside the viewpoint (the best 3D point of view) and the single side 3D points of view. 4POV: one of the the four default software side point of view; BPOV: the best point of view, i.e., the viewpoint maximizing the 3D geometric objects' view area within the viewport.

#### 4.5.6 Do the user's attributes (background training, decision-making level, and experience in 3D visualization) influence the usability of the 3D viewpoint that maximizes the 3D geometric objects' view area inside the viewport?

As all participants of the survey successfully detected the right number of bad condition assets with the 3D precomputed viewpoint, there is thus no effect on the accuracy criterion. Then, the results show that the training background, the decision-making level, and the experience in 3D visualization have no significant effect on the response time (at the confidence level of 95%). Note that, since there was only one participant from the construction industry, this attribute was not taken into account in this statistical analysis. Finally, the results also indicate that the training background, the decision-making level (except for the strategic level for which the number of observations per category did not meet the statistical test conditions), and the experience in 3D visualization have no significant effect on the level of certainty.

## 4.6 Discussion

### 4.6.1 Back to the research questions

Within the given framework of facility management, the results support that a 3D viewpoint that maximizes the 3D geometric objects' view area inside the viewport improves the accuracy and user's certainty of a visual counting task compared to the four default combined software side points of view. The statistical analyses even show that these two criteria are

highly enhanced (p-value < 0.001). These findings are therefore promising in the perspective of including 3D spatial data visualization in decision-making procedures, especially when it comes to safety procedures. In the case of fire detection or propagation, the company in charge of the building safety might, for instance, provide a quicker and better evaluation to the emergency services. The deployment of required resources (both human and material) might then be enhanced and lead to facilitating the work in the field.

However, the hypothesis that our point of view makes the visual counting of objects faster compared to a single side point of view could not be demonstrated at the 5% significance threshold. However, we can still notice that the best 3D point of view shows a lower variance, which may be explained by a higher consistency in the visibility of 3D geometric objects within the viewport. Moreover, the single side point of view greatly limited the choice of objects to be visualized due to their visibility requirement inside the viewport; the objects were usually close to each other, which may have facilitated the visual task achievement and reduced its completion time. In contrast, the precomputed point of view was applied on a more scattered spatial distribution of objects, which is more representative in practice. As a result, although no statistical effect could be found on the visual counting speed, our point of view still seems a promising solution for conducting such a visual task as it still performs faster than the four default combined software side points of view and is more suitable for actual scenarios in facility management.

Finally, visual counting accuracy and speed (linked to the best 3D viewpoint) are not influenced by the background training, the decision-making level, and the experience in 3D visualization. The same applies to the certainty degree of the 3D best point of view, except for the strategic level for which the number of observations per category did not meet the statistical test conditions. To deeply analyze the effect of this decision-making level on the certainty degree, a higher number of participants is required and is vital to develop user-centered design strategies.

### 4.6.2 3D viewpoint in the 3D geovisualization process

Within the 3D geovisualization process, the results tend to support the key role of 3D viewpoint in achieving specific visual tasks. While the visualization techniques applied to the 3D building model were kept constant throughout the experiment, we show that the achievement of a selective task (visual counting) can be greatly enhanced from a suitable 3D point of view. Initially included into the rendering aspect as variables of vision (Semmo et al., 2015), the camera settings should thus be removed and considered as an external processing stage, since they clearly impact the completion of the visual task.

Beyond the theoretical outcomes, this work also proposes a first RESTful web application for managing 3D viewpoint. Developed as a client-server application that can leverage the power of remote computers, the application could become a promising operational solution to be incorporated to existing online 3D viewers. This architecture could even be deployed on any kind of device (from desktop computers and laptops

to tablets and smartphones), as the processing stage is performed remotely. The only parameters sent by the server to the client are two sets of three dimension coordinates that automatically locate and orient the camera inside the 3D scene. Note that these two sets of coordinates could even be incorporated into the visualization of the OGC Web Terrain Service as a powerful way to improve the understanding of the 3D scene (Open Geospatial Consortium, 2001). For that purpose, the 3D coordinates of the best camera location should be converted into the OGC specifications: the distance from the point of interest (which is the 3D vector that fits the camera viewing direction), the pitch and yaw angles.

### 4.6.3 Limitations and perspectives

First of all, only 36 experts participated in the survey, which is too small for the development of real user-centered design strategies. Consequently, the results must be interpreted with caution and a higher number of participants is required to achieve a greater confidence in the findings. Whilst the questionnaire was only deployed on the web for facilitating access during the interviews, no publicity actions were undertaken to introduce the questionnaire to a wider audience. Yet, this latter step should be required in the future in order to increase the sample size, although it does not guarantee the same degree of reliability as for interviews. Note that professional social networking sites (e.g., LinkedIn) could also be used so as to reach worldwide experts from the field.

Then, the visual counting task was only carried out on the windows of the 3D building, i.e., on objects visible from the outside. A more practical use

case in facility management also requires 3D assets located inside the building, e.g., temperature or carbon monoxide sensors, ducts, and cabling. Since these objects are fundamentally occluded from an exterior 3D point of view, additional visualization techniques should be simultaneously applied.

Then, the experiment was only performed on one specific selective task: visual counting. However, the selectivity interpretation task also includes other assignments, such as the location of one or multiple asset(s) or the extraction of semantic information. As such, additional investigations could therefore be conducted in the future.

Furthermore, the maximization of the 3D geometric objects' view area within the viewport was used as the only indicator that defined the viewpoint optimality criterion. This choice was driven by the selective task (visual counting) and the visualization conditions (the objects of interest were clearly contrasted from their surrounding). In the future, new or additional indicators could be proposed to specifically meet the requirements of other visual tasks. For that matter, an existing list of descriptors can be found in (Lee et al., 2005; Page et al., 2003; Polonsky et al., 2005; Vazquez et al., 2001).

Beyond its use in facility management, the viewpoint management algorithm could be extended to the design phase of buildings as a way to facilitate the understanding of clash (or collision) detection. To date, current BIM software already provides algorithms to automatically detect clashes among architectural, structural, and MEP components (Azhar,

Sattineni, & Hein, 2010), along with a log and clash images. However, we noted that the software illustrations are not based on any specific design guidance. A 3D viewpoint management module linked to suitable visualization techniques could therefore enhance the comprehension and solution of clash detections.

Finally, to date, our proposal has only been applied on 3D spatial data visualized through monitor-based displays, and thus via the monoscopic vision. With the ongoing and growing development of virtual reality, the automatic 3D viewpoint selection could be applied to enhance the stereoscopic experience, such as fly and walk-troughs, for better interaction with the designed space. For instance, it could be a part of a BIM-game system, i.e., an approach integrating both building information modeling and gaming, to improve architectural visualization and education (Yan et al., 2011). In such systems, the algorithm could also enhance the visualization and understanding of simulations of physical building dynamics and behaviors of virtual building users.

## 4.7 Conclusions

In this chapter, we propose the preliminary experiment to validate the general hypothesis that there exists at least one optimal 3D viewpoint for visualizing a set of 3D geometric objects and that this point of view is a function of the objects' view area inside the viewport. Applied to visual counting of assets based on a BIM model in facility management, the study shows that visual counting accuracy is significantly enhanced with our 3D viewpoint compared to the four default combined software side points of

view. The same is also true with respect to the certainty with which users undertake the visual task. In facility management, the viewpoint processing algorithm could therefore enhance the safety monitoring of buildings and the communication process with emergency services. The algorithm could even be a part of existing 3D online viewers, as it is already implemented as a web application.

The findings from this research also enrich the knowledge in the 3D geovisualization field as they stress the importance of 3D viewpoint as a key parameter in the visualization process of 3D models.

Moreover, only a few works in the domain use the experimental approach to validate their results, making the developed experimental setup innovative. In the future, 3D geovisualization-related studies could thus take advantage of this scientific approach.

Note taht the hypothesis that a 3D viewpoint that maximizes the 3D geometric objects' view area makes the visual counting of 3D geometric objects faster compared to a single side point of view could not be demonstrated. However, the statistical analysis shows promising results, leading to the conducting of additional surveys. Eventually, this work also lays the foundation of eventual future investigations in the 3D viewpoint usability evaluation, in terms of visual tasks to be performed, 3D objects to be visualized, and visualization supports.

CHAPTER 5

# Back to this research

## 5.1 Preface

This chapter proposes a reflexive feedback on Chapters 2, 3 & 4, and more generally, on this four years of research. It also deals with a set of research opportunities and give details on how these research directions could be addressed in the future. Eventually, this chapter also presents preliminary results of an ongoing study related to the 3D visualization of topological relationships among geometric objects.

## 5.2 Reflexive feedback

### 5.2.1 Chapter 2 - 3D Geovisualization

Shifting from the 2nd to the 3rd dimension (in terms of visualization) offers new opportunities in the transformation process of geospatial data into geoinformation, especially as it is more consistent with the human visual system. However, although 3D virtual worlds enable a more intuitive interaction with the spatial content, they bring more fields of expertise into play. Beyond 2D cartography, 3D geovisualization incorporates approaches from computer graphics and vision, psychological and physiological aspects, social sciences… This interdisciplinary nature is fascinating but makes the research more challenging.

In this thesis, we specifically considered the 3D geovisualization domain from a geomatics engineering perspective and we attempted to contribute to the field development from a semiotics-related approach. Based on the literature review, we noted that 3D geovisualization lacked of consistency in the visual communication process, especially in putting the domain

knowledges (visualization techniques and visual targeted purposes) in perspective. Graphical (and potentially semantic) inconsistency was therefore wide open, which brought the need to support users in the 3D graphical design of virtual geospatial models.

Hence, in Chapter 2, we proposed the first attempt to formalize (as a knowledge network) the 3D geovisualization process, especially from a semiotics point of view, i.e. including both an expression (i.e., visual stimuli) and content plan (i.e., the semantic world). We did not pretend to solve all graphical conflicts occurring in the 3D visualization process of geospatial data, but we do believe that this formalization framework will reduce their development, and subsequently will allow a more suitable visualization of 3D geospatial data.

Note that, to date, the proposed knowledge network only incorporates a limited number of visualization techniques and visual targeted purposes. In the future, the network should therefore be updated with the outcomes of additional (and more recent) studies. Furthermore, the usability of our knowledge network for achieving given user-centered visual purposes should still be evaluated. Empirical studies should thus be conducted in order to demonstrate how a design support tool (that implements our knowledge network) could assist the graphical design of virtual 3D models, and thus be of benefit to users of 3D geospatial data.

### 5.2.2 Chapter 3 - 3D Viewpoint Management

In the previous chapter, we undertook a formalization process aiming to give structure to the 3D geovisualization field. Through this work, we realized that moving to the 3rd dimension strengthens the role of the viewpoint. Indeed, as the camera is no longer simply only oriented in a classic top-down direction (which is usually the case when visualizing data in 2D), the point of view now needs to be configured, especially in order to optimize the visualization techniques relevance in achieving given visual targeted purposes; and, due to the 3D graphical representation of geometric objects, this configuration is complex, in particular because occlusion issues are inevitable. That is why the viewpoint selection becomes a real research issue in 3D, and for this purpose, this thesis addresses this topic.

Hence, in Chapter 3, we provided two algorithms (called viewpoint management and flythrough creation algorithms), aiming to assist users in the 3D viewpoint selection of a set of geometric objects to which visualization techniques have been applied. In this research, the maximization of 3D geometric objects' view area within the viewport was used as the only indicator that defines the point of view optimality criterion. Note, however, that additional descriptors (both geometric and/or image-related) could be proposed to widen the application scope of these algorithms (e.g., for the recognition and classification processes).

Eventually, to date, the algorithms are only incorporated as additional modules following the filtering, mapping and rendering stages. However,

in the future, these algorithms could also be integrated at the beginning of the visualization pipeline. Indeed, the viewpoint management algorithm could be used to support and automate the generalization operators choice to be applied within the 3D model. For instance, the algorithm could be initially applied on the only selected 3D objects of interest. Then, from the best precomputed viewpoint, the 3D model would be automatically generalized in order to locally reduce the occlusion on the selected features: e.g., via an automatic selection of visualization context objects (VCOs) to be displayed (filtering stage), an appropriate level of details and/or the application of occlusion management techniques to be applied to VCOs (mapping stage).

### 5.2.3 Chapter 4 – Experimental study

In Chapter 3, we proposed a geocomputational method that assists the 3D viewpoint selection in the visualization process of a set of geometric objects of interest to which visualization techniques have been applied. However, this solution had still to be validated, which was performed in Chapter 4 via the elaboration of an experimental study aiming to answer the three specific research questions, summarized as follows:

> Does a 3D viewpoint based on the maximization of 3D geometric objects' view area **enhance (1) the accuracy, (2) the user's certainty, and (3) the speed** when visually selecting a set of objects within a virtual 3D building model compared to the default combined software points of view?

In May and June 2019, we therefore conducted a study with experts, specifically in the form of interviews using an online questionnaire. Based on a BIM model (provided by Autodesk Revit®), participants had to deal with a set of twelve independent and non-correlated simulations related to a given selectivity task: visual counting. The results of this study (36 participants) showed that, based solely on a 3D viewpoint that maximizes the 3D geometric objects' view area, **(1) visual counting accuracy is significantly improved** compared to the four combined default software side points of view. **The same applies to the (2) certainty with which users** conduct visual counting. Nevertheless, in comparison to a single side point of view, **users do not undertake (3) the visual task faster**.

Note that this study assessed the usability of our viewpoint in relation to the four combined default software side points of view, which is one specific point of comparison (amongst others). This choice is not meaningless as these viewpoints allowed a global view of the whole 3D building model (similarly to a user who navigates inside the 3 model). However, in practice, users usually go beyond these static viewpoints. In the future, it would therefore be interesting to evaluate our 3D point of view compared to an interactive user's experience with the 3D spatial content: e.g., the amount of time spent searching an optimal 3D viewpoint, the proximity with our precomputed point of view…

Nevertheless, it should be noted this new point of comparison induces the appearance of a carry-over effect (i.e., the effect that the knowledge of a previous experimental condition affects the participant's performance in

further tests) if performed on the same 3D geometric objects. Special attention should therefore be addressed to perform such tests on different sections of a 3D model (for instance).

## 5.3 Perspectives

Following the outcomes and limits of this thesis, we propose a set of research opportunities for future investigations.

### 5.3.1 How to model and visualize 3D topological relationships?

In this thesis, the geocomputational method (on best 3D viewpoints identification) has only be validated within the visual counting task (selectivity purpose). With this in mind, in September 2019, a new survey, in association with the City of Montreal, has been launched in order to evaluate the geocomputational method usability in the visual identification of 3D topological relationships among disjoined and intersected geometric objects. Although preliminary, the results of this investigation supports that a 3D viewpoint that maximizes the 3D geometric objects' view area enhances the accuracy and users' certainty in the visual identification of 3D topological relationships (among disjoined and intersected objects). A more detailed analysis of this survey is provided below.

#### *5.3.1.1 Context*

The case study was carried out on a virtual 3D model of the *Planetarium Rio Tinto Alcan* (provided free of charge by the city of Montreal) in which property issues take place. Indeed, the city of Montreal reported difficulties in visualizing (in 3D) easements, specifically in the visual identification of 3D topological relationships between existing easements and geometric objects (Figure 39). For that purpose, we conducted an investigation aiming to demonstrate the 3D viewpoint management algorithm usability in visually identifying 3D topological relationships (in particular among disjoined and intersected geometric objects) compared to the four combined default software points of view: top-down, side (pointing to the two planimetric axes), and at 45 degrees.

Due to the relatively short period of time available for this survey, we still compared the geocomputational method usability with the default software points of view. However, note that this methodology is not meaningless in this specific case study, since it avoids the carry-over effect that could have be induced with an interactive experience of the 3D model.

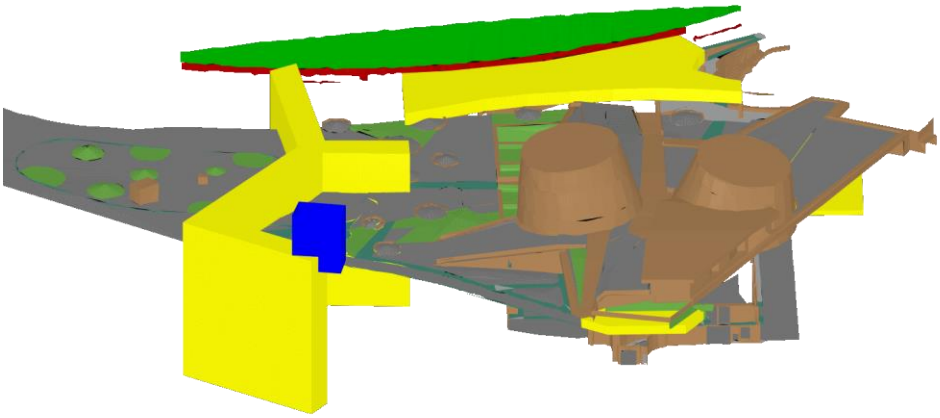

**Figure 39**: Virtual 3D model of the Planetarium Rio Tinto Alcan (Montreal) in which easements are represented in yellow. In this survey, participants have to identify the topological relationship between an object in blue and an easement in yellow. In this example, the blue object intersects an easement (in yellow).

#### *5.3.1.2 Online questionnaire*

Similarly to the experimental study presented in chapter 4, an online questionnaire has been produced. Participants dealt with a set of twelve non-correlated simulations in which they had to identify the topological relationship between one of the existing easements of the 3D model and a fictive geometric object (e.g, air conditioner unit, and locker). Among these

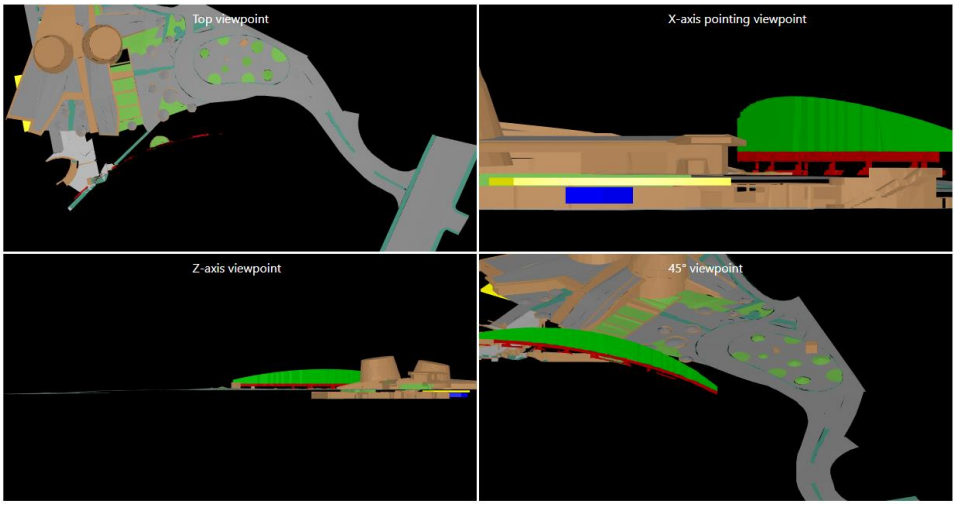


**Figure 40**: Example of simulations visualized from the four combined default software points of view (disjoined objects): top viewpoint (upper left), side viewpoints (upper right and lower left) and 45° viewpoint (lower right)

simulations, six were visualized from the four combined default software points of view (Figure 40) and six from a point of view that maximizes the 3D geometric objects' view area (Figure 41). Eventually, in each group, half of the simulations were related to a 3D intersection topological relationship and the other half to disjoined geometric objects.

For each simulation, two questions were systematically asked:

- Question 1: Does the geometric object (in blue) intersect the easement (in yellow)?

**Figure 41**: Example of simulations visualized from a point of view that maximizes the visibility of 3D geometric objects' view area inside the viewport (intersected objects)

- Question 2: What is the degree of certainty of your answer? Possible options: totally certain, quite certain, quite uncertain, and totally uncertain.

#### *5.3.1.3 Statistical analysis*

Within the framework of this study, the viewpoint management algorithm usability has been evaluated with the two following indicators: the accuracy (as a measure of the effectiveness) and the user's certainty with which the visual task is performed. Thanks to the participation of 40

students (in geomatics or related-topics) of the Université Laval (Canada) and Université de Liège (Belgium)[6], the following results were obtained.

Is a 3D viewpoint based on the maximization of 3D geometric objects' view area more accurate for visual 3D topological relationship identification of disjoined and intersected geometric objects compared to the default combined software points of view?

The exact binomial test shows that maximizing the 3D geometric objects' view area inside the viewport significantly improves the success rate of visual 3D topological relation identification among disjoined and intersected geometrics objects compared to the traditional software points of view (Figure 42 and Figure 43). Indeed, the overall success rate is about 96.5% (for both disjoined and intersected topological relationships) compared to a success rate of 86% (disjoined geometric objects) and 77.5% (intersected geometric objects) with the four combined default software points of view. As a result, the use of the default software viewpoints reduces the accuracy in visually identifying the 3D topological relationship among geometric objects, in particular when geometric objects intersect each other.

[6] We want to sincerely thank Prof. Dr. Marc Gervais (from Université Laval) and Prof. Dr. Pierre Hallot (from Université de Liège) for their cooperation throughout this investigation.

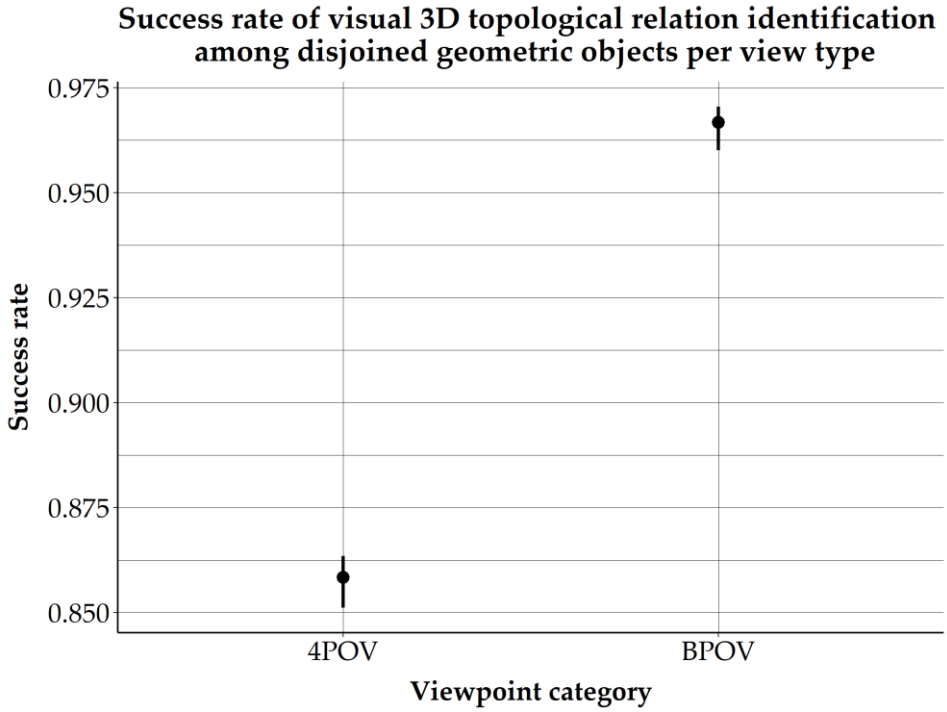


**Figure 42**: Exact binomial test. Success rate of visual 3D topological relation identification among disjoined geometric objects per view type. 4POV: the four combined default software points of view; BPOV: the best point of view, i.e., the viewpoint maximizing the 3D geometric objects' view area within the viewport.

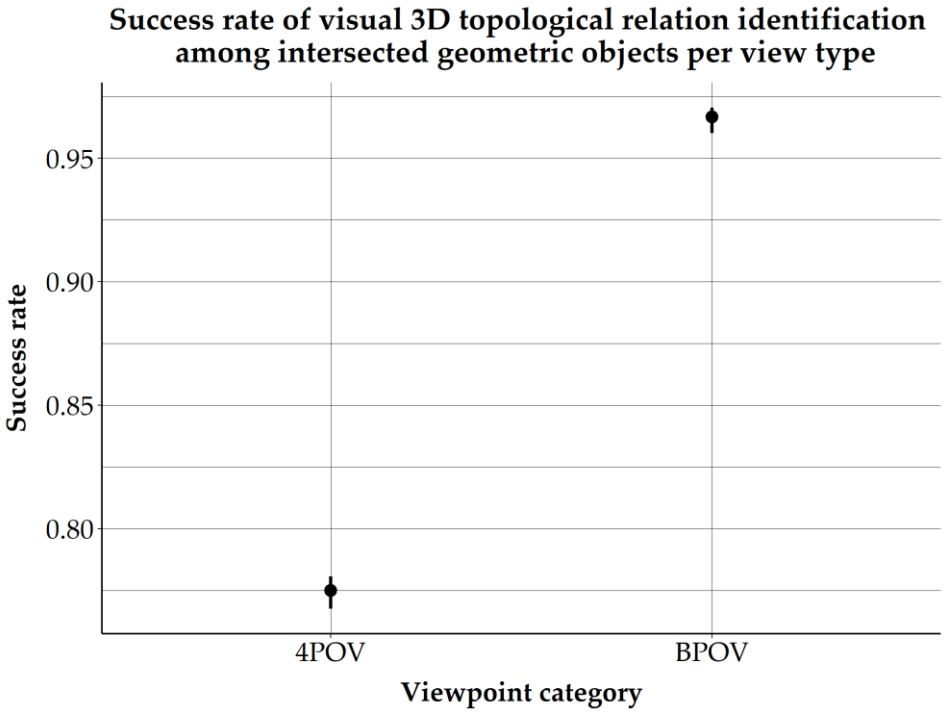


**Figure 43**: Exact binomial test. Success rate of visual 3D topological relation identification among intersected geometric objects per view type. 4POV: the four combined default software points of view; BPOV: the best point of view, i.e., the viewpoint maximizing the 3D geometric objects' view area within the viewport.

Does a 3D viewpoint based on the maximization of 3D geometric objects' view area enhance the user's certainty when visually identifying the visual 3D topological relationship identification of disjoined and intersected geometric objects compared to the default combined software points of view?

Prior to the statistical Chi-2 test, the initial measurement scale was reduced to two categories in order to meet the minimum number of observations per class (5). To achieve that, the frequencies associated to the totally uncertain, quite uncertain, and quite certain classes were merged; the totally certain class was not rearranged. Then, the application of the Chi-2 test showed that maximizing the 3D geometric objects' view area significantly improves the degree of certainty of participants in the visual identification of the 3D topological relationship among disjoined and intersected geometric objects: p-value of $8.77 \times 10^{-9}$ (disjoined objects) and $1.20 \times 10^{-12}$ (intersected objects). Indeed, participants are generally less confident when dealing with the four combined default software points of view (Figure 44 and Figure 45). Besides, note that participants are also less certain in the visual identification of intersected objects compared to disjoined objects (in particular with the default software points of view).

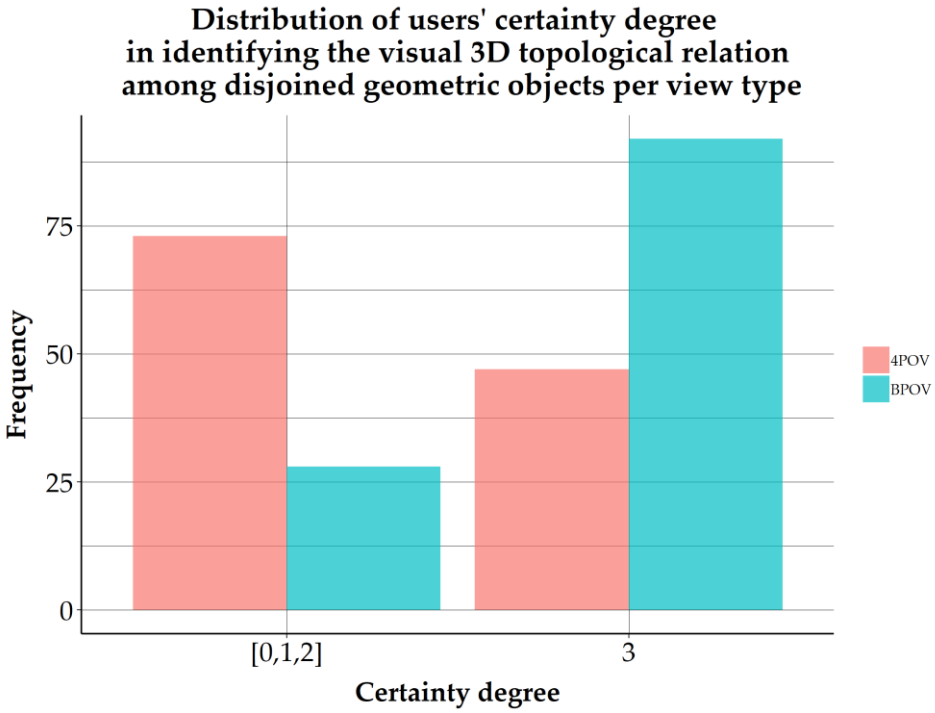


**Figure 44**: Distribution of users' certainty degree in identifying the visual 3D topological relation among disjoined geometric objects per view type; 4POV: the four combined default software points of view; BPOV: the best point of view, i.e., the viewpoint maximizing the 3D geometric objects' view area within the viewport. The categories 0, 1, and 2 (respectively, totally uncertain, quite uncertain, and quite certain) have been merged to meet the minimum number of observations per class (5).

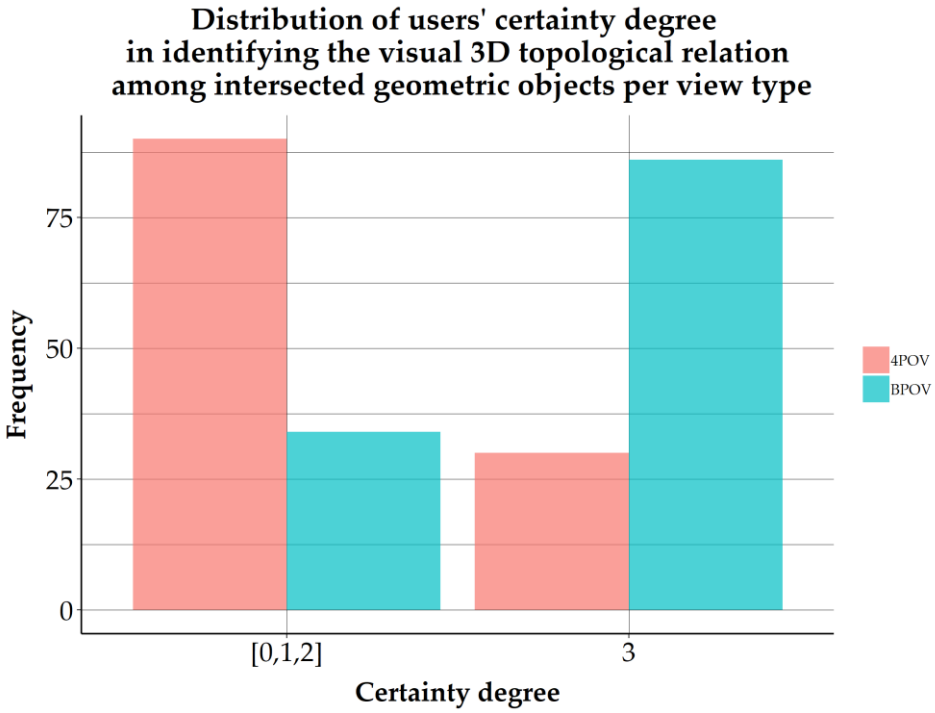


**Figure 45**: Distribution of users' certainty degree in identifying the visual 3D topological relation among intersected geometric objects per view type; 4POV: the four combined default software points of view; BPOV: the best point of view, i.e., the viewpoint maximizing the 3D geometric objects' view area within the viewport. The categories 0, 1, and 2 (respectively, totally uncertain, quite uncertain, and quite certain) have been merged to meet the minimum number of observations per class (5).

#### *5.3.1.4 Preliminary conclusion*

Within the framework of this survey, we propose the first evaluation of our geocomputational method in the visual identification of spatial relationships among disjoined and intersected geometric objects. Although preliminary, the results of this investigation support that a 3D viewpoint that maximizes the 3D geometric objects' view area enhances the accuracy and user's certainty in the visual identification of 3D topological relationships among disjoined and intersected objects. As such, this study brings additional evidence that reinforce the viewpoint management algorithm usability in achieving further visual tasks, i.e., beyond the former visual selectivity task of this research.

Then, this survey also brings new research opportunities in order to enhance the identification of the best 3D viewpoint for 3D topological relationships. Indeed, to date, the algorithm only maximizes the view area of disjoined and intersected geometric objects; although it would be more relevant to maximize the view of area of the disjoined or intersected section as it constitutes the "object of interest" from which the 3D topological relationship evaluation can be undertaken. Hence, a new research question arises: how should these topological relationships be modeled (especially the disjoined section among geometric objects) and visualized (in particular the visualization techniques to be applied in order to graphically represent the intersection among geometrics objects)? Note that solutions for automatic 3D topological relationships detection can already be found in (Zhang & Hu, 2011). Furthermore, dynamic

transparency could also be a promising solution in the visual identification of these relationships.

### 5.3.2 How to benefit from the viewpoint management algorithm within the 3D data acquisition process?

To date, our geocomputational method has only been developed and incorporated in the 3D visualization process of geospatial data. However, it could be extended to the geospatial data acquisition in order to automate flight planning (e.g., drone) with precomputed camera viewpoints for capturing data in the field. For that purpose, an orthophoto of the study area could be employed to locate one or multiple zone(s) to be photographed. Then, these analysis areas would be marked out on a georeferenced LiDAR dataset, from which the viewpoint management algorithm could be used to identify the best 3D points of view(s). Note that further data could be incorporated into the original dataset so as to take into account additional obstacles on the field (e.g., electrical girds, wind turbines). Eventually, in the same context, our algorithm could also assist the drone pilot's location in the field: e.g., to keep a constant visual line of sight over the full duration of the flight, as mandated by law in some countries (in Belgium for instance).

In another context, our geocomputational method could be used to support terrestrial laser scanning, especially in the sensors location. For instance, based on existing LiDAR datasets or 3D CAD files (for indoor scanning), the algorithm could be used to guarantee an overall scan of the study area, and thus reduce occlusion in the data acquisition process.

### 5.3.3 How to use deep learning to automatically extract features that define the viewpoint optimality?

In this thesis, the viewpoint optimality has been defined on the geometric object's view area maximization within the viewport. Although relatively straightforward, this solution is not meaningless as we showed that, compared to combined default software points of view, it enhances the accuracy and user's certainty in achieving given retinal tasks: visual counting and visual identification of 3D topological relationships. However, in the future, additional descriptors (both 2D image and 3D geometric objects-related features) could be used to widen the usability scope of the geocomputational method: e.g., to geometric objects' recognition and classification processes.

To address this issue, the scientific literature could be reviewed, looking for further existing descriptors: e.g., the ratio of visible area, the surface area entropy, the silhouette length, the silhouette entropy, the curvature entropy, and the mesh saliency (Lee et al., 2005; Page et al., 2003; Polonsky et al., 2005; Vazquez et al., 2001). Although useful, these indicators are, however, difficult to apply in practice since they are often specific to a given visual task and/or application context.

Hence, the use of artificial intelligence, in particular convolutional neural networks, could be a promising solution to automatically extract optimality descriptors. To achieve that, a dataset of 2D images of a given category of 3D geometric objects (e.g., churches with the same architectural style) could be used as inputs of a convolutional neural

network in order to detect features (i.e., descriptors) that define the viewpoint optimality. Once completed, this knowledge base could then be used to identify the best point of view of a selected geometric object within the 3D scene.

### 5.3.4 How to take advantage of the viewpoint management algorithm to produce visual cues that assist navigation and interaction within geovirtual environments visualized through stereoscopic vision?

In this research, 3D geospatial data have only been visualized through monitor-based displays, and thus via the monoscopic vision. However, at the present time, the immersive experience via the use of a head-mounted display (for instance) becomes more affordable[7] and thus accessible to a wider audience. General speaking, moving to geovirtual world visualized through an immersive headset has some advantages compared to classic desktop geovirtual environment. Indeed, whilst this latter has the potential to reach a wider audience, the former has the ability to enhance the user's spatial presence (i.e., the sense of "being there"); and combined with an embodiment (via the use of an avatar), it may improve the user's involvement and awareness of given issues (e.g., environmental) (Fuhrmann & MacEachren, 2001; Hruby et al., 2019).

[7] The new *Oculus Quest* head-mounted display costs less than 500€ and allows a complete stereoscopic experience with an all-one headset, i.e. without the need of an external computer.

However, to fully benefit from such geovirtual environments (e.g., for exploration and discovery purposes), it is crucial to keep users oriented within the 3D world as disorientation may cause discomfort and anxiety, which is detrimental for spatial knowledge acquisition (Darken & Peterson, 2001). For that purpose, several scientific studies have already been conducted in order to enhance the navigation process: e.g., automatically reaching a destination from a current position within a 3D city model (Ropinski et al., 2005) or optimizing the design of virtual environments for route learning (Lokka & Çöltekin, 2019).

Nevertheless, we noted that, once the final destination has been reached, user is usually not assisted in the visualization of his/her points of interest: e.g., finding the most appropriate location within a public square to simultaneously visualize one or multiple feature(s). In that case, our geocomputational method could be employed to identify the best viewpoint(s), and ultimately visual cues could even be produced to automatically guide users towards the most suitable point of view(s). Note that, to deal with occlusion issues (e.g., objects enclosed or contained within other objects), a mixed reality could even be considered, similarly to (Devaux et al., 2018).

### 5.3.5 How to use the viewpoint management algorithm to assist a multi-LODs graphical representation of virtual 3D city models?

Modelling virtual 3D city models is inherently linked to the concept of level of details (LOD), which represents the degree of spatio-semantic

adherence (of the model) to its corresponding subset of reality (Biljecki et al., 2014). This definition incorporates both:

- the presence and complexity of the objects and their elements,
- the level of quality (Döllner & Buchholz, 2005a),
- the level of abstraction (Glander & Döllner, 2009),
- and the level of completeness (Tempfli & Pilouk, 1996).

While fully incorporated into the modelling stage, this concept is usually no longer considered as an issue of concern in the visualization process, in particular when the 3D model is displayed with the same level of details as modelled. However, from a cartographic point of view, it is necessary to go over the static aspect of a given LOD, especially when visualization is used well beyond the information presentation (e.g., for knowledge construction) (MacEachren & Kraak, 2001). Indeed, too much detailed 3D city models (both in terms of geometric objects' density and their associated level of details) may drastically reduce knowledge extraction due to a cognitive overload (Resch et al., 2013).

To support this process, it is essential to apply generalization operators, dealing both on the presence/absence of city objects and their elements, the features complexity, their dimensionality, and/or appearance (Foerster et al., 2007; Semmo et al., 2015). In this context, an interesting approach has already been proposed in (Semmo et al., 2012). Nevertheless, an automation of this generalization process is still missing and could be performed with our geocomputational method. As mentioned in section 5.2.2, the viewpoint management algorithm could be used to generalize

the 3D model in order to reduce the occlusion of selected geometric objects: e.g., via an automatic selection of visualization context objects to be displayed, an appropriate level of details and/or the application of occlusion management techniques. As such, our geocomputational method could reduce the user's cognitive overload and thus favor the knowledge extraction.

CHAPTER 6

# Conclusions and recommendations

## 6.1 Preface

This chapter returns to the research objectives, summarizes the main results of this thesis, and highlights the findings to the contribution of knowledge. It also resumes future research topics, both linked to the visualization process of 3D geospatial data and their acquisition.

## 6.2 Back to the research objectives

The achievement of the global aim of this research, i.e., **the enhancement of the 3D visualization process of virtual building models in achieving given user-centered visual targeted purposes**, has been carried through three specific objectives, which are discussed in detail in the next sections.

### 6.2.1 Formalizing the 3D visualization process of geospatial data

As discussed in chapter 2, formalizing the 3D geovisualization field was an important issue as the process remained unstructured, leading to potential graphic (and subsequently semantic) incoherence in the 3D visualization of geospatial data. The main outcome of this objective was thus the recognition of the lack of a theoretical framework, and subsequently the need to develop a semiotic model of the 3D geoinformation, including both an expression and content plan. Furthermore, this conceptualization process also highlighted the camera significance in optimizing the visualization techniques relevance for achieving given visual targeted purposes, and therefore supporting assistance in the occlusion issue.

### 6.2.2 Proposing a theoretical and operational solution to the 3D viewpoint selection issue in order to enhance the visualization of the underlying semantic information

In chapter 3, we addressed the ubiquitous 3D viewpoint selection issue via the development of a theoretical and operational solution that automates and optimizes the 3D point of view identification in the visualization of a set of 3D geometric objects to which visualization techniques have been applied. Specific attention has been carried out to incorporate this geocomputational method into a semantic driven visualization process so as to be fully integrated in the 3D geovisualization field. Eventually, the method has been incorporated into a client-server application, dividing the visualization and processing stages between the client and the server respectively.

### 6.2.3 Evaluating the proposal for a given visual task related to the selectivity purpose.

In chapter 4, we provided empirical evidence related to the geocomputational method usability in achieving a given selectivity purpose (visual counting) compared to the four combined default software points of view. This validation stage has been carried out in the form of interviews with a group of experts, and the collected data provided valuable information to evaluate the 3D viewpoint management algorithm developed in chapter 3.

## 6.3 Back to the research questions

In this thesis, we hypothesized that **there exists at least one optimal 3D viewpoint for visualizing a set of 3D geometric objects within 3D building models**. Applied to visual selectivity purpose (visual counting), this research aimed to demonstrate the usability of a 3D viewpoint that maximizes the 3D geometric objects' view area, specifically compared to the four combined default software points of view.

To address and demonstrate this proposal, we developed a geocomputational method on best 3D viewpoint identification and tested its usability within an investigation in the facility management framework using a BIM model (chapter 4). Our study showed that **visual counting accuracy is significantly enhanced** with a 3D viewpoint that maximizes the 3D geometric objects' view area compared to the four combined default software points of view (specific research question 1). **The same is also true with respect to the certainty with which users undertake the visual counting** (specific research question 2). However, the hypothesis that our point of view makes the visual counting of objects faster compared to a single side point of view (specific research question 3) could not be demonstrated at the 5% significance threshold. Nevertheless, the statistical analysis showed promising results (e.g., a lower variance in users' responses).

## 6.4 Contribution to Knowledge

The formalization of the 3D geovisualization field, as a knowledge network, is a clear contribution of this research as no such proposal could not be found in the scientific literature or practices. Since it has been generically written, it is applicable to any 3D geospatial data and aims to assist both domain experts in the definition of their own graphic design guidelines and non-professional users that manipulate and visualize geospatial data.

Then, this thesis formalized and highlighted the key role of the viewpoint in the 3D geovisualization process. Based on the conducted empirical study, we showed that a point of view that maximizes the 3D geometric objects' view area significantly enhances the accuracy and user's certainty with which visual counting is carried out. As such, this conclusion points out the potential of such a 3D point of view as a new suitable tool to be incorporated within 3D modeling and visualization software (complementary to current 3D default software viewpoints).

Next, the geocomputational method itself is also a real contribution of this work as it is the first theoretical proposal that supports and optimizes the 3D viewpoint selection within a semantic driven visualization process. Moreover, its implementation into a client-server application that can leverage the power of remote computers constitutes a promising and deployable solution to existing online 3D viewers (e.g., as an external plugin).

Eventually, the validation experimental framework contributes to the development of the 3D geovisualization too as it is a step forward in bringing empirical evidence in the field, contrary to classic subjective evaluations. Future 3D geovisualization-related researches could thus benefit from this scientific approach.

## 6.5 Future Research

The results of this thesis brings out a set of perspectives for future researches in 3D geovisualization and geospatial data acquisition.

1. As mentioned in Chapter 5, the geocomputational method should be validated with additional visual tasks and application contexts to really demonstrate its usability in meeting user-centered requirements. Beyond selectivity purpose and 3D topological relationships visual identification, visibility analysis (e.g., for locating surveillance cameras) and flooding extent estimation (e.g., for mitigating damage to utilities) are interesting topics to be investigated for security and risk management purposes. Note that our algorithm could also be used in video games as the point of view location plays a key role in the player's presence feeling (Krichane, 2019; Ryan, 1999; Sheridan, 1992).

2. Then, to date, the viewpoint management algorithm has only been incorporated in the 3D visualization process of geospatial data. In the future, it could be extended to the geospatial data acquisition as a way to improve drone flight planning (e.g., in providing automatic best viewpoints for capturing data) and pilot's location in the field (e.g., in

keeping a constant visual line of sight over the full duration of the flight). Moreover, the algorithm could also assist terrestrial laser scanning in the sensors location in order to reduce occluded areas in the data acquisition process.

3. Then, the utility function (that defines the viewpoint optimality) is currently only based on the *3D geometric object's view area maximization* descriptor. Whilst this solution is valuable for visualizing well-defined semantic 3D objects, the function could incorporate additional descriptors (both 2D image and 3D geometric object's related features) in order to extend the geocomputational method usage for the recognition and classification processes. These descriptors could even be extracted and combined through artificial intelligence, in particular convolutional neural networks.

4. Afterwards, this thesis only deals with 3D geospatial data visualized through monoscopic vision. However, the increasing access to virtual reality (both in terms of cost and computer resources) extends the use of the geocomputational method to geovirtual immersive environments visualized through stereoscopic vision. Applications in education, BIM and urban planning are promising as the algorithm could enhance (for instance) the presentation of physical dynamics, users' activities simulations and architectural features. Indeed, the viewpoint management algorithm could support the stereoscopic experience by providing visual assistance to users: e.g., supplying visual cues to users in

order to assist immersive guided tours (such as fly and walk-throughs), and thus improve the navigation and interaction with the designed space.

5. Eventually, a multi-LODs graphical representation of 3D city models should be investigated in the future as it could enhance the readability of virtual urban environments in high density urban areas. Indeed, applying a higher LOD to objects of interest (i.e., extracted by semantic and/or spatial queries) compared to visualization context objects (VCOs) could enhance the user's focus on the essential piece of geoinformation, and subsequently reduce the cognitive overload. To achieve that, the viewpoint management algorithm could be used to assist the initial selection of VCOs to be displayed (filtering stage), their level(s) of details and/or the application of occlusion management techniques (mapping stage). In the future, it should thus be possible to automatically go beyond the static aspect of a given LOD dataset, especially to favor the knowledge extraction.

# Bibliography

Abbasnejad, B., & Moud, H. I. (2013). BIM and Basic Challenges Associated with its Definitions, Interpretations and Expectations. *International Journal of Engineering Research and Applications*, *3*, 287-294.

Abdul-Rahman, A., & Pilouk, M. (2008). *Spatial Data Modelling for 3D GIS*. Springer-Verlag Berlin Heidelberg.

Abran, A., Khelifi, A., & Suryn, W. (2003). Usability Meanings and Interpretations in ISO Standards. *Software Quality Journal*, *11*(4), 325-338.

Akcamete, A, Akinci, B., & Garrett, J. H. (2010). Potential utilization of building information models for planning maintenance activities. *Proceedings of the International Conference on Computing in Civil and Building Engineering*, 151-157. Nottingham, UK.

Akcamete, Asli, Liu, X., Akinci, B., & Garrett, J. H. (2011). Integrating and Visualizing Maintenance and Repair Work Orders in BIM: Lessons Learned from a Prototype. *Proceedings of the 11th International Conference on Construction Applications of Virtual Reality (CONVR)*, 639-649. Weimar, Germany.

Altmaier, A., & Kolbe, T. H. (2003). Applications and Solutions for Interoperable 3d Geo-Visualization. *Proceedings of the Photogrammetric Week 2003*, 1-15. Stuttgart, Germany.

American Society of Civil Engineers. (1994). *Glossary of the Mapping Sciences*. New York, NY, USA: ASCE Publications.

Andrienko, G., Andrienko, N., Dykes, J., Fabrikant, S. I., & Wachowicz, M. (2008). Geovisualization of Dynamics, Movement and Change : Key Issues and Developing Approaches in Visualization Research. *Information Visualization*, *7*(3-4), 173-180. https://doi.org/10.1057/IVS.2008.23

Avery, B., Sandor, C., & Thomas, B. H. (2009). Improving spatial perception for augmented reality x-ray vision. *Virtual Reality Conference, 2009. VR 2009. IEEE*, 79–82. IEEE.

Azhar, S. (2011). Building Information Modeling (BIM) : Trends, Benefits, Risks, and Challenges for the AEC Industry. *Leadership and Management in Engineering*, *11*(3), 241-252. https://doi.org/10.1061/(ASCE)LM.1943-5630.0000127

Azhar, S., Nadeem, A., Mok, J. Y. N., & Leung, B. H. Y. (2008). Building Information Modeling (BIM) : A New Paradigm for Visual

Interactive Modeling and Simulation for Construction Projects. *Advancing and Integrating Construction Education, Research & Practice"*, 435-446. Karachi, Pakistan.

Azhar, S., Sattineni, A., & Hein, M. (2010). BIM Undergraduate Capstone Thesis : Student Perceptions and Lessons Learned. *Proceedings of the 46th ASC Annual Conference, Boston, MA*, 8.

Baddeley, A. D., Kopelman, M. D., & Wilson, B. A. (2002). *The Handbook of Memory Disorders*. Wiley.

Bandrova, T. (2005). Innovative technology for the creation of 3D maps. *Data Science Journal*, *4*, 53–58.

Barral, P., Dorme, G., & Plemenos, D. (1999). *Visual Understanding of a Scene by Automatic Movement of a Camera*. 7. Moscow, Russia.

Batty, M., Chapman, D., Evans, S., Haklay, M., Kueppers, S., Shiode, N., … Torrens, P. M. (2000). *Visualizing the city : Communicating urban design to planners and decision-makers*.

Bazargan, K., & Falquet, G. (2009). Specifying the representation of non-geometric information in 3D virtual environments. *International Conference on Human-Computer Interaction*, 773–782. Springer.

Becerik-Gerber, B., Jazizadeh, F., Li, N., & Calis, G. (2012). Application Areas and Data Requirements for BIM-Enabled Facilities Management. *Journal of Construction Engineering and Management*, *138*(3), 431-442. https://doi.org/10.1061/(ASCE)CO.1943-7862.0000433

Benner, J., Geiger, A., & Leinemann, K. (2005). Flexible generation of semantic 3D building models. *Proceedings of the 1st international workshop on next generation 3D city models, Bonn*, 17–22.

Bertin, J. (1967). *Sémiologie graphique : Les diagrammes, les réseaux et les cartes* (Gauthier-Villars, Mouton & Cie). Paris, France.

Biljecki, F. (2017). *Level of detail in 3D city models*. TU Delft.

Biljecki, Filip, Ledoux, H., & Stoter, J. (2016). An improved LOD specification for 3D building models. *Computers, Environment and Urban Systems*, *59*, 25-37. https://doi.org/10.1016/j.compenvurbsys.2016.04.005

Biljecki, Filip, Ledoux, H., Stoter, J., & Zhao, J. (2014). Formalisation of the level of detail in 3D city modelling. *Computers, Environment and Urban Systems*, *48*, 1-15. https://doi.org/10.1016/j.compenvurbsys.2014.05.004

Biljecki, Filip, Stoter, J., Ledoux, H., Zlatanova, S., & Çöltekin, A. (2015). Applications of 3D City Models : State of the Art Review. *ISPRS International Journal of Geo-Information*, *4*(4), 2842-2889. https://doi.org/10.3390/ijgi4042842

Billen, M. I., Kreylos, O., Hamann, B., Jadamec, M. A., Kellogg, L. H., Staadt, O., & Sumner, D. Y. (2008). A geoscience perspective on immersive 3D gridded data visualization. *Computers & Geosciences*, *34*(9), 1056-1072. https://doi.org/10.1016/j.cageo.2007.11.009

Billen, R., Cutting-Decelle, A.-F., Marina, O., de Almeida, J.-P., Caglioni, M., Falquet, G., … Zlatanova, S. (2014). *3D City Models and urban information : Current issues and perspectives: European COST Action TU0801*. Consulté à l'adresse http://3u3d.edpsciences.org/10.1051/TU0801/201400001

Bleisch, S. (2012). *3D GEOVISUALIZATION–DEFINITION AND STRUCTURES FOR THE ASSESSMENT OF USEFULNESS*. ISPRS Annals of Photogrammetry, Remote Sensing and Spatial Information Sciences, *I-2*, 129-134.

Boukhelifa, N., Bezerianos, A., Isenberg, T., & Fekete, J.-D. (2012). Evaluating sketchiness as a visual variable for the depiction of

qualitative uncertainty. *IEEE Transactions on Visualization and Computer Graphics*, *18*(12), 2769–2778.

Brasebin, M., Christophe, S., Buard, É., & Pelloie, F. (2015). *A KNOWLEDGE BASE TO CLASSIFY AND MIX 3D RENDERING STYLES*. In Proceedings of the 27th International Cartographic Conference, Rio de Janeiro, Rio de Janeiro, Brazil, 23-28.

Buchroithner, M., Schenkel, R., & Kirschenbauer, S. (2000). 3D display techniques for cartographic purposes : Semiotic aspects. *International Archives of Photogrammetry and Remote Sensing*, *33*(B5/1; PART 5), 99–106.

Calabrese, F., Colonna, M., Lovisolo, P., Parata, D., & Ratti, C. (2011). Real-Time Urban Monitoring Using Cell Phones : A Case Study in Rome. *IEEE Transactions on Intelligent Transportation Systems*, *12*(1), 141-151. https://doi.org/10.1109/TITS.2010.2074196

Calcagno, P., Chilès, J. P., Courrioux, G., & Guillen, A. (2008). Geological modelling from field data and geological knowledge. *Physics of the Earth and Planetary Interiors*, *171*(1-4), 147-157. https://doi.org/10.1016/j.pepi.2008.06.013

Carpendale, M. S. T. (2003). *Considering Visual Variables as a Basis for Information Visualisation*. Consulté à l'adresse http://prism.ucalgary.ca//handle/1880/45758

Cemellini, B., Thompson, R., De Vries, M., & Van Oosterom, P. (2018). Visualization/dissemination of 3D Cadastre. *FIG Congress 2018*, 30. Istanbul, Turkey.

Cemellini, B., Thompson, R., & Oosterom, P. V. (2018). Usability testing of a web-based 3D Cadastral visualization system. *6th International FIG Workshop on 3D Cadastres*, 20. Delft, The Netherlands.

Chittaro, L., & Burigat, S. (2004). 3D location-pointing as a navigation aid in Virtual Environments. *Proceedings of the Working Conference on Advanced Visual Interfaces - AVI '04*, 267-274. https://doi.org/10.1145/989863.989910

Congote, J., Moreno, A., Kabongo, L., Pérez, J.-L., San-José, R., & Ruiz, O. (2012). Web based hybrid volumetric visualisation of urban GIS data : Integration of 4D Temperature and Wind Fields with LoD-2 CityGML models. In T. Leduc, G. Moreau, & R. Billen (Éd.), *Usage, Usability, and Utility of 3D City Models – European COST Action TU0801* (p. 03001). https://doi.org/10.1051/3u3d/201203001

Coors, V. (2003). 3D-GIS in networking environments. *Computers, Environment and Urban Systems*, *27*(4), 345–357.

Czmoch, I., & Pękala, A. (2014). Traditional Design versus BIM Based Design. *Procedia Engineering*, *91*, 210-215. https://doi.org/10.1016/j.proeng.2014.12.048

Darken, R., & Peterson, B. (2001). Spatial Orientation, Wayfinding, and Representation. In K. Hale & K. Stanney, *Handbook of Virtual Environments* (Vol. 20143245, p. 467-491). https://doi.org/10.1201/b17360-24

Devaux, A., Hoarau, C., Brédif, M., & Christophe, S. (2018). 3D urban geovisualization : In situ augmented and mixed reality experiments. *ISPRS Annals of Photogrammetry, Remote Sensing and Spatial Information Sciences*, *IV-4*, 41-48. https://doi.org/10.5194/isprs-annals-IV-4-41-2018

DiCarlo, J. J., Zoccolan, D., & Rust, N. C. (2012). How Does the Brain Solve Visual Object Recognition? *Neuron*, *73*(3), 415-434. https://doi.org/10.1016/j.neuron.2012.01.010

Döllner, J., Baumann, K., & Buchholz, H. (2006). *Virtual 3D City Models a s Foundation of Complex Urban Information Spaces*. Présenté à

Proceedings of the 11th International Conference on Urban Planning and Spatial Development in the Information Society, Vienna.

Döllner, Jürgen, & Buchholz, H. (2005a). Continuous level-of-detail modeling of buildings in 3D city models. *Proceedings of the 2005 International Workshop on Geographic Information Systems - GIS '05*, 173. https://doi.org/10.1145/1097064.1097089

Döllner, Jürgen, & Buchholz, H. (2005b). Expressive virtual 3D city models. *XXII international cartographic conference (ICC2005), A Coruda, Global Congress*.

Döllner, Jürgen, Kolbe, T. H., Liecke, F., Sgouros, T., & Teichmann, K. (2006, mai 15). *The Virtual 3D City Model of Berlin—Managing, Integrating and Communicating Complex Urban Information*. Présenté à 25th Urban Data Management Symposium, Aalborg, Denmark.

Dubel, S., Rohlig, M., Schumann, H., & Trapp, M. (2014). 2D and 3D presentation of spatial data : A systematic review. *2014 IEEE VIS International Workshop on 3DVis (3DVis)*, 11-18. https://doi.org/10.1109/3DVis.2014.7160094

Dutagaci, H., Cheung, C. P., & Godil, A. (2010). A benchmark for best view selection of 3D objects. *Proceedings of the ACM Workshop on 3D Object Retrieval - 3DOR '10*, 45-50. https://doi.org/10.1145/1877808.1877819

Edeline, F., Klinkenberg, J. M., & Minguet, P. (1992). *Traité du signe visuel : Pour une rhétorique de l'image.* Seuil, 419.

Egenhofer, M. J., & Mark, D. M. (1995). *Naive geography*. Consulté à l'adresse http://link.springer.com/chapter/10.1007/3-540-60392-1_1

Ellul, C., & Altenbuchner, J. (2014). Investigating approaches to improving rendering performance of 3D city models on mobile devices. *Geo-Spatial Information Science*, *17*(2), 73-84. https://doi.org/10.1080/10095020.2013.866620

Elmqvist, N., Assarsson, U., & Tsigas, P. (2007). Employing dynamic transparency for 3D occlusion management : Design issues and evaluation. *IFIP Conference on Human-Computer Interaction*, 532–545. Springer.

Elmqvist, N., & Tsigas, P. (2007). A taxonomy of 3D occlusion management techniques. *Virtual Reality Conference, 2007. VR'07. IEEE*, 51–58. IEEE.

Elmqvist, N., & Tudoreanu, M. E. (2007). *Occlusion Management in Immersive and Desktop 3D Virtual Environments : Theory and Evaluation*. *6*(1), 13.

Foerster, T., Stoter, J., & Köbben, B. (2007). Towards a formal classification of generalization operators. *Proceedings of the 23rd International Cartographic Conference*.

Franke, H. W. (1977). Observations Concerning Practical Visual Languages. *Visible Language*, *11*(2), 22.

Fuhrmann, S., & MacEachren, A. M. (2001). Navigation in desktop geovirtual environments : Usability assessment. *20th ICA/ACI International Cartographic Conference*, 2444-2453. Beijing.

Glander, T., & Döllner, J. (2009). Abstract representations for interactive visualization of virtual 3D city models. *Computers, Environment and Urban Systems*, *33*(5), 375-387. https://doi.org/10.1016/j.compenvurbsys.2009.07.003

Green, M. (1998). Toward a Perceptual Science of Multidimensional Data Visualization : Bertin and Beyond. *ERGO/GERO Human Factors Science*, *8*, 1-30.

Gröger, G., & Plümer, L. (2012). CityGML – Interoperable semantic 3D city models. *ISPRS Journal of Photogrammetry and Remote Sensing*, *71*, 12-33. https://doi.org/10.1016/j.isprsjprs.2012.04.004

Häberling, C., Bär, H., & Hurni, L. (2008). Proposed Cartographic Design Principles for 3D Maps : A Contribution to an Extended Cartographic Theory. *Cartographica: The International Journal for Geographic Information and Geovisualization*, *43*(3), 175-188. https://doi.org/10.3138/carto.43.3.175

Haeberling, C. (2002). 3D Map Presentation–A Systematic Evaluation of Important Graphic Aspects. *Proceedings of ICA Mountain Cartography Workshop" Mount Hood*, 11.

Hajji, R., & Billen, R. (2016). Collaborative 3D Modeling : Conceptual and Technical Issues. I*nternational Journal of 3-D Information Modeling (IJ3DIM)*, 5(3), 47-67.

He, J., Wang, L., Zhou, W., Zhang, H., Cui, X., & Guo, Y. (2017). Viewpoint Selection for Photographing Architectures. *ArXiv:1703.01702 [Cs]*. Consulté à l'adresse http://arxiv.org/abs/1703.01702

Heim, M. (2000). *Virtual realism* (Oxford University Press).

Herbert, G., & Chen, X. (2015). A comparison of usefulness of 2D and 3D representations of urban planning. *Cartography and Geographic Information Science*, *42*(1), 22-32. https://doi.org/10.1080/15230406.2014.987694

Hruby, F., Ressl, R., & de la Borbolla del Valle, G. (2019). Geovisualization with immersive virtual environments in theory and practice. *International Journal of Digital Earth*, *12*(2), 123-136. https://doi.org/10.1080/17538947.2018.1501106

Hu, J., You, S., & Neumann, U. (2003). Approaches to large-scale urban modeling. *IEEE Computer Graphics and Applications*, *23*(6), 62–69.

Huk, T. (2006). Who benefits from learning with 3D models? The case of spatial ability: 3D-models and spatial ability. *Journal of Computer Assisted Learning*, *22*(6), 392-404. https://doi.org/10.1111/j.1365-2729.2006.00180.x

Jaubert, B., Tamine, K., & Plemenos, D. (2006). Techniques for off-line scene exploration using a virtual camera. *International Conference 3IA*, 14.

Jazayeri, I., Rajabifard, A., & Kalantari, M. (2014). A geometric and semantic evaluation of 3D data sourcing methods for land and

property information. *Land Use Policy*, *36*, 219-230. https://doi.org/10.1016/j.landusepol.2013.08.004

Jobst, M., Dollner, J., & Lubanski, O. (2010). Communicating Geoinformation effectively with virtual 3D city models. In *Handbook of Research on E-Planning : ICTs for Urban Development and Monitoring*, IGI Global, 2010. 120-142.

Jobst, Markus, & Döllner, J. (2008). Better Perception of 3D-Spatial Relations by Viewport Variations. In M. Sebillo, G. Vitiello, & G. Schaefer (Éd.), *Visual Information Systems. Web-Based Visual Information Search and Management*, 7-18. https://doi.org/10.1007/978-3-540-85891-1_4

Jobst, Markus, & Germanchis, T. (2007). The employment of 3D in cartography—An overview. In *Multimedia Cartography*, 217–228).

Jobst, Markus, Kyprianidis, J. E., & Döllner, J. (2008). Mechanisms on Graphical Core Variables in the Design of Cartographic 3D City Presentations. In A. Moore & I. Drecki (Éd.), *Geospatial Vision*, 45-59.

Kaden, R., & Kolbe, T. H. (2013). CITY-WIDE TOTAL ENERGY DEMAND ESTIMATION OF BUILDINGS USING SEMANTIC 3D CITY

MODELS AND STATISTICAL DATA. *ISPRS Annals of Photogrammetry, Remote Sensing and Spatial Information Sciences*, *II-2/W1*, 163-171. https://doi.org/10.5194/isprsannals-II-2-W1-163-2013

Kaňuk, J., Gallay, M., & Hofierka, J. (2015). Generating time series of virtual 3-D city models using a retrospective approach. *Landscape and Urban Planning*, *139*, 40-53. https://doi.org/10.1016/j.landurbplan.2015.02.015

Khan, M., & Khan, S. S. (2011). Data and information visualization methods, and interactive mechanisms : A survey. *International Journal of Computer Applications*, *34*(1), 1–14.

Kim, JS., Yoo, SJ., & Li, K. J. (2014). Integrating IndoorGML and CityGML for Indoor Space. In *Lecture Notes in Computer Science*: *Vol. 8470*. *Web and Wireless Geographical Information Systems* (Springer). Berlin, Heidelberg.

Kolbe, T. H. (2009). Representing and exchanging 3D city models with CityGML. In *3D geo-information sciences*, Springer, 15–31.

Kraak, M. J. (1988). Computer Assisted Cartographic Three-Dimensional Imaging Technique. *Taylor & Francis*.

Kraak, M.-J. (2003). Geovisualization illustrated. *ISPRS Journal of Photogrammetry and Remote Sensing*, *57*(5-6), 390-399. https://doi.org/10.1016/S0924-2716(02)00167-3

Krichane, S. (2019). *La caméra imaginaire : Jeux vidéo et modes de visualisation* (Georg).

Kwan, M. P., & Lee, J. (2004). Geovisualization-of-Human-Activity-Patterns-Using-3D-GIS-A-time-geographic-approach.pdf. *Spatially integrated social sciences*, *27*, 721-744.

Kwan, M.-P. (2000). Interactive geovisualization of activity-travel patterns using three-dimensional geographical information systems : A methodological exploration with a large data set. *Transportation Research Part C: Emerging Technologies*, *8*(1-6), 185–203.

Kwan, M.-P., & Lee, J. (2005). Emergency response after 9/11 : The potential of real-time 3D GIS for quick emergency response in micro-spatial environments. *Computers, Environment and Urban Systems*, *29*(2), 93-113. https://doi.org/10.1016/j.compenvurbsys.2003.08.002

Kyle, B. R., Vanier, D. J., Kosovac, B., & Froese, T. M. (2002). Visualizer-an-interactive-graphical-decision-support-tool-for-service-life-

prediction-for-asset-managers.pdf. *Proceedings of the 9th International Conference on durability of building materials and components*, 15. Brisbane, Australia.

Lazar, J., Feng, J. H., & Hochheiser, H. (2010). *Research methods in human-computer interaction* (Wiley).

Lee, C. H., Varshney, A., & Jacobs, D. W. (2005). Mesh saliency. *ACM Transactions on Graphics*, *24*(3), 656-659.

Lee, K. (2012). Augmented Reality in Education and Training. *TechTrends*, *56*(2), 9.

Lee, W.-L., Tsai, M.-H., Yang, C.-H., Juang, J.-R., & Su, J.-Y. (2016). V3DM+: BIM interactive collaboration system for facility management. *Visualization in Engineering*, *4*(1), 15. https://doi.org/10.1186/s40327-016-0035-9

Li, X., & Zhu, H. (2009). Modeling and Visualization of Underground Structures. *Journal of Computing in Civil Engineering*, p. 7.

Liu, H.-C., & Sung, W.-P. (2014). Computer aided design system based on 3D GIS for park design. In *Computer Intelligent Computing and Education Technology* (p. 413-416). London, UK: CRC Press.

Liu, X., Wang, X., Wright, G., Cheng, J., Li, X., & Liu, R. (2017). A State-of-the-Art Review on the Integration of Building Information Modeling (BIM) and Geographic Information System (GIS). *ISPRS International Journal of Geo-Information*, p. 53.

Lokka, I. E., & Çöltekin, A. (2019). Toward optimizing the design of virtual environments for route learning : Empirically assessing the effects of changing levels of realism on memory. *International Journal of Digital Earth*, *12*(2), 137-155. https://doi.org/10.1080/17538947.2017.1349842

Lorenz, H., Trapp, M., Döllner, J., & Jobst, M. (2008). Interactive multi-perspective views of virtual 3D landscape and city models. In *The European Information Society*, 301–321.

Löwner, M.-O., Benner, J., Gröger, G., & Häfele, K.-H. (2013). New concepts for structuring 3D city models–an extended level of detail concept for CityGML buildings. *International Conference on Computational Science and Its Applications*, 466–480. Springer.

Lu, L., Becker, T., & Löwner, M.-O. (2017). 3D Complete Traffic Noise Analysis Based on CityGML. In Alias Abdul-Rahman (Éd.),

*Advances in 3D Geoinformation*, 265-283. https://doi.org/10.1007/978-3-319-25691-7_15

Luebke, D., Reddy, M., Cohen, J. D., Varshney, A., Watson, B., & Huebner, R. (2012). *Level of details for 3D graphics* (Morgan Kaufmann publishers ed.).

MacEachren, A. M. (1995). *How Maps Work* (Guilford).

MacEachren, Alan M., Edsall, R., Haug, D., Baxter, R., Otto, G., Masters, R., … Qian, L. (1999). Virtual environments for geographic visualization : Potential and challenges. *Proceedings of the 1999 workshop on new paradigms in information visualization and manipulation in conjunction with the eighth ACM internation conference on Information and knowledge management*, 35–40. ACM.

MacEachren, Alan M., & Kraak, M.-J. (2001). Research Challenges in Geovisualization. *Cartography and Geographic Information Science*, *28*(1), 3-12. https://doi.org/10.1559/152304001782173970

Meijers, M., Zlatanova, S., & Pfeifer, N. (2005). 3D geoinformation indoors : Structuring for evacuation. *Proceedings of Next generation 3D city models*, *6*. Germany Bonn.

Métral, C., Ghoula, N., & Falquet, G. (2012). *An ontology of 3D visualization techniques for enriched 3D city models* (T. Leduc, G. Moreau, & R. Billen, Éd.). https://doi.org/10.1051/3u3d/201202005

Métral, Claudine, Ghoula, N., Silva, V., & Falquet, G. (2014). A repository of information visualization techniques to support the design of 3D virtual city models. In *Innovations in 3D Geo-Information Sciences*, 175–194.

Milgram, P., & Kishino, F. (1994). A taxonomy of mixed reality visual displays. *IEICE TRANSACTIONS on Information and Systems*, *77*(12), 1321–1329.

Morrison, J. L. (1974). A theoretical framework for cartographic generalization with the emphasis on the process of symbolization. *International Yearbook of Cartography*, *14*, 115-127.

Moser, J., Albrecht, F., & Kosar, B. (2010). Beyonf viusalisation—3D GIS analysis for virtual city models. *International Archives of the Photogrammetry, Remote Sensing and Spatial Information Sciences*, *XXXVIII-4/W15*, 143-146.

Motamedi, A., Hammad, A., & Asen, Y. (2014). Knowledge-assisted BIM-based visual analytics for failure root cause detection in facilities

management. *Automation in Construction*, *43*, 73-83. https://doi.org/10.1016/j.autcon.2014.03.012

Neubauer, S., & Zipf, A. (2007). *Suggestions for Extending the OGC Styled Layer Descriptor (SLD) Specification into 3D – Towards Visualization Rules for 3D City Models*. 10.

Neuville, R., Pouliot, J., & Billen, R. (2019). Identification of the Best 3D Viewpoint within the BIM Model : Application to Visual Tasks Related to Facility Management. *Buildings*, *9*(7), 167. https://doi.org/10.3390/buildings9070167

Neuville, R., Pouliot, J., Poux, F., & Billen, R. (2019). 3D Viewpoint Management and Navigation in Urban Planning : Application to the Exploratory Phase. *Remote Sensing*, *11*(3), 236. https://doi.org/10.3390/rs11030236

Neuville, R., Pouliot, J., Poux, F., De Rudder, L., & Billen, R. (2018). A Formalized 3D Geovisualization Illustrated to Selectivity Purpose of Virtual 3D City Model. *ISPRS International Journal of Geo-Information*, *7*(5), 194.

Neuville, R., Pouliot, J., Poux, F., Hallot, P., De Rudder, L., & Billen, R. (2017). Towards a decision support tool for 3D visualisation :

Application to selectivity purpose on single object in a 3D city scene. *ISPRS Annals of Photogrammetry, Remote Sensing and Spatial Information Sciences*, *IV-4/W5*, 91-97. https://doi.org/10.5194/isprs-annals-IV-4-W5-91-2017

Neuville, R., Poux, F., Hallot, P., & Billen, R. (2016). Towards a normalised 3D Geovisualisation : The viewpoint management. *ISPRS Annals of the Photogrammetry, Remote Sensing and Spatial Information Sciences*, *4*, 179-186.

Ninger, A. K., & Bartel, S. (1998). 3D-GIS for Urban Purposes. *GeoInformatica*, p. 79-103.

Ogao, P. J., & Kraak, M.-J. (2002). Defining visualization operations for temporal cartographic animation design. *International journal of applied earth observation and geoinformation*, *4*(1), 23–31.

Okoshi, T. (1976). *Three-Dimensional Imaging Techniques* (Academic press). New York.

Oosterom, P. V., Stoter, J., Ploeger, H., Thompson, R., & Karki, S. (2010). *World-wide Inventory of the Status of 3D Cadastres in 2010 and Expectations for 2014*. 21. Marrakech, Morocco.

Open Geospatial Consortium. (2001). *Web Terrain Server (WTS)* (R. R. Singh, Éd.).

Open Geospatial Consortium. (2006). *Candidate OpenGIS® CityGML Implementation Specification (City Geography Markup Language)* (G. Gröger, T. Kolbe, & A. Czerwinski, Éd.).

Open Geospatial Consortium. (2018). *OGC® IndoorGML: Corrigendum* (J. Lee, K.-J. Li, S. Zlatanova, T. H. Kolbe, C. Nagel, & T. Becker, Éd.).

Page, D. L., Koschan, A. F., Sukumar, S. R., Roui-Abidi, B., & Abidi, M. A. (2003). Shape analysis algorithm based on information theory. *Proceedings 2003 International Conference on Image Processing (Cat. No.03CH37429)*, *1*, I-229-232. https://doi.org/10.1109/ICIP.2003.1246940

Philips, A., Walz, A., Bergner, A., Graeff, T., Heistermann, M., Kienzler, S., … Zeilinger, G. (2015). Immersive 3D geovisualization in higher education. *Journal of Geography in Higher Education*, *39*(3), 437-449. https://doi.org/10.1080/03098265.2015.1066314

Plemenos, D. (2003). *Exploring virtual worlds : Current techniques and future issues*. 5-10.

Polonsky, O., Patané, G., Biasotti, S., Gotsman, C., & Spagnuolo, M. (2005). What's in an image? : Towards the computation of the "best" view of an object. *The Visual Computer*, *21*(8-10), 840-847. https://doi.org/10.1007/s00371-005-0326-y

Pouliot, J., Badard, T., Desgagné, E., Bédard, K., & Thomas, V. (2008). Development of a Web Geological Feature Server (WGFS) for sharing and querying of 3D objects. In P. van Oosterom, S. Zlatanova, F. Penninga, & E. M. Fendel (Éd.), *Advances in 3D Geoinformation Systems* (p. 115-130). https://doi.org/10.1007/978-3-540-72135-2_7

Pouliot, J., Ellul, C., Hubert, F., Wang, C., Rajabifard, A., Kalantari, M., Shojaei, D., Atazadeh, B., Van Oosterom, P., De Vries, M & Ying, S. (2018). Visualization and New Opportunities. In *Best Practices 3D Cadastre* (p. 77).

Pouliot, J., Wang, C., Fuchs, V., Hubert, F., & Bédard, M. (2013). Experiments with Notaries about the Semiology of 3D Cadastral Models. *ISPRS - International Archives of the Photogrammetry, Remote Sensing and Spatial Information Sciences*, *XL-2/W2*, 53-57. https://doi.org/10.5194/isprsarchives-XL-2-W2-53-2013

Pouliot, J., Wang, C., & Hubert, F. (2014). *Transparency Performance in the 3D Visualization of Bounding Legal and Physical Objects : Preliminary Results of a Survey*. 173-182. Dubai.

Pouliot, J., Wang, C., Hubert, F., & Fuchs, V. (2014). Empirical Assessment of the Suitability of Visual Variables to Achieve Notarial Tasks Established from 3D Condominium Models. In U. Isikdag (Éd.), *Innovations in 3D Geo-Information Sciences* (p. 195-210). https://doi.org/10.1007/978-3-319-00515-7_12

Poux, F., Neuville, R., Hallot, P., Van Wersch, L., Luczfalvy Jancsó, A., & Billen, R. (2017). Digital Investigations of an Archaeological Smart Point Cloud : A Real Time Web-Based Platform To Manage the Visualisation of Semantical Queries. *The International Archives of the Photogrammetry, Remote Sensing and Spatial Information Sciences*, *Volume XLII-5/W1*, 581–588. Florence, Italy.

Poux, F., Neuville, R., Nys, G.-A., & Billen, R. (2018). 3D Point Cloud Semantic Modelling : Integrated Framework for Indoor Spaces and Furniture. *Remote Sensing*, *10*(9), 1412. https://doi.org/10.3390/rs10091412

Poux, F., Neuville, R., Van Wersch, L., Nys, G.-A., & Billen, R. (2017). 3D Point Clouds in Archaeology : Advances in Acquisition, Processing and Knowledge Integration Applied to Quasi-Planar Objects. *Geosciences*, *7*(4), 96. https://doi.org/10.3390/geosciences7040096

Ranzinger, M., & Gleixner, G. (1997). GIS datasets for 3D urban planning. *Computers, Environment and Urban Systems*, *21*(2), 159-173. https://doi.org/10.1016/S0198-9715(97)10005-9

Rautenbach, V., Coetzee, S., Schiewe, J., & Çöltekin, A. (2015). An Assessment of Visual Variables for the Cartographic Design of 3D Informal Settlement Models. *Proceedings of the 27th International Cartographic Conference*. Présenté à Proceedings of the 27th International Cartographic Conference, Rio de Janeiro, Brazil.

Resch, B., Hillen, F., Reimer, A., & Spitzer, W. (2013). Towards 4D Cartography – Four-dimensional Dynamic Maps for Understanding Spatio-temporal Correlations in Lightning Events. *The Cartographic Journal*, *50*(3), 266-275. https://doi.org/10.1179/1743277413Y.0000000062

Röhlig, M., & Schumann, H. (2016). Visibility Widgets : Managing Occlusion of Quantitative Data in 3D Terrain Visualization. *Proceedings of the 9th International Symposium on Visual Information Communication and Interaction - VINCI '16*, 51-58. https://doi.org/10.1145/2968220.2968230

Ropinski, T., Steinicke, F., & Hinrichs, K. (2005). A constrained road-based VR navigation technique for travelling in 3D city models. *Proceedings of the 2005 International Conference on Augmented Tele-Existence - ICAT '05*, 228. https://doi.org/10.1145/1152399.1152441

Ryan, M. L. (1999). Immersion vs. Interactivity : Virtual Reality and Literary Theory. *SubStance*, *28*(2), 110-137.

Semmo, A., Trapp, M., Jobst, M., & Döllner, J. (2015). Cartography-Oriented Design of 3D Geospatial Information Visualization – Overview and Techniques. *The Cartographic Journal*, *52*(2), 95-106. https://doi.org/10.1080/00087041.2015.1119462

Semmo, A., Trapp, M., Kyprianidis, J. E., & Döllner, J. (2012). Interactive Visualization of Generalized Virtual 3D City Models using Level-of-Abstraction Transitions. *Computer Graphics Forum*, *31*(3pt1), 885-894. https://doi.org/10.1111/j.1467-8659.2012.03081.x

Sheridan, T. B. (1992). Musings on Telepresence and Virtual Presence. *Presence: Teleoperators and Virtual Environments*, *1*(1), 120-126.

Shojaei, D., Kalantari, M., Bishop, I. D., Rajabifard, A., & Aien, A. (2013). Visualization requirements for 3D cadastral systems. *Computers, Environment and Urban Systems*, *41*, 39-54. https://doi.org/10.1016/j.compenvurbsys.2013.04.003

Sinning-Meister, M., Gruen, A., & Dan, H. (1996). 3D City models for CAAD-supported analysis and design of urban areas. *ISPRS Journal of Photogrammetry and Remote Sensing*, *51*(4), 196–208.

Slocum, T. A., McMaster, R. B., Kessler, F. C., & Howard, H. H. (2010). *Thematic Cartography and geovisualization* (Pearson Education LTD). London.

Snyder, J. P. (1987). *Map projections—A working manual*. Washington, D.C.: US Government Printing Office.

Sokolov, D., Plemenos, D., & Tamine, K. (2006). Methods and data structures for virtual world exploration. *The Visual Computer*, *22*(7), 506-516. https://doi.org/10.1007/s00371-006-0025-3

Stadler, A., & Kolbe, T. H. (2007). Spatio-semantic coherence in the integration of 3D city models. *Proceedings of the 5th International*

*ISPRS Symposium on Spatial Data Quality ISSDQ 2007 in Enschede, The Netherlands, 13-15 June 2007*.

Stein, T., & Décoret, X. (2008). *Dynamic label placement for improved interactive exploration*. 15. https://doi.org/10.1145/1377980.1377986

Stevens, S. S. (1946). *On the Theory of Scales of Measurement*. *103*(2684), 677-680.

Tempfli, K., & Pilouk, M. (1996). Practicable photogrammetry for 3D-GIS. *International archives of photogrammetry, remote sensing and spatial information sciences*, 859-867. Vienna, Austria.

Tjan, B. S., & Legge, G. E. (1998). The viewpoint complexity of an object-recognition task. *Vision Research*, *38*(15-16), 2335-2350. https://doi.org/10.1016/S0042-6989(97)00255-1

Trapp, M., Beesk, C., Pasewaldt, S., & Döllner, J. (2011). Interactive Rendering Techniques for Highlighting in 3D Geovirtual Environments. In T. H. Kolbe, G. König, & C. Nagel (Éd.), *Advances in 3D Geo-Information Sciences* (p. 197-210). https://doi.org/10.1007/978-3-642-12670-3_12

Van Velsen, L., Van Der Geest, T., Klaassen, R., & Steehouder, M. (2008). User-centered evaluation of adaptive and adaptable systems : A

literature review. *The Knowledge Engineering Review*, *23*(03). https://doi.org/10.1017/S0269888908001379

Vazquez, P.-P., Feixas, M., Sbert, M., & Heidrich, W. (2001). Viewpoint Selection using Viewpoint Entropy. *Proceedings of the Vision Modeling and Visualization Conference*, 273-280. Aka GlbH.

Virzi, R. (1992). Refining the test phase of usability evaluation : How many subjects is enough? *Human factors*, *34*(4), 457-468.

Wallach, D., & Scholz, S. C. (2012). User-Centered Design : Why and How to Put Users First in Software Development. In A. Maedche, A. Botzenhardt, & L. Neer (Éd.), *Software for People* (p. 11-38). https://doi.org/10.1007/978-3-642-31371-4_2

Wang, C., Pouliot, J., & Hubert, F. (2012). *Visualization Principles in 3D Cadastre : A First Assessment of Visual Variables*. Présenté à 3rd International Workshop on 3D Cadastres, Shenzhen.

Wang, Chen. (2015). *3D Visualization of Cadastre : Assessing the Suitability of Visual Variables and Enhancement Techniques in the 3D Model of Condominium Property Units*. Université Laval, Québec.

Wang, Chen, Pouliot, J., & Hubert, F. (2017). How users perceive transparency in the 3D visualization of cadastre : Testing its

usability in an online questionnaire. *GeoInformatica*, *21*(3), 599-618. https://doi.org/10.1007/s10707-016-0281-y

Wang, Y., Wang, X., Wang, J., Yung, P., & Jun, G. (2013). Engagement of Facilities Management in Design Stage through BIM : Framework and a Case Study. *Advances in Civil Engineering*, *2013*, 1-8. https://doi.org/10.1155/2013/189105

Ward, M. O., Grinstein, G., & Keim, D. (2010). *Interactive Data Visualization : Foundations, Techniques, and Applications*. CRC Press.

Ware, C. (2012). *Information Visualization Perception for Design* (3rd ed..). Burlington: Elsevier Science.

Ware, C., Hui, D., & Franck, G. (1993). *Visualizing Object Oriented Software in Three Dimensions*. 612-620. Torronto, Ontario, Canada.

Wetzel, E. M., & Thabet, W. Y. (2016). *The use of a BIM-based framework to support safe facility management processes* (Virginia Polytechnic Institute and State University).

Willenborg, B., Sindram, M., & Kolbe, T. (2018). Applications of 3D City Models for a Better Understanding of the Built Environment. In M. Behnisch & G. Meinel (Éd.), *Trends in Spatial Analysis and Modelling* (Vol. 19, p. 167-191). https://doi.org/10.1007/978-3-319-52522-8_9

Wu, H., He, Z., & Gong, J. (2010). A virtual globe-based 3D visualization and interactive framework for public participation in urban planning processes. *Computers, Environment and Urban Systems*, *34*(4), 291-298. https://doi.org/10.1016/j.compenvurbsys.2009.12.001

Yan, W., Culp, C., & Graf, R. (2011). Integrating BIM and gaming for real-time interactive architectural visualization. *Automation in Construction*, *20*(4), 446-458. https://doi.org/10.1016/j.autcon.2010.11.013

Zhang, J. P., & Hu, Z. Z. (2011). BIM- and 4D-based integrated solution of analysis and management for conflicts and structural safety problems during construction : 1. Principles and methodologies. *Automation in Construction*, *20*(2), 155-166. https://doi.org/10.1016/j.autcon.2010.09.013

Zhang, X., Arayici, Y., Wu, S., Abbott, C., & Aouad, G. (2009). Integrating BIM and GIS for large scale (building) asset management : A critical review. *Proceedings 12th International Conference on Civil Structural and Environmental Engineering Computing*, 16. Madeira, Portugal: Civil-Comp Press.

Zhou, Y., Dao, T. H. D., Thill, J.-C., & Delmelle, E. (2015). Enhanced 3D visualization techniques in support of indoor location planning. *Computers, Environment and Urban Systems*, *50*, 15-29. https://doi.org/10.1016/j.compenvurbsys.2014.10.003

Zhu, Q., Hu, M., Zhang, Y., & Du, Z. (2009). Research and practice in three-dimensional city modeling. *Geo-Spatial Information Science*, *12*(1), 18-24. https://doi.org/10.1007/s11806-009-0195-z

Zlatanova, S., Van Oosterom, P., & Verbree, E. (2004). 3D technology for improving Disaster Management : Geo-DBMS and positioning. *Proceedings of the XXth ISPRS congress*.

# Appendix 1 – Online questionnaire results

| Question | Participant | Answer | Solution | Correctness | Speed (s) | Certainty | Point of view (POV) | Background training | Decision-making level | 3D Visualization experience |
|---|---|---|---|---|---|---|---|---|---|---|
| **1** | 1 | 6 | 6 | 1 | 59,7 | 2 | 4POV | surveyor | technical | never |
| **2** | 1 | 7 | 7 | 1 | 19,9 | 1 | SPOV | surveyor | technical | never |
| **3** | 1 | 4 | 4 | 1 | 9,2 | 3 | BPOV | surveyor | technical | never |
| **4** | 1 | 5 | 5 | 1 | 37,7 | 2 | 4POV | surveyor | technical | never |
| **5** | 1 | 7 | 7 | 1 | 9,4 | 3 | BPOV | surveyor | technical | never |
| **6** | 1 | 4 | 4 | 1 | 7,7 | 3 | SPOV | surveyor | technical | never |
| **7** | 1 | 5 | 7 | 0 | 21,7 | 3 | 4POV | surveyor | technical | never |
| **8** | 1 | 5 | 6 | 0 | 13,5 | 3 | SPOV | surveyor | technical | never |
| **9** | 1 | 5 | 5 | 1 | 17,8 | 3 | BPOV | surveyor | technical | never |
| **10** | 1 | 4 | 4 | 1 | 14,1 | 3 | 4POV | surveyor | technical | never |
| **11** | 1 | 6 | 6 | 1 | 7 | 3 | BPOV | surveyor | technical | never |
| **12** | 1 | 5 | 5 | 1 | 6,3 | 3 | SPOV | surveyor | technical | never |
| **1** | 2 | 5 | 6 | 0 | 41,2 | 2 | 4POV | surveyor | technical | often |
| **2** | 2 | 6 | 7 | 0 | 29,3 | 3 | SPOV | surveyor | technical | often |
| **3** | 2 | 4 | 4 | 1 | 22,6 | 3 | BPOV | surveyor | technical | often |
| **4** | 2 | 5 | 5 | 1 | 30,8 | 3 | 4POV | surveyor | technical | often |
| **5** | 2 | 7 | 7 | 1 | 9,2 | 3 | BPOV | surveyor | technical | often |
| **6** | 2 | 4 | 4 | 1 | 6,9 | 2 | SPOV | surveyor | technical | often |

| | | | | | | | | | | |
|---|---|---|---|---|---|---|---|---|---|---|
| **7** | 2 | 7 | 7 | 1 | 32 | 2 | 4PO V | surveyo r | technic al | often |
| **8** | 2 | 6 | 6 | 1 | 13,9 | 3 | SPO V | surveyo r | technic al | often |
| **9** | 2 | 5 | 5 | 1 | 9,5 | 3 | BPO V | surveyo r | technic al | often |
| **10** | 2 | 4 | 4 | 1 | 27,6 | 2 | 4PO V | surveyo r | technic al | often |
| **11** | 2 | 6 | 6 | 1 | 7,9 | 3 | BPO V | surveyo r | technic al | often |
| **12** | 2 | 5 | 5 | 1 | 9,4 | 3 | SPO V | surveyo r | technic al | often |
| **1** | 3 | 6 | 6 | 1 | 71,5 | 2 | 4PO V | surveyo r | technic al | often |
| **2** | 3 | 7 | 7 | 1 | 25,2 | 3 | SPO V | surveyo r | technic al | often |
| **3** | 3 | 4 | 4 | 1 | 15,3 | 3 | BPO V | surveyo r | technic al | often |
| **4** | 3 | 5 | 5 | 1 | 44,6 | 2 | 4PO V | surveyo r | technic al | often |
| **5** | 3 | 7 | 7 | 1 | 14 | 2 | BPO V | surveyo r | technic al | often |
| **6** | 3 | 4 | 4 | 1 | 10,8 | 2 | SPO V | surveyo r | technic al | often |
| **7** | 3 | 8 | 7 | 0 | 47,1 | 1 | 4PO V | surveyo r | technic al | often |
| **8** | 3 | 6 | 6 | 1 | 26,6 | 2 | SPO V | surveyo r | technic al | often |
| **9** | 3 | 5 | 5 | 1 | 9,3 | 3 | BPO V | surveyo r | technic al | often |
| **10** | 3 | 4 | 4 | 1 | 111,5 | 1 | 4PO V | surveyo r | technic al | often |
| **11** | 3 | 6 | 6 | 1 | 10,6 | 2 | BPO V | surveyo r | technic al | often |
| **12** | 3 | 5 | 5 | 1 | 14,3 | 2 | SPO V | surveyo r | technic al | often |
| **1** | 4 | 5 | 6 | 0 | 52,8 | 2 | 4PO V | surveyo r | technic al | often |
| **2** | 4 | 7 | 7 | 1 | 32,1 | 3 | SPO V | surveyo r | technic al | often |
| **3** | 4 | 4 | 4 | 1 | 15,4 | 3 | BPO V | surveyo r | technic al | often |
| **4** | 4 | 5 | 5 | 1 | 44,4 | 2 | 4PO V | surveyo r | technic al | often |
| **5** | 4 | 7 | 7 | 1 | 8,5 | 3 | BPO V | surveyo r | technic al | often |
| **6** | 4 | 4 | 4 | 1 | 8,8 | 3 | SPO V | surveyo r | technic al | often |
| **7** | 4 | 7 | 7 | 1 | 103 | 2 | 4PO V | surveyo r | technic al | often |

| | | | | | | | | | | |
|---|---|---|---|---|---|---|---|---|---|---|
| **8** | 4 | 6 | 6 | 1 | 14 | 3 | SPOV | surveyor | technical | often |
| **9** | 4 | 5 | 5 | 1 | 6,9 | 3 | BPOV | surveyor | technical | often |
| **10** | 4 | 4 | 4 | 1 | 42 | 2 | 4POV | surveyor | technical | often |
| **11** | 4 | 6 | 6 | 1 | 8,2 | 3 | BPOV | surveyor | technical | often |
| **12** | 4 | 5 | 5 | 1 | 12 | 3 | SPOV | surveyor | technical | often |
| **1** | 5 | 6 | 6 | 1 | 56,7 | 3 | 4POV | surveyor | technical | often |
| **2** | 5 | 6 | 7 | 0 | 113,7 | 1 | SPOV | surveyor | technical | often |
| **3** | 5 | 4 | 4 | 1 | 82,8 | 3 | BPOV | surveyor | technical | often |
| **4** | 5 | 5 | 5 | 1 | 59,2 | 3 | 4POV | surveyor | technical | often |
| **5** | 5 | 7 | 7 | 1 | 62,5 | 3 | BPOV | surveyor | technical | often |
| **6** | 5 | 4 | 4 | 1 | 93,3 | 3 | SPOV | surveyor | technical | often |
| **7** | 5 | 6 | 7 | 0 | 92,5 | 2 | 4POV | surveyor | technical | often |
| **8** | 5 | 6 | 6 | 1 | 36,7 | 3 | SPOV | surveyor | technical | often |
| **9** | 5 | 5 | 5 | 1 | 40,3 | 3 | BPOV | surveyor | technical | often |
| **10** | 5 | 4 | 4 | 1 | 62,1 | 3 | 4POV | surveyor | technical | often |
| **11** | 5 | 6 | 6 | 1 | 44,6 | 3 | BPOV | surveyor | technical | often |
| **12** | 5 | 5 | 5 | 1 | 35,3 | 3 | SPOV | surveyor | technical | often |
| **1** | 6 | 7 | 6 | 0 | 71,7 | 2 | 4POV | surveyor | technical | sometimes |
| **2** | 6 | 7 | 7 | 1 | 32,9 | 3 | SPOV | surveyor | technical | sometimes |
| **3** | 6 | 4 | 4 | 1 | 13,9 | 3 | BPOV | surveyor | technical | sometimes |
| **4** | 6 | 5 | 5 | 1 | 76,2 | 2 | 4POV | surveyor | technical | sometimes |
| **5** | 6 | 7 | 7 | 1 | 19,6 | 3 | BPOV | surveyor | technical | sometimes |
| **6** | 6 | 4 | 4 | 1 | 15,1 | 3 | SPOV | surveyor | technical | sometimes |
| **7** | 6 | 7 | 7 | 1 | 42,3 | 2 | 4POV | surveyor | technical | sometimes |
| **8** | 6 | 5 | 6 | 0 | 13,7 | 3 | SPOV | surveyor | technical | sometimes |

| | | | | | | | | | | |
|---|---|---|---|---|---|---|---|---|---|---|
| **9** | 6 | 5 | 5 | 1 | 11,6 | 3 | BPO V | surveyor | technical | sometimes |
| **10** | 6 | 4 | 4 | 1 | 46,5 | 2 | 4PO V | surveyor | technical | sometimes |
| **11** | 6 | 6 | 6 | 1 | 10,8 | 3 | BPO V | surveyor | technical | sometimes |
| **12** | 6 | 5 | 5 | 1 | 15,8 | 3 | SPO V | surveyor | technical | sometimes |
| **1** | 7 | 5 | 6 | 0 | 58,6 | 2 | 4PO V | engineer | technical | sometimes |
| **2** | 7 | 7 | 7 | 1 | 14,5 | 3 | SPO V | engineer | technical | sometimes |
| **3** | 7 | 4 | 4 | 1 | 8,5 | 3 | BPO V | engineer | technical | sometimes |
| **4** | 7 | 8 | 5 | 0 | 30 | 1 | 4PO V | engineer | technical | sometimes |
| **5** | 7 | 7 | 7 | 1 | 8,1 | 3 | BPO V | engineer | technical | sometimes |
| **6** | 7 | 4 | 4 | 1 | 5,6 | 3 | SPO V | engineer | technical | sometimes |
| **7** | 7 | 6 | 7 | 0 | 16,4 | 2 | 4PO V | engineer | technical | sometimes |
| **8** | 7 | 6 | 6 | 1 | 6,4 | 2 | SPO V | engineer | technical | sometimes |
| **9** | 7 | 5 | 5 | 1 | 5,2 | 3 | BPO V | engineer | technical | sometimes |
| **10** | 7 | 6 | 4 | 0 | 17,7 | 1 | 4PO V | engineer | technical | sometimes |
| **11** | 7 | 6 | 6 | 1 | 5,7 | 3 | BPO V | engineer | technical | sometimes |
| **12** | 7 | 5 | 5 | 1 | 5,4 | 3 | SPO V | engineer | technical | sometimes |
| **1** | 8 | 6 | 6 | 1 | 23,4 | 2 | 4PO V | engineer | technical | never |
| **2** | 8 | 7 | 7 | 1 | 13,2 | 1 | SPO V | engineer | technical | never |
| **3** | 8 | 4 | 4 | 1 | 8,2 | 3 | BPO V | engineer | technical | never |
| **4** | 8 | 7 | 5 | 0 | 26,7 | 2 | 4PO V | engineer | technical | never |
| **5** | 8 | 7 | 7 | 1 | 8,1 | 3 | BPO V | engineer | technical | never |
| **6** | 8 | 4 | 4 | 1 | 5,5 | 3 | SPO V | engineer | technical | never |
| **7** | 8 | 7 | 7 | 1 | 22,2 | 1 | 4PO V | engineer | technical | never |
| **8** | 8 | 6 | 6 | 1 | 10,1 | 3 | SPO V | engineer | technical | never |
| **9** | 8 | 5 | 5 | 1 | 7,4 | 3 | BPO V | engineer | technical | never |

| | | | | | | | | | | |
|---|---|---|---|---|---|---|---|---|---|---|
| **10** | 8 | 4 | 4 | 1 | 22,1 | 2 | 4PO V | enginee r | technic al | never |
| **11** | 8 | 6 | 6 | 1 | 9 | 3 | BPO V | enginee r | technic al | never |
| **12** | 8 | 5 | 5 | 1 | 9,8 | 3 | SPO V | enginee r | technic al | never |
| **1** | 9 | 4 | 6 | 0 | 59,8 | 3 | 4PO V | architec t | technic al | often |
| **2** | 9 | 7 | 7 | 1 | 24,5 | 3 | SPO V | architec t | technic al | often |
| **3** | 9 | 4 | 4 | 1 | 17,8 | 3 | BPO V | architec t | technic al | often |
| **4** | 9 | 5 | 5 | 1 | 23,7 | 2 | 4PO V | architec t | technic al | often |
| **5** | 9 | 7 | 7 | 1 | 11,6 | 3 | BPO V | architec t | technic al | often |
| **6** | 9 | 4 | 4 | 1 | 11 | 3 | SPO V | architec t | technic al | often |
| **7** | 9 | 5 | 7 | 0 | 43,2 | 3 | 4PO V | architec t | technic al | often |
| **8** | 9 | 6 | 6 | 1 | 14,7 | 3 | SPO V | architec t | technic al | often |
| **9** | 9 | 5 | 5 | 1 | 15,5 | 3 | BPO V | architec t | technic al | often |
| **10** | 9 | 4 | 4 | 1 | 14,1 | 2 | 4PO V | architec t | technic al | often |
| **11** | 9 | 6 | 6 | 1 | 12,7 | 3 | BPO V | architec t | technic al | often |
| **12** | 9 | 5 | 5 | 1 | 12,3 | 3 | SPO V | architec t | technic al | often |
| **1** | 10 | 4 | 6 | 0 | 87,9 | 1 | 4PO V | architec t | technic al | someti mes |
| **2** | 10 | 7 | 7 | 1 | 31,7 | 3 | SPO V | architec t | technic al | someti mes |
| **3** | 10 | 4 | 4 | 1 | 12,9 | 3 | BPO V | architec t | technic al | someti mes |
| **4** | 10 | 5 | 5 | 1 | 60,2 | 2 | 4PO V | architec t | technic al | someti mes |
| **5** | 10 | 7 | 7 | 1 | 21,9 | 3 | BPO V | architec t | technic al | someti mes |
| **6** | 10 | 4 | 4 | 1 | 9,7 | 3 | SPO V | architec t | technic al | someti mes |
| **7** | 10 | 5 | 7 | 0 | 56,8 | 2 | 4PO V | architec t | technic al | someti mes |
| **8** | 10 | 5 | 6 | 0 | 8,8 | 3 | SPO V | architec t | technic al | someti mes |
| **9** | 10 | 5 | 5 | 1 | 11,8 | 3 | BPO V | architec t | technic al | someti mes |
| **10** | 10 | 4 | 4 | 1 | 21,9 | 2 | 4PO V | architec t | technic al | someti mes |

| | | | | | | | | | | |
|---|---|---|---|---|---|---|---|---|---|---|
| **11** | 10 | 6 | 6 | 1 | 13,5 | 3 | BPOV | architect | technical | sometimes |
| **12** | 10 | 5 | 5 | 1 | 14,2 | 3 | SPOV | architect | technical | sometimes |
| **1** | 11 | 6 | 6 | 1 | 32,4 | 2 | 4POV | architect | technical | often |
| **2** | 11 | 7 | 7 | 1 | 30 | 2 | SPOV | architect | technical | often |
| **3** | 11 | 4 | 4 | 1 | 14 | 2 | BPOV | architect | technical | often |
| **4** | 11 | 5 | 5 | 1 | 19,2 | 1 | 4POV | architect | technical | often |
| **5** | 11 | 7 | 7 | 1 | 14,2 | 2 | BPOV | architect | technical | often |
| **6** | 11 | 4 | 4 | 1 | 9,6 | 2 | SPOV | architect | technical | often |
| **7** | 11 | 7 | 7 | 1 | 21,8 | 2 | 4POV | architect | technical | often |
| **8** | 11 | 6 | 6 | 1 | 14 | 2 | SPOV | architect | technical | often |
| **9** | 11 | 5 | 5 | 1 | 7,9 | 2 | BPOV | architect | technical | often |
| **10** | 11 | 4 | 4 | 1 | 23,5 | 1 | 4POV | architect | technical | often |
| **11** | 11 | 6 | 6 | 1 | 6,4 | 2 | BPOV | architect | technical | often |
| **12** | 11 | 5 | 5 | 1 | 11,6 | 2 | SPOV | architect | technical | often |
| **1** | 12 | 5 | 6 | 0 | 48,1 | 3 | 4POV | surveyor | strategic | often |
| **2** | 12 | 7 | 7 | 1 | 27,8 | 3 | SPOV | surveyor | strategic | often |
| **3** | 12 | 4 | 4 | 1 | 12,1 | 3 | BPOV | surveyor | strategic | often |
| **4** | 12 | 5 | 5 | 1 | 39,1 | 3 | 4POV | surveyor | strategic | often |
| **5** | 12 | 7 | 7 | 1 | 16 | 3 | BPOV | surveyor | strategic | often |
| **6** | 12 | 4 | 4 | 1 | 8,9 | 3 | SPOV | surveyor | strategic | often |
| **7** | 12 | 6 | 7 | 0 | 64,8 | 2 | 4POV | surveyor | strategic | often |
| **8** | 12 | 6 | 6 | 1 | 12,9 | 3 | SPOV | surveyor | strategic | often |
| **9** | 12 | 5 | 5 | 1 | 7,8 | 3 | BPOV | surveyor | strategic | often |
| **10** | 12 | 4 | 4 | 1 | 46,9 | 3 | 4POV | surveyor | strategic | often |
| **11** | 12 | 6 | 6 | 1 | 8,4 | 3 | BPOV | surveyor | strategic | often |

| | | | | | | | | | | |
|---|---|---|---|---|---|---|---|---|---|---|
| **12** | 12 | 5 | 5 | 1 | 10 | 3 | SPOV | surveyor | strategic | often |
| **1** | 13 | 5 | 6 | 0 | 55,4 | 2 | 4POV | surveyor | operational | often |
| **2** | 13 | 7 | 7 | 1 | 21,3 | 1 | SPOV | surveyor | operational | often |
| **3** | 13 | 4 | 4 | 1 | 15,7 | 2 | BPOV | surveyor | operational | often |
| **4** | 13 | 5 | 5 | 1 | 51,1 | 2 | 4POV | surveyor | operational | often |
| **5** | 13 | 7 | 7 | 1 | 14,7 | 2 | BPOV | surveyor | operational | often |
| **6** | 13 | 4 | 4 | 1 | 257,9 | 2 | SPOV | surveyor | operational | often |
| **7** | 13 | 7 | 7 | 1 | 100,4 | 1 | 4POV | surveyor | operational | often |
| **8** | 13 | 6 | 6 | 1 | 15,9 | 2 | SPOV | surveyor | operational | often |
| **9** | 13 | 5 | 5 | 1 | 9,5 | 2 | BPOV | surveyor | operational | often |
| **10** | 13 | 4 | 4 | 1 | 27,5 | 1 | 4POV | surveyor | operational | often |
| **11** | 13 | 6 | 6 | 1 | 10,3 | 2 | BPOV | surveyor | operational | often |
| **12** | 13 | 5 | 5 | 1 | 10,2 | 2 | SPOV | surveyor | operational | often |
| **1** | 14 | 6 | 6 | 1 | 154,8 | 1 | 4POV | surveyor | operational | sometimes |
| **2** | 14 | 7 | 7 | 1 | 33,7 | 2 | SPOV | surveyor | operational | sometimes |
| **3** | 14 | 4 | 4 | 1 | 12,3 | 2 | BPOV | surveyor | operational | sometimes |
| **4** | 14 | 6 | 5 | 0 | 75,2 | 2 | 4POV | surveyor | operational | sometimes |
| **5** | 14 | 7 | 7 | 1 | 15 | 2 | BPOV | surveyor | operational | sometimes |
| **6** | 14 | 4 | 4 | 1 | 14,9 | 2 | SPOV | surveyor | operational | sometimes |
| **7** | 14 | 9 | 7 | 0 | 72 | 2 | 4POV | surveyor | operational | sometimes |
| **8** | 14 | 6 | 6 | 1 | 17,7 | 2 | SPOV | surveyor | operational | sometimes |
| **9** | 14 | 5 | 5 | 1 | 15,1 | 2 | BPOV | surveyor | operational | sometimes |
| **10** | 14 | 6 | 4 | 0 | 40,2 | 2 | 4POV | surveyor | operational | sometimes |
| **11** | 14 | 6 | 6 | 1 | 13,2 | 2 | BPOV | surveyor | operational | sometimes |
| **12** | 14 | 5 | 5 | 1 | 16,7 | 2 | SPOV | surveyor | operational | sometimes |

| | | | | | | | | | | |
|---|---|---|---|---|---|---|---|---|---|---|
| **1** | 15 | 4 | 6 | 0 | 115,6 | 1 | 4POV | construction | technical | never |
| **2** | 15 | 7 | 7 | 1 | 34,5 | 1 | SPOV | construction | technical | never |
| **3** | 15 | 4 | 4 | 1 | 12,7 | 3 | BPOV | construction | technical | never |
| **4** | 15 | 5 | 5 | 1 | 24 | 2 | 4POV | construction | technical | never |
| **5** | 15 | 7 | 7 | 1 | 12,7 | 2 | BPOV | construction | technical | never |
| **6** | 15 | 4 | 4 | 1 | 13 | 3 | SPOV | construction | technical | never |
| **7** | 15 | 6 | 7 | 0 | 63,3 | 2 | 4POV | construction | technical | never |
| **8** | 15 | 6 | 6 | 1 | 11,2 | 3 | SPOV | construction | technical | never |
| **9** | 15 | 5 | 5 | 1 | 58,2 | 3 | BPOV | construction | technical | never |
| **10** | 15 | 4 | 4 | 1 | 26,4 | 2 | 4POV | construction | technical | never |
| **11** | 15 | 6 | 6 | 1 | 9,7 | 3 | BPOV | construction | technical | never |
| **12** | 15 | 5 | 5 | 1 | 13,5 | 3 | SPOV | construction | technical | never |
| **1** | 16 | 4 | 6 | 0 | 96,5 | 3 | 4POV | engineer | strategic | sometimes |
| **2** | 16 | 7 | 7 | 1 | 29,3 | 1 | SPOV | engineer | strategic | sometimes |
| **3** | 16 | 4 | 4 | 1 | 30,1 | 2 | BPOV | engineer | strategic | sometimes |
| **4** | 16 | 5 | 5 | 1 | 73,6 | 2 | 4POV | engineer | strategic | sometimes |
| **5** | 16 | 7 | 7 | 1 | 26,6 | 3 | BPOV | engineer | strategic | sometimes |
| **6** | 16 | 4 | 4 | 1 | 30,4 | 2 | SPOV | engineer | strategic | sometimes |
| **7** | 16 | 6 | 7 | 0 | 62,2 | 1 | 4POV | engineer | strategic | sometimes |
| **8** | 16 | 6 | 6 | 1 | 25,6 | 2 | SPOV | engineer | strategic | sometimes |
| **9** | 16 | 5 | 5 | 1 | 22,8 | 3 | BPOV | engineer | strategic | sometimes |
| **10** | 16 | 4 | 4 | 1 | 35,6 | 2 | 4POV | engineer | strategic | sometimes |
| **11** | 16 | 6 | 6 | 1 | 21,5 | 3 | BPOV | engineer | strategic | sometimes |
| **12** | 16 | 5 | 5 | 1 | 24,3 | 3 | SPOV | engineer | strategic | sometimes |
| **1** | 17 | 6 | 6 | 1 | 152 | 2 | 4POV | engineer | technical | often |

| | | | | | | | | | | |
|---|---|---|---|---|---|---|---|---|---|---|
| **2** | 17 | 7 | 7 | 1 | 31,6 | 3 | SPOV | engineer | technical | often |
| **3** | 17 | 4 | 4 | 1 | 10,5 | 3 | BPOV | engineer | technical | often |
| **4** | 17 | 5 | 5 | 1 | 83,4 | 2 | 4POV | engineer | technical | often |
| **5** | 17 | 7 | 7 | 1 | 9,7 | 3 | BPOV | engineer | technical | often |
| **6** | 17 | 4 | 4 | 1 | 9,6 | 2 | SPOV | engineer | technical | often |
| **7** | 17 | 6 | 7 | 0 | 44,8 | 1 | 4POV | engineer | technical | often |
| **8** | 17 | 6 | 6 | 1 | 14,7 | 3 | SPOV | engineer | technical | often |
| **9** | 17 | 5 | 5 | 1 | 11,5 | 3 | BPOV | engineer | technical | often |
| **10** | 17 | 4 | 4 | 1 | 43 | 2 | 4POV | engineer | technical | often |
| **11** | 17 | 6 | 6 | 1 | 7,4 | 3 | BPOV | engineer | technical | often |
| **12** | 17 | 5 | 5 | 1 | 12,8 | 3 | SPOV | engineer | technical | often |
| **1** | 18 | 6 | 6 | 1 | 65,4 | 2 | 4POV | engineer | technical | never |
| **2** | 18 | 7 | 7 | 1 | 22,7 | 3 | SPOV | engineer | technical | never |
| **3** | 18 | 4 | 4 | 1 | 8,4 | 3 | BPOV | engineer | technical | never |
| **4** | 18 | 6 | 5 | 0 | 52,5 | 1 | 4POV | engineer | technical | never |
| **5** | 18 | 7 | 7 | 1 | 10,2 | 3 | BPOV | engineer | technical | never |
| **6** | 18 | 4 | 4 | 1 | 6,6 | 3 | SPOV | engineer | technical | never |
| **7** | 18 | 8 | 7 | 0 | 38,8 | 1 | 4POV | engineer | technical | never |
| **8** | 18 | 6 | 6 | 1 | 12,5 | 2 | SPOV | engineer | technical | never |
| **9** | 18 | 5 | 5 | 1 | 8,4 | 3 | BPOV | engineer | technical | never |
| **10** | 18 | 6 | 4 | 0 | 38,2 | 2 | 4POV | engineer | technical | never |
| **11** | 18 | 6 | 6 | 1 | 11 | 3 | BPOV | engineer | technical | never |
| **12** | 18 | 5 | 5 | 1 | 11,6 | 3 | SPOV | engineer | technical | never |
| **1** | 19 | 5 | 6 | 0 | 55,8 | 1 | 4POV | surveyor | technical | never |
| **2** | 19 | 7 | 7 | 1 | 21,2 | 1 | SPOV | surveyor | technical | never |

| | | | | | | | | | | |
|---|---|---|---|---|---|---|---|---|---|---|
| **3** | 19 | 4 | 4 | 1 | 13 | 2 | BPO V | surveyo r | technic al | never |
| **4** | 19 | 5 | 5 | 1 | 43,4 | 2 | 4PO V | surveyo r | technic al | never |
| **5** | 19 | 7 | 7 | 1 | 10,9 | 3 | BPO V | surveyo r | technic al | never |
| **6** | 19 | 4 | 4 | 1 | 11,2 | 0 | SPO V | surveyo r | technic al | never |
| **7** | 19 | 7 | 7 | 1 | 87,8 | 1 | 4PO V | surveyo r | technic al | never |
| **8** | 19 | 5 | 6 | 0 | 24,3 | 2 | SPO V | surveyo r | technic al | never |
| **9** | 19 | 5 | 5 | 1 | 7,5 | 3 | BPO V | surveyo r | technic al | never |
| **10** | 19 | 4 | 4 | 1 | 24,5 | 2 | 4PO V | surveyo r | technic al | never |
| **11** | 19 | 6 | 6 | 1 | 8,4 | 2 | BPO V | surveyo r | technic al | never |
| **12** | 19 | 5 | 5 | 1 | 8,7 | 1 | SPO V | surveyo r | technic al | never |
| **1** | 20 | 6 | 6 | 1 | 26,3 | 2 | 4PO V | enginee r | technic al | often |
| **2** | 20 | 7 | 7 | 1 | 17,4 | 3 | SPO V | enginee r | technic al | often |
| **3** | 20 | 4 | 4 | 1 | 8,8 | 3 | BPO V | enginee r | technic al | often |
| **4** | 20 | 6 | 5 | 0 | 49,6 | 1 | 4PO V | enginee r | technic al | often |
| **5** | 20 | 7 | 7 | 1 | 11,9 | 3 | BPO V | enginee r | technic al | often |
| **6** | 20 | 4 | 4 | 1 | 15,7 | 2 | SPO V | enginee r | technic al | often |
| **7** | 20 | 8 | 7 | 0 | 49,2 | 0 | 4PO V | enginee r | technic al | often |
| **8** | 20 | 6 | 6 | 1 | 9,6 | 2 | SPO V | enginee r | technic al | often |
| **9** | 20 | 5 | 5 | 1 | 8,5 | 2 | BPO V | enginee r | technic al | often |
| **10** | 20 | 5 | 4 | 0 | 40,4 | 0 | 4PO V | enginee r | technic al | often |
| **11** | 20 | 6 | 6 | 1 | 7,2 | 3 | BPO V | enginee r | technic al | often |
| **12** | 20 | 5 | 5 | 1 | 14,4 | 3 | SPO V | enginee r | technic al | often |
| **1** | 21 | 5 | 6 | 0 | 172,8 | 1 | 4PO V | enginee r | technic al | never |
| **2** | 21 | 7 | 7 | 1 | 18,8 | 2 | SPO V | enginee r | technic al | never |
| **3** | 21 | 4 | 4 | 1 | 13 | 3 | BPO V | enginee r | technic al | never |

| | | | | | | | | | | |
|---|---|---|---|---|---|---|---|---|---|---|
| **4** | 21 | 5 | 5 | 1 | 33,9 | 2 | 4PO V | enginee r | technic al | never |
| **5** | 21 | 7 | 7 | 1 | 15,1 | 3 | BPO V | enginee r | technic al | never |
| **6** | 21 | 4 | 4 | 1 | 10,9 | 3 | SPO V | enginee r | technic al | never |
| **7** | 21 | 5 | 7 | 0 | 84,5 | 2 | 4PO V | enginee r | technic al | never |
| **8** | 21 | 6 | 6 | 1 | 12 | 3 | SPO V | enginee r | technic al | never |
| **9** | 21 | 5 | 5 | 1 | 9,8 | 3 | BPO V | enginee r | technic al | never |
| **10** | 21 | 4 | 4 | 1 | 26,6 | 2 | 4PO V | enginee r | technic al | never |
| **11** | 21 | 6 | 6 | 1 | 69,1 | 3 | BPO V | enginee r | technic al | never |
| **12** | 21 | 5 | 5 | 1 | 11,4 | 3 | SPO V | enginee r | technic al | never |
| **1** | 22 | 6 | 6 | 1 | 199,6 | 2 | 4PO V | enginee r | technic al | often |
| **2** | 22 | 7 | 7 | 1 | 36,7 | 3 | SPO V | enginee r | technic al | often |
| **3** | 22 | 4 | 4 | 1 | 8,8 | 3 | BPO V | enginee r | technic al | often |
| **4** | 22 | 6 | 5 | 0 | 38,8 | 2 | 4PO V | enginee r | technic al | often |
| **5** | 22 | 7 | 7 | 1 | 11,7 | 3 | BPO V | enginee r | technic al | often |
| **6** | 22 | 4 | 4 | 1 | 8,8 | 3 | SPO V | enginee r | technic al | often |
| **7** | 22 | 5 | 7 | 0 | 28,7 | 3 | 4PO V | enginee r | technic al | often |
| **8** | 22 | 5 | 6 | 0 | 9,6 | 3 | SPO V | enginee r | technic al | often |
| **9** | 22 | 5 | 5 | 1 | 8,2 | 3 | BPO V | enginee r | technic al | often |
| **10** | 22 | 4 | 4 | 1 | 18,2 | 3 | 4PO V | enginee r | technic al | often |
| **11** | 22 | 6 | 6 | 1 | 9,6 | 3 | BPO V | enginee r | technic al | often |
| **12** | 22 | 5 | 5 | 1 | 13,5 | 3 | SPO V | enginee r | technic al | often |
| **1** | 23 | 7 | 6 | 0 | 117,4 | 2 | 4PO V | surveyo r | strategi c | often |
| **2** | 23 | 7 | 7 | 1 | 17 | 3 | SPO V | surveyo r | strategi c | often |
| **3** | 23 | 4 | 4 | 1 | 13,9 | 3 | BPO V | surveyo r | strategi c | often |
| **4** | 23 | 6 | 5 | 0 | 44,4 | 2 | 4PO V | surveyo r | strategi c | often |

| | | | | | | | | | | |
|---|---|---|---|---|---|---|---|---|---|---|
| **5** | 23 | 7 | 7 | 1 | 8,7 | 3 | BPO V | surveyor | strategic | often |
| **6** | 23 | 4 | 4 | 1 | 11,2 | 3 | SPO V | surveyor | strategic | often |
| **7** | 23 | 6 | 7 | 0 | 175,6 | 2 | 4PO V | surveyor | strategic | often |
| **8** | 23 | 5 | 6 | 0 | 14,9 | 3 | SPO V | surveyor | strategic | often |
| **9** | 23 | 5 | 5 | 1 | 7 | 3 | BPO V | surveyor | strategic | often |
| **10** | 23 | 5 | 4 | 0 | 41 | 2 | 4PO V | surveyor | strategic | often |
| **11** | 23 | 6 | 6 | 1 | 7,6 | 3 | BPO V | surveyor | strategic | often |
| **12** | 23 | 5 | 5 | 1 | 19,7 | 3 | SPO V | surveyor | strategic | often |
| **1** | 24 | 4 | 6 | 0 | 21,4 | 3 | 4PO V | engineer | operational | never |
| **2** | 24 | 7 | 7 | 1 | 16,8 | 3 | SPO V | engineer | operational | never |
| **3** | 24 | 4 | 4 | 1 | 10,5 | 3 | BPO V | engineer | operational | never |
| **4** | 24 | 5 | 5 | 1 | 13,9 | 3 | 4PO V | engineer | operational | never |
| **5** | 24 | 7 | 7 | 1 | 12,2 | 3 | BPO V | engineer | operational | never |
| **6** | 24 | 4 | 4 | 1 | 8,3 | 3 | SPO V | engineer | operational | never |
| **7** | 24 | 5 | 7 | 0 | 105,6 | 2 | 4PO V | engineer | operational | never |
| **8** | 24 | 5 | 6 | 0 | 8,8 | 3 | SPO V | engineer | operational | never |
| **9** | 24 | 5 | 5 | 1 | 10,4 | 3 | BPO V | engineer | operational | never |
| **10** | 24 | 5 | 4 | 0 | 35 | 2 | 4PO V | engineer | operational | never |
| **11** | 24 | 6 | 6 | 1 | 13,5 | 3 | BPO V | engineer | operational | never |
| **12** | 24 | 5 | 5 | 1 | 9,1 | 3 | SPO V | engineer | operational | never |
| **1** | 25 | 6 | 6 | 1 | 55,4 | 2 | 4PO V | engineer | operational | sometimes |
| **2** | 25 | 7 | 7 | 1 | 40,2 | 3 | SPO V | engineer | operational | sometimes |
| **3** | 25 | 4 | 4 | 1 | 25,7 | 3 | BPO V | engineer | operational | sometimes |
| **4** | 25 | 5 | 5 | 1 | 55,5 | 2 | 4PO V | engineer | operational | sometimes |
| **5** | 25 | 7 | 7 | 1 | 26,6 | 3 | BPO V | engineer | operational | sometimes |

| | | | | | | | | | | |
|---|---|---|---|---|---|---|---|---|---|---|
| **6** | 25 | 4 | 4 | 1 | 24,5 | 3 | SPOV | engineer | operational | sometimes |
| **7** | 25 | 7 | 7 | 1 | 35 | 3 | 4POV | engineer | operational | sometimes |
| **8** | 25 | 5 | 6 | 0 | 33,3 | 3 | SPOV | engineer | operational | sometimes |
| **9** | 25 | 5 | 5 | 1 | 16,7 | 3 | BPOV | engineer | operational | sometimes |
| **10** | 25 | 4 | 4 | 1 | 25,6 | 2 | 4POV | engineer | operational | sometimes |
| **11** | 25 | 6 | 6 | 1 | 24,9 | 3 | BPOV | engineer | operational | sometimes |
| **12** | 25 | 5 | 5 | 1 | 21,1 | 3 | SPOV | engineer | operational | sometimes |
| **1** | 26 | 6 | 6 | 1 | 80,6 | 1 | 4POV | engineer | operational | never |
| **2** | 26 | 7 | 7 | 1 | 39,2 | 2 | SPOV | engineer | operational | never |
| **3** | 26 | 4 | 4 | 1 | 17,7 | 3 | BPOV | engineer | operational | never |
| **4** | 26 | 5 | 5 | 1 | 59 | 2 | 4POV | engineer | operational | never |
| **5** | 26 | 7 | 7 | 1 | 24,7 | 3 | BPOV | engineer | operational | never |
| **6** | 26 | 4 | 4 | 1 | 18,5 | 3 | SPOV | engineer | operational | never |
| **7** | 26 | 7 | 7 | 1 | 90,8 | 2 | 4POV | engineer | operational | never |
| **8** | 26 | 5 | 6 | 1 | 20 | 2 | SPOV | engineer | operational | never |
| **9** | 26 | 5 | 5 | 1 | 11,8 | 3 | BPOV | engineer | operational | never |
| **10** | 26 | 4 | 4 | 1 | 21,9 | 2 | 4POV | engineer | operational | never |
| **11** | 26 | 6 | 6 | 1 | 10,5 | 3 | BPOV | engineer | operational | never |
| **12** | 26 | 5 | 5 | 1 | 9,1 | 3 | SPOV | engineer | operational | never |
| **1** | 27 | 6 | 6 | 1 | 37,2 | 2 | 4POV | engineer | operational | sometimes |
| **2** | 27 | 6 | 7 | 0 | 29,8 | 3 | SPOV | engineer | operational | sometimes |
| **3** | 27 | 4 | 4 | 1 | 22,5 | 3 | BPOV | engineer | operational | sometimes |
| **4** | 27 | 5 | 5 | 1 | 44,9 | 2 | 4POV | engineer | operational | sometimes |
| **5** | 27 | 7 | 7 | 1 | 15,1 | 3 | BPOV | engineer | operational | sometimes |
| **6** | 27 | 4 | 4 | 1 | 11,1 | 3 | SPOV | engineer | operational | sometimes |

| | | | | | | | | | | |
|---|---|---|---|---|---|---|---|---|---|---|
| **7** | 27 | 7 | 7 | 1 | 50,1 | 2 | 4POV | engineer | operational | sometimes |
| **8** | 27 | 5 | 6 | 0 | 12,3 | 3 | SPOV | engineer | operational | sometimes |
| **9** | 27 | 5 | 5 | 1 | 14 | 3 | BPOV | engineer | operational | sometimes |
| **10** | 27 | 4 | 4 | 1 | 49,1 | 3 | 4POV | engineer | operational | sometimes |
| **11** | 27 | 6 | 6 | 1 | 17,2 | 3 | BPOV | engineer | operational | sometimes |
| **12** | 27 | 5 | 5 | 1 | 13,8 | 3 | SPOV | engineer | operational | sometimes |
| **1** | 28 | 6 | 6 | 1 | 136,4 | 3 | 4POV | architect | technical | often |
| **2** | 28 | 7 | 7 | 1 | 47,6 | 2 | SPOV | architect | technical | often |
| **3** | 28 | 4 | 4 | 1 | 25,4 | 3 | BPOV | architect | technical | often |
| **4** | 28 | 5 | 5 | 1 | 36,7 | 3 | 4POV | architect | technical | often |
| **5** | 28 | 7 | 7 | 1 | 19,5 | 3 | BPOV | architect | technical | often |
| **6** | 28 | 4 | 4 | 1 | 16,6 | 3 | SPOV | architect | technical | often |
| **7** | 28 | 7 | 7 | 1 | 29,4 | 3 | 4POV | architect | technical | often |
| **8** | 28 | 6 | 6 | 1 | 30,5 | 3 | SPOV | architect | technical | often |
| **9** | 28 | 5 | 5 | 1 | 76,5 | 3 | BPOV | architect | technical | often |
| **10** | 28 | 4 | 4 | 1 | 363,9 | 3 | 4POV | architect | technical | often |
| **11** | 28 | 6 | 6 | 1 | 12,8 | 3 | BPOV | architect | technical | often |
| **12** | 28 | 5 | 5 | 1 | 25,4 | 3 | SPOV | architect | technical | often |
| **1** | 29 | 6 | 6 | 1 | 182,4 | 2 | 4POV | engineer | technical | often |
| **2** | 29 | 6 | 7 | 0 | 35,1 | 2 | SPOV | engineer | technical | often |
| **3** | 29 | 4 | 4 | 1 | 15,1 | 2 | BPOV | engineer | technical | often |
| **4** | 29 | 6 | 5 | 0 | 126,9 | 2 | 4POV | engineer | technical | often |
| **5** | 29 | 7 | 7 | 1 | 40,9 | 2 | BPOV | engineer | technical | often |
| **6** | 29 | 4 | 4 | 1 | 17,8 | 2 | SPOV | engineer | technical | often |
| **7** | 29 | 7 | 7 | 1 | 81,4 | 2 | 4POV | engineer | technical | often |

| | | | | | | | | | | |
|---|---|---|---|---|---|---|---|---|---|---|
| **8** | 29 | 5 | 6 | 0 | 11,8 | 2 | SPOV | engineer | technical | often |
| **9** | 29 | 5 | 5 | 1 | 14 | 3 | BPOV | engineer | technical | often |
| **10** | 29 | 3 | 4 | 0 | 25,2 | 2 | 4POV | engineer | technical | often |
| **11** | 29 | 6 | 6 | 1 | 10,4 | 2 | BPOV | engineer | technical | often |
| **12** | 29 | 5 | 5 | 1 | 12,3 | 2 | SPOV | engineer | technical | often |
| **1** | 30 | 6 | 6 | 1 | 69,3 | 2 | 4POV | surveyor | technical | often |
| **2** | 30 | 7 | 7 | 1 | 11,6 | 2 | SPOV | surveyor | technical | often |
| **3** | 30 | 4 | 4 | 1 | 10,1 | 3 | BPOV | surveyor | technical | often |
| **4** | 30 | 5 | 5 | 1 | 52,1 | 3 | 4POV | surveyor | technical | often |
| **5** | 30 | 7 | 7 | 1 | 22,8 | 3 | BPOV | surveyor | technical | often |
| **6** | 30 | 4 | 4 | 1 | 7,8 | 2 | SPOV | surveyor | technical | often |
| **7** | 30 | 5 | 7 | 0 | 72,6 | 1 | 4POV | surveyor | technical | often |
| **8** | 30 | 6 | 6 | 1 | 10,4 | 3 | SPOV | surveyor | technical | often |
| **9** | 30 | 5 | 5 | 1 | 10,1 | 3 | BPOV | surveyor | technical | often |
| **10** | 30 | 4 | 4 | 1 | 38,8 | 2 | 4POV | surveyor | technical | often |
| **11** | 30 | 6 | 6 | 1 | 8,2 | 3 | BPOV | surveyor | technical | often |
| **12** | 30 | 5 | 5 | 1 | 12,5 | 3 | SPOV | surveyor | technical | often |
| **1** | 31 | 5 | 6 | 0 | 34,1 | 2 | 4POV | architect | technical | often |
| **2** | 31 | 7 | 7 | 1 | 38,4 | 3 | SPOV | architect | technical | often |
| **3** | 31 | 4 | 4 | 1 | 11,9 | 3 | BPOV | architect | technical | often |
| **4** | 31 | 5 | 5 | 1 | 39,9 | 1 | 4POV | architect | technical | often |
| **5** | 31 | 7 | 7 | 1 | 16,5 | 3 | BPOV | architect | technical | often |
| **6** | 31 | 4 | 4 | 1 | 11,6 | 3 | SPOV | architect | technical | often |
| **7** | 31 | 5 | 7 | 0 | 28,7 | 0 | 4POV | architect | technical | often |
| **8** | 31 | 5 | 6 | 0 | 9,6 | 3 | SPOV | architect | technical | often |

| | | | | | | | | | | |
|---|---|---|---|---|---|---|---|---|---|---|
| **9** | 31 | 5 | 5 | 1 | 10,9 | 3 | BPOV | architect | technical | often |
| **10** | 31 | 4 | 4 | 1 | 20 | 1 | 4POV | architect | technical | often |
| **11** | 31 | 6 | 6 | 1 | 11 | 3 | BPOV | architect | technical | often |
| **12** | 31 | 5 | 5 | 1 | 11,9 | 3 | SPOV | architect | technical | often |
| **1** | 32 | 5 | 6 | 0 | 45,6 | 2 | 4POV | architect | technical | often |
| **2** | 32 | 7 | 7 | 1 | 30,9 | 2 | SPOV | architect | technical | often |
| **3** | 32 | 4 | 4 | 1 | 20,8 | 2 | BPOV | architect | technical | often |
| **4** | 32 | 5 | 5 | 1 | 42,9 | 2 | 4POV | architect | technical | often |
| **5** | 32 | 7 | 7 | 1 | 17,1 | 2 | BPOV | architect | technical | often |
| **6** | 32 | 4 | 4 | 1 | 17,4 | 2 | SPOV | architect | technical | often |
| **7** | 32 | 5 | 7 | 0 | 32,6 | 2 | 4POV | architect | technical | often |
| **8** | 32 | 5 | 6 | 0 | 19,6 | 2 | SPOV | architect | technical | often |
| **9** | 32 | 5 | 5 | 1 | 12,7 | 2 | BPOV | architect | technical | often |
| **10** | 32 | 4 | 4 | 1 | 34,1 | 2 | 4POV | architect | technical | often |
| **11** | 32 | 6 | 6 | 1 | 14,4 | 2 | BPOV | architect | technical | often |
| **1** | 33 | 5 | 6 | 0 | 32,4 | 2 | 4POV | architect | technical | often |
| **2** | 33 | 7 | 7 | 1 | 15,8 | 2 | SPOV | architect | technical | often |
| **3** | 33 | 4 | 4 | 1 | 16,1 | 2 | BPOV | architect | technical | often |
| **4** | 33 | 5 | 5 | 1 | 16,2 | 2 | 4POV | architect | technical | often |
| **5** | 33 | 7 | 7 | 1 | 16,4 | 2 | BPOV | architect | technical | often |
| **6** | 33 | 0 | 4 | 0 | 9,5 | 2 | SPOV | architect | technical | often |
| **7** | 33 | 7 | 7 | 1 | 20,5 | 2 | 4POV | architect | technical | often |
| **8** | 33 | 4 | 6 | 0 | 9,1 | 2 | SPOV | architect | technical | often |
| **9** | 33 | 5 | 5 | 1 | 9 | 2 | BPOV | architect | technical | often |
| **10** | 33 | 4 | 4 | 1 | 15,2 | 2 | 4POV | architect | technical | often |

| | | | | | | | | | | |
|---|---|---|---|---|---|---|---|---|---|---|
| **11** | 33 | 6 | 6 | 1 | 7,2 | 2 | BPOV | architect | technical | often |
| **1** | 34 | 6 | 6 | 0 | 56,5 | 2 | 4POV | architect | technical | often |
| **2** | 34 | 7 | 7 | 1 | 20,7 | 2 | SPOV | architect | technical | often |
| **3** | 34 | 4 | 4 | 1 | 14,3 | 2 | BPOV | architect | technical | often |
| **4** | 34 | 6 | 5 | 0 | 14,5 | 2 | 4POV | architect | technical | often |
| **5** | 34 | 7 | 7 | 1 | 13,7 | 2 | BPOV | architect | technical | often |
| **6** | 34 | 4 | 4 | 1 | 9,2 | 2 | SPOV | architect | technical | often |
| **7** | 34 | 7 | 7 | 1 | 15,7 | 2 | 4POV | architect | technical | often |
| **8** | 34 | 6 | 6 | 1 | 17,8 | 2 | SPOV | architect | technical | often |
| **9** | 34 | 5 | 5 | 1 | 48,5 | 2 | BPOV | architect | technical | often |
| **10** | 34 | 4 | 4 | 1 | 18,7 | 2 | 4POV | architect | technical | often |
| **11** | 34 | 6 | 6 | 1 | 8 | 2 | BPOV | architect | technical | often |
| **1** | 35 | 4 | 6 | 0 | 42,3 | 3 | 4POV | architect | technical | often |
| **2** | 35 | 7 | 7 | 1 | 20,9 | 2 | SPOV | architect | technical | often |
| **3** | 35 | 4 | 4 | 1 | 19,6 | 3 | BPOV | architect | technical | often |
| **4** | 35 | 5 | 5 | 1 | 40,5 | 3 | 4POV | architect | technical | often |
| **5** | 35 | 7 | 7 | 1 | 14,3 | 3 | BPOV | architect | technical | often |
| **6** | 35 | 4 | 4 | 1 | 21,8 | 2 | SPOV | architect | technical | often |
| **7** | 35 | 6 | 7 | 0 | 56,1 | 3 | 4POV | architect | technical | often |
| **8** | 35 | 5 | 6 | 0 | 23,4 | 1 | SPOV | architect | technical | often |
| **9** | 35 | 5 | 5 | 1 | 7,8 | 3 | BPOV | architect | technical | often |
| **10** | 35 | 4 | 4 | 1 | 29 | 3 | 4POV | architect | technical | often |
| **11** | 35 | 6 | 6 | 1 | 6,9 | 3 | BPOV | architect | technical | often |
| **1** | 36 | 7 | 6 | 0 | 30,2 | 3 | 4POV | surveyor | technical | often |
| **2** | 36 | 7 | 7 | 1 | 19,4 | 3 | SPOV | surveyor | technical | often |

| | | | | | | | | | | |
|---|---|---|---|---|---|---|---|---|---|---|
| **3** | 36 | 4 | 4 | 1 | 16,2 | 3 | BPOV | surveyor | technical | often |
| **4** | 36 | 5 | 5 | 1 | 47,5 | 2 | 4POV | surveyor | technical | often |
| **5** | 36 | 7 | 7 | 1 | 19 | 3 | BPOV | surveyor | technical | often |
| **6** | 36 | 4 | 4 | 1 | 17,4 | 3 | SPOV | surveyor | technical | often |
| **7** | 36 | 7 | 7 | 1 | 27 | 3 | 4POV | surveyor | technical | often |
| **8** | 36 | 5 | 6 | 0 | 23,8 | 2 | SPOV | surveyor | technical | often |
| **9** | 36 | 5 | 5 | 1 | 11,4 | 2 | BPOV | surveyor | technical | often |
| **10** | 36 | 5 | 4 | 0 | 90,5 | 2 | 4POV | surveyor | technical | often |
| **11** | 36 | 6 | 6 | 1 | 12 | 2 | BPOV | surveyor | technical | often |

# Appendix 2 – Online questionnaire statistical analyses

## 1 – Analysis of the visual counting accuracy via an exact binomial test (Software R)

```
#Loading libraries

require(xlsx)

require(Hmisc)

require(ggplot2)

require(extrafont)

#Loading data

data = read.xlsx("3dviewpoint-survey.xlsx",2)

#Speed column extraction

successRate = data[,c(5,8)]

successRate = successRate[which(successRate[,2] == "4POV" | successRate[,2] ==
"BPOV"),]

#Sum per category

pov = sum(successRate[which(successRate[,2] == "4POV"),1])

bpov = sum(successRate[which(successRate[,2] == "BPOV"),1])

n = nrow(successRate)/2

#Exact binomial distribution

binpov = binconf(pov, n, 0.95, method = "all")

binbpov = binconf(bpov, n, 0.95, method = "all")

#Success rate
```

```
pov = pov/(nrow(successRate)/2)

bpov = bpov/(nrow(successRate)/2)

#Extract upper and lower limits

binpov = binpov[1,c(2,3)]

binbpov =  binbpov[1,c(2,3)]

povend = as.vector(c(binpov,binbpov))

index = c("4POV"," BPOV")

#Plot

d = data.frame(POV=(index),
mean=c(pov,bpov),lower=c(binpov[1],binbpov[1]),upper=c(binpov[2],binbpov[2]))

plot = ggplot()+

geom_pointrange(data=d, mapping=aes(x=index, y=mean, ymin=upper, ymax=lower),
alpha=1.0, size=1.0, color="black", fill="black", shape=20) +

labs(title="Visual counting success rate per view type",x="Viewpoint category",y="Success
rate") +

theme_linedraw() +

theme(panel.border = element_blank()) +

theme(text = element_text(family="Palatino Linotype"),

plot.title = element_text(hjust = 0.5,color = "black", size = 18, face = "bold",margin =
margin(t = 0, r = 0, b = 10, l = 0)),

axis.text=element_text(size=16),axis.title=element_text(size=16,face="bold"),

axis.title.y = element_text(margin = margin(t = 0, r = 10, b = 0, l = 0)),

axis.title.x = element_text(margin = margin(t = 10, r = 0, b = 0, l = 0)),

axis.line = element_line(colour = "black"),

axis.ticks = element_line(colour = "black"))

#Saving plot

ggsave("successRate.png", plot = last_plot(), device = NULL, path = NULL,
```

```
scale = 1, width = 20, height = 15, units = c("cm"),
dpi = 300, limitsize = TRUE)
```

## 2 – Analysis of the users' certainty via a Chi-squared test (Software R)

```
#Loading data
require("xlsx")
data = read.xlsx("3dviewpoint-survey.xlsx",2)
#Certainty column extraction
certainty = data[,7:8]
#Frequency for each certainty category
length = length(certainty$Certainty)
pov = rep(-1,length/3)
bpov = rep(-1,length/3)
#Extracting 4POV and BPOV
pov = certainty[which(certainty[,2] == "4POV"),]
bpov = certainty[which(certainty[,2] == "BPOV"),]
pov = pov[,1]
bpov = bpov[,1]
#Extracting category
category = sort(unique(c(pov,bpov)))

#Frequency per category
fpov = numeric(length(category))
fbpov = numeric(length(category))
fpov = as.vector(table(pov))
fbpov = as.vector(c(0,0,table(bpov)))
#Regroup categories (0,1,2) & (3)
```

```
if (length(category) == 4) {
  fpovr = c(sum(fpov[1],fpov[2],fpov[3]),sum(fpov[4]))
  fbpovr = c(sum(fbpov[1],fbpov[2],fbpov[3]),fbpov[4])
} else{
  fpovr = c(sum(fpov[1],fpov[2]),sum(fpov[3]))
  fbpovr = c(sum(fbpov[1],fbpov[2]),sum(fbpov[3]))
}
#Chi-Squared test
array = matrix(c(fpovr,fbpovr),2,length(fpovr), byrow=T)
chi_squared = chisq.test(array)
#Plot preparation
vector = as.vector(array)
two = vector[1] + vector[2]
three = vector[3] + vector[4]
two = rep(2,two)
three = rep(3,three)
together = c(two,three)
categ = c(rep("4POV",vector[1]),rep("BPOV",vector[2]),rep("4POV",vector[3]),rep("BPOV",vector[4]))
end = cbind(together,categ)
end2 = as.data.frame(end)
#Plot
plot = ggplot(end2 ,aes(end2$together, fill=end2$categ))+
geom_bar(alpha = 0.7, position="dodge") +
scale_x_discrete(labels=c("2" = "[0,1,2]", "3" = "3")) +
```

```
ggtitle("Distribution of users' certainty degree \n in performing the visual counting per view type") +

xlab("Certainty degree") + ylab("Frequency") +

theme_linedraw() +

theme(panel.border = element_blank(),legend.title = element_blank()) +

theme(text = element_text(family="Palatino Linotype", face="bold"),

plot.title = element_text(hjust = 0.5,color = "black", size = 18, face = "bold",margin = margin(t = 0, r = 0, b = 10, l = 0)),

axis.text=element_text(size=16),axis.title=element_text(size=16,face="bold"),

axis.title.y = element_text(margin = margin(t = 0, r = 10, b = 0, l = 0)),

axis.title.x = element_text(margin = margin(t = 10, r = 0, b = 0, l = 0)),

axis.line = element_line(colour = "black"))

#Saving plot

ggsave("certainty.png", plot = last_plot(), device = NULL, path = NULL,

 scale = 1, width = 20, height = 15, units = c("cm"),

 dpi = 300, limitsize = TRUE)
```

## 3 – Analysis of the visual counting speed via an one-way ANOVA test (Software R)

```
#Loading libraries

require(xlsx)

require(ggplot2)

require(extrafont)

#Loading data

data = read.xlsx("3dviewpoint-survey.xlsx",2)

#Speed column extraction

speedAll = data[,c(5,6,8)]

speed = speedAll[which((speedAll[,3] == "SPOV" & speedAll[,1] == "1") | (speedAll[,3] == "BPOV") & speedAll[,1] == "1"),]

speedOrder = speed[order(speed$POV),]

speedOrder[,2] = round(((speedOrder[,2] / speedOrder[,1])/10),3)

speedOrder = speedOrder[c(2,3)]

#BPOV and SPOV

bpov = speedOrder[which(speedOrder[,2] == "BPOV"),]

spov = speedOrder[which(speedOrder[,2] == "SPOV"),]

bpovMean = mean(bpov[,1])

spovMean = mean(spov[,1])


#Coding BPOV and SPOV (0 and 1)

bpov = bpov[,1]

ibpov = numeric(length(bpov))

ibpov[]=1
```

```
spov = spov[,1]

ispov = numeric(length(spov))

ispov[]=2

ibspov = c(ibpov, ispov)

#Data

data = cbind(speedOrder, ibspov)

as.data.frame(data)

#One-way Anova

anovaOneWay = aov(Speed~ibspov, data)

analysis = summary(anovaOneWay)

plot = ggplot(end,aes(x = ibspov, y = Speed, group = ibspov))+

geom_boxplot() +

geom_jitter() +

scale_x_discrete(limits=c("BPOV", "4POV")) +

scale_y_continuous(breaks=c(0,1,2,3,6,10), limits = c(0,10)) +

ggtitle("Visual counting speed per view type") +

xlab("Viewpoint category") + ylab("Visual counting time per 3D geometric object (second)")
+

theme_minimal() +

theme(text = element_text(family="Palatino Linotype"),

plot.title = element_text(hjust = 0.5,color = "black", size = 18, face = "bold",margin = margin(t
= 0, r = 0, b = 10, l = 0)),

axis.text=element_text(size=16),axis.title=element_text(size=16,face="bold"),

axis.title.y = element_text(margin = margin(t = 0, r = 10, b = 0, l = 0)),

axis.title.x = element_text(margin = margin(t = 10, r = 0, b = 0, l = 0)),

axis.line = element_line(colour = "black"))
```

```
#Saving plot
ggsave("Speed.png", plot = last_plot(), device = NULL, path = NULL,
  scale = 1, width = 20, height = 15, units = c("cm"),
  dpi = 300, limitsize = TRUE)
```

# Abstract

Geospatial data visualization, known as geovisualization, often provides great support in the comprehension of the geographic information. For instance, geovisualization is fully integrated in urban planning, from the exploratory phase (e.g., for facilitating the diagnosis of areas where something needs to be done) to the monitoring stage (e.g., for evaluating dynamics phenomena). Initially carried out in 2D, this process increasingly extents to the third dimension as a way to enhance the visual perception of the surrounding world, which is fundamentally 3D. However, this shift is not without pitfalls, both in the graphical design of 3D model and the viewpoint selection. To promote the use of the third dimension, it is therefore essential to propose new strategies that facilitate this transition. As a result, this thesis intends to contribute to 3D geovisualization field development via the first proposal that aims to formalize its process into a knowledge network including both an expression (i.e., visual stimuli) and content plan (i.e., semantic world). Following this formalization effort, we realized that moving to the 3rd dimension strengthens the role of the viewpoint, especially in order to enhance the visualization techniques relevance in achieving visual targeted purposes. Indeed, as the camera is no longer simply oriented in a classic top-down direction (which is usually the case in 2D), the point of view needs now to be configured; and, due to the 3D graphical representation, this configuration is complex, in particular because occlusion issues are inevitable. This is why this research mainly tackles the best 3D viewpoint selection issue via a geocomputational method that automates and optimizes its identification within 3D scene. Note that specific attention has been carried out to incorporate the solution into a global semantic driven visualization process. Eventually, the proposal is validated through the development of an experimental framework that aims to evaluate our solution for a given visual selectivity task: visual counting. For that purpose, an empirical test has been conducted with experts in the form of interviews using an online questionnaire.